NUTRIENT REMOVAL SIMULATION OF RENDERING WASTEWATER IN SBR SYSTEMS

by
Elias Daniel David Nova Burgos

Master's thesis in partial fulfilment of the requirements for the degree of master's in environmental engineering

Advisors
Diana Catalina Rodríguez
Julio César Saldarriaga Molina

Universidad de Antioquia
Facultad de Ingeniería
Maestría en Ingeniería Ambiental
Grupo de Investigación Diagnóstico y Control de la Contaminación (GDCON)
Medellín, Antioquia, Colombia
2024

Maestría en Ingeniería Ambiental.

Grupo de Investigación Diagnóstico y Control de la Contaminación.

Sede de Investigación Universitaria (SIU).

ACKNOWLEDGMENTS

I thank my academic advisors Diana Catalina and Julio Saldarriaga from the Universidad de Antioquia for their guidance and support during the research process, as well as for giving me the opportunity to process the collected data. I would also like to thank Markus Ahnert from the Technical University of Dresden for introducing me to the world of activated sludge simulation and for collaborating with me in the calibration process of the simulations. Thank Carlos Lopez Vasquez for being my first direct contact with activated sludge simulation at international level and for his recommendation to participate in the last cohort of the activated sludge simulation course in the Netherlands. To Daniel Nolasco for managing to obtain access to the licensing of the BioWin software, which the simulations were run. To Celeste Jenisch for helping me in the English editing process. I thank the Universidad de Antioquia for granting me the scholarship that allowed me to complete my master's degree, the IHE Institute for granting me the scholarship to take the course on process modeling of wastewater treatment plants which filled gaps in specific knowledge of sludge simulation, and the GDCON research group for the collected and analyzed data.

TABLE OF CONTENTS

TABLE OF FIGURES

TABLE LIST

ABBREVIATIONS

ADM: Anaerobic Digestion Models
ANO: autotrophic nitrifying organisms
ASM: Activated sludge model.
BOD_5: Biochemical oxygen demand at the fifth day
COD: Chemical oxygen demand
COD_S: Soluble (filtrated) chemical oxygen demand
CWW: Condensate wastewater
DO: dissolved oxygen
FOG: Fats, Oil and Grease
GAOs: Glycogen Accumulating Organisms.
HKWW: Housekeeping Wastewater
HRT: Hydraulic retention time
K_La: Oxygen transfer rate
LCFA: Long chain fatty acids
NH_4^+: Ammonia
N_2O: Nitrous oxide
NO_3^- :Nitrate
NO_2^-: Nitrite
OHO: ordinary heterotrophic organisms
OUR: Oxygen uptake rate
PAOs: Polyphosphate accumulating organisms
PO_4^-: Orthophosphate
PO_4^{3-}: Polyphosphates
SBR: Sequencing batch reactor
SO_4^{2-}: Sulfate
S_S: readily soluble biodegradable COD.
SRT: Sludge retention time
SVI: Sludge volume index
TKN: Total Kjeldahl nitrogen
TN: Total Nitrogen
TOC: Total organic carbon
TP: Total phosphorus
TSS: Total suspended solids
VFA: Volatile fatty acids
VSS: Volatile suspended solids
WWTP: Wastewater treatment plant

ASM PARAMETERS (BioWin nomenclature)

μ_{AUT} (Z_{AOB} & Z_{NOB}): Maximum specific nitrifier growth rate (d^{-1})
μ_H (Z_{BH}): Maximum specific heterotrophic growth rate (d^{-1})
b_{Aut}: autotrophic decay coefficient (d^{-1})
b_H: heterotrophic decay coefficient (d^{-1})
f_i: fraction of inert particulate matter
i_{XB}: mass Nper mass COD in biomass (gN/gCOD)
K_N: half-saturation parameter for autotrophic biomass (gNH4/m^3)
K_{ND}: Ammonification rate (d^{-1})
k_R: rate of rapid hydrolysis (d^{-1})
K_S: half saturation parameter for heterotrophic biomass (gCOD/m^3)
S_s= S_A+S_F: readily degradable substrate (gCOD/m^3)
S_A (S_{BSA}) or COD_A: volatile fatty acids (Acetate, gCOD/m^3)
S_F (S_{BSC}): readily biodegradable complex organics (gCOD/m^3)
S_I (S_{US}): inert orgnic matter. (gCOD/m^3)
S_{NHx} (NH_3-N): ammonium and ammonia nitrogen (gN/m^3)
S_{NOx} (NO_3-N): nitrate and nitrite nitrogen (gN/m^3)
S_{PO4}: inorganic soluble phosphate (gP/m^3)
S_N: ammonium concentration (gN/m^3)
S_{ND}: soluble organic nitrogen (gN/m^3)
S_{O2} (DO): dissolved oxygen (gO_2/m^3)
X: total particulate matter (gVSS/m^3)
X_I (X_I): inert organic matter (gCOD/m^3)
X_R: rapidly hydrolysable matter (gCOD/m^3)
X_S (X_{SP}): entrapped slowly hydrolysable matter (gCOD/m^3)
X_{ND}: particulate organic nitrogen (gN/m^3)
X_H: heterotrophic organism/biomass (gCOD/m^3)
X_{PAO} (Z_{BP}): phosphate accumulating organism (gCOD/m^3)
X_{PP} (PP_{LO}): poly-phosphate organism (gP/m^3)
X_{GLY}: glycogen organism (gCOD/m^3)
X_{AUT}: autotrophic nitrifying organisms/biomass (gCOD/m^3)
Y_H: heterotrophic yield coefficient (gCOD/gCOD)
Y_{AUT}: autotrophic yield coefficient (gCOD/gCOD)

1. INTRODUCTION

The meat rendering process transforms waste from the meat industry to useful and valuable material as by-products (i.e. animal feed supplements), soaps and rustproofing paints. To produce animal feed supplements the hydrolysis process of lipids and proteins is fundamental to prevent the spread of diseases, during this hydrolysis process and housekeeping procedures large amounts of wastewater with high organic substances, acids, and nutrients are released to the environment imposing a huge pollution challenge, especially for biological treatment stages in developing countries with basic industrial wastewater infrastructure.

Wastewater simulation is an alternative treatment forecasting of biological process, that could help to control and operate such a complex system under both dynamic and steady-state conditions. However, the influent and model parameters calibration is not an easy task, because of the lack of knowledge and standardized procedures for industrial wastewater systems. Thus, the main objective of this work is to evaluate the removal of carbon and nitrogen from an sequencing batch reactor (SBR) of housekeeping wastewater (HKWW), condensate wastewater (CWW), and the differential overload of both wastewater lines by means of simulations, following the recommendations of the activated sludge modelling (ASM) unified protocol from the good modelling practices task group, defining the two different wastewaters production, processing and analyzing the collected data, setting the plan model layout, proposing a calibration methodology for simulations of meat industry effluents based on sludge production, carbon and nitrogen performance, and analyzing how the influent fractionation, and model parameter influence the sensitivity of the treatment representations.

The HKWW simulation presents that the organic matter is partially and physically removed rather than biologically since the phosphorus deficit, and pH inhibition that limits ordinary heterotrophic organisms (OHO) growth. While nitrogen presents almost no removal as a result of low pH, ammonia inhibition, and low inorganic carbon source for autotrophic nitrifying organisms (ANO). On the other hand, the CWW simulations present a higher organic matter removal for this matrix than for HKWW, since it presents a higher biodegradable content. In this case the major stripped macronutrient removal is nitrogen rather than carbon, because CWW matrix presents a higher nitrogen content and basic pH that promotes the ammonium formation and its later release to the atmosphere. Thus, for the correct biological treatment performance, the system requires adjustment in the preliminary and primary treatment for free, disperse and emulsifying oils removal to avoid fats, oil and grease (FOG) overloading and hereafter microorganism’s washout, the reduction in the aeration pattern to promote nitrifiers growth due to the increment in CO_2 concentrations, and the addition of alkali species to prevent nitrifiers inhibition.

2. PROBLEM STATEMENT

Meat rendering is a separation process of fat from animal tissue. It begins with the disgregation of fat and proteinaceous materials by use of either heat "cooking", chemicals, pressure, or vacuum to sterilize against pathogens, like the spread of bovine spongiform encephalopathy and Creutzfeldt–Jacob disease (Brennan et al., 2021), and to reduce the amount of water enhancing the product lifetime and storage (Kosseva, 2020). Then, the centrifugation stage produces "stick water" or "condensate water" detaching oil from the liquids and small solid materials (protein meal). Finally, by means of evaporation in a wet scrubber the condensate is separated from the solids, then this liquid is cooled and discharged in form of raw rendering condensate wastewater. During the whole meat rendering process the housekeeping effluent, a secondary relevant source of wastewater, is produced mostly from raw material washing, followed by equipment cleaning (e.g. cookers, mixers, grinders, and emulsifiers) and from machinery, floor, and container cleaning operations. Both the rendering condensate and cleaning wastewater produce large amounts hydrolyzed FOG and proteins that trigger socio-environment impacts.

Rendering industry pipes and municipal sewers are mostly affected by FOG fouling, which is the process of saponification, solidification and deposition of glycerol and metal ions that blocks the drains and produces unpleasant odors (Sultan et al. (2024). Saponification also clogs gas collection systems (Cammarota & Freire, 2006), and even in thinning layers causes decreasing of light and oxygen transfer in channels and rivers banks (Klaucans & Sams, 2018). Additionally, lipids hydrolysis produces high biodegradable organic acids like VFA, that produces death of aquatic organisms by oxygen depletion (Cuadros et al., 2011; Brennan et al., 2021), creates a negative impact on K_La coefficient that difficult re-aeration of natural water bodies (Auterská & Novák, 2006), and transports toxic micropollutants that also present low affinity to water like lipids (Pintor et al., 2016). On other side, protein hydrolysis produces large amounts of nutrients (e.g. NH_4^+, NO_2^-, NO_3^-, amino acids and nucleic acids) that promote eutrophication, threatening aquatic life as a result of toxic algal bloom (Rahman et al., 2014). Also, those nutrients are released to the water-bulk in forms of free NH_4^+ and NO_2^- that along with a nutritional deficit of readily biodegradable carbon and phosphorous, produce high toxicity to aquatic environments (Brønd & Sund, 1994; Auterská & Novák, 2006), the NO_3^- could be carried out by the drinking water and endanger human population, mainly infants, causing the "blue baby syndrome" interfering with blood oxygenation (Knobeloch et al., 2000). Furthermore, emissions of greenhouse gases (GHG) as nitrogen oxides (NOx, as NO, NO_2) into the atmosphere could occur for the whole meat industry effluents, as another issue of water enrichment with nitrogen and incomplete denitrification due to nutrient disbalance (Domingo et al., 2017), excess of aeration, and insufficient anoxic conditions (not anaerobic) (Tian et al., 2020).

To reduce and avoid the socio-environmental impacts, rendering wastewater is commonly treated by means of preliminary (e.g. gravity separation), primary (e.g. flotation), and secondary treatment (e.g. biological process). Although the high removal effect of preliminary and primary treatment against free oil, remaining dispersed and emulsifying oils affects the secondary treatment, and hereafter, do not comply with the pollutant standards. New technologies and combinations of technologies aroused from the sustainable environment to polishing the secondary treatment, but most of them have not practical application due to the economical constraints. Therefore, best practicable-, sustainable- and economically achievable -technologies like biological process are still being matter of study.

Biological process is commonly affected by rendering wastewater, since hydrolyzed FOG reduces the transport rate between cells and aqueous phase, exposes microorganisms to inhibition (e.g. Nitrifiers) and washout due to the toxic effect of long chain fatty acids (LCFA) (Brønd & Sund, 1994). Oleic acid, another volatile fatty acids (VFA) that is also released during lipid hydrolysis, affects the rendering wastewater treatment leading to pH inhibition of the anaerobic environment (Nakhla et al., 2003). Additionally, this type of effluents is very unstable due to the macronutrient deficiency (i.e. low readily COD/N and readily COD/P ratio), the longer the wastewater storage time, the greater the nutrition deficit, since materials are received in advanced decay state (Metzner & Temper, 1990), this nutritional deficit affects the OHO, Nitrifiers and PAOs growth that are essential bio communities for the secondary treatment (Nowak et al., 1996). Finally, the secondary process is also affected by the high heat transfer (temperature up to 40°C) that promotes filamentous and viscous sludge bulking, damaging the solids settling, and hereafter the effluent Total suspended solids (TSS) removal (Brønd & Sund, 1994; Auterská & Novák, 2006).

To control the complexity of the biological process of meat wastewater, plant-wide models (WWTP simulation) became a great alternative to meet the standards, give insight into plant performance, and support on management decisions at the lower cost (Orhon et al., 2009; Makinia & Zaborowska, 2020). Biological processes simulation is represented by means of biokinetic models such as ASM. However, ASM from the IWA-type have been developed for municipal wastewater systems, thus, for industrial applications ASM may be additionally calibrated on influent composition, kinetic, and stoichiometric parameters (Melcer, 2004; Meijer & Brdjanovic, 2012). The right correction of those parameters could cause some troubles for many beginners due to the lack of knowledge and standardized procedures in both domestic and industrial applications (Hauduc et al., 2009; Chen et al., 2020). In the later, it is unclear how to select and fit the right subset of parameters to the specific industrial application, which are limited by the available observed data, and it is also difficult to recognize which fixed parameters may bias the simulated response (Makinia & Zaborowska, 2020).

Rendering effluent simulations is an under-studied matrix, which is represented by few simulation studies. Nowak et al. (1996) have investigated kinetics of nitrification under phosphorous deficiency, O'Flynn (1999) simulated the treatment of this type of effluent with anaerobic activated sludge systems but were not given too many details about simulations. Finally, Nakhla, Liu & Bassi (2006) modeled the reaction kinetics of an aerobic continuous activated sludge system, and suggested correction of modelling for biomass growth, and hydrolysis by Monod's models. However, the rendering wastewater treatment analysis of plant performance while changing the proportion between condensate and housekeeping activities have still not been simulated and analyzed.

3. OBJECTIVE

Evaluate the removal of carbon and nitrogen from an SBR treatment system of meat by-product wastewater by means of simulations.

3.1. SPECIFIC OBJECTIVES

- Configure the SBR system layout, based on secondary information, with their operational cycles and controllers, input and output signals, parameters, and models.
- Calibrate the kinetic, stoichiometric, and operational parameters with observed data to define the simulation baseline.
- Simulate scenarios of differential loads of Carbon: Nitrogen (C: N) to determine its biological removal.

4. REFERENCE FRAMEWORK

At next, it will present the reference framework that helps to understand the baseline of the wastewater simulation theory. This framework consists of an urban management system, plant-wide models, and simulation protocols of wastewater, emphasizing industrial wastewater applications.

4.1. URBAN WASTEWATER MANAGEMENT

To manage (tracking and following) wastewater pollution in a whole catchment area, urban wastewater models, also called spatial extended simulation, are used by integration of data gathering, components, and interfaces. Industrial wastewater is an essential component in the extended simulation (Meijer, & Brdjanovic, 2012), and thus the industrial simulation outputs are fundamental in urban wastewater management. Some examples of components and interfaces are generated by the catchment area, sewer system (e.g. KOSIM), plant-wide models (BSM1, benchmarking that include ASMs), and river quality models or receiving water bodies (e.g. RWQM1) (Makinia & Zaborowska, 2020; Chen et al., 2020). Data gathering is an important component to face such as complex systems and can be managed by means of instrumentation, process control, and automatization (Alex et al., 2020). While components and interfaces are integrated into urban wastewater models.

4.1.1. PLANT-WIDE MODELS

Industrial wastewater components and interfaces to feed urban wastewater models are generated by plant-wide models (whole WWTP simulation). Those models arose as a necessary strategy to design, retrofit (upgrade), optimize operational plant cost, operators train, control evaluation (what if? scenarios), removal efficiency optimization, and energy recovery (e.g. biogas) (Chen et al., 2020). Plant wide models also improve realism of the exiting model by better understanding of physicochemical process, process extensions (as side-stream process like SHARON), and water resource recovery facilities (WRRF) due the awareness of climate change and sustainability. The new trends support the idea that WWTP should not only reduce the pollution to water bodies but also should keep an eye on energy balances, operational cost, process risk, and life cycle assessment (Makinia & Zaborowska, 2020).

Plant-wide models consist of the next three material models: sludge, gas and liquid-lines (Lopez-Vazquez et al., 2017). The sludge line, which is the concentrated waste of the liquid line, is referring to the entire treatment that sludge suffers to be stabilized (by digestion mostly). The sludge line plays an important role in the wastewater line and consecutively for the whole plant performance, sometimes the wastewater line is overloaded by a surplus of ammonia in rejected water that comes from the dewatering sludge process (Makinia & Zaborowska, 2020). On the other side, the gas line is necessary to operate environmentally friendly WWTP by modelling greenhouse gases emission (e.g. Nitrogen oxides) in nutrient removal facilities. Finally, the liquid line, which probably is one of the most well-known and controlled lines (Melcer, 2004), is controlled and operated by a simulator (computer program), and simulation protocol.

The simulator integrates among others, the next models: Bioreactor model, hydraulic model, influent model (characterization), oxygen transfer (aeration), heat transfer (temperature changes), and sedimentation tank (Gernaey et al., 2004; Makinia & Zaborowska, 2020). Similarly, the bioreactor model integrates ASM, ADM and physicochemical processes that take place during the reacting phase. The former is used to simulate the heart of the biological (secondary) process, while ADM and physicochemical process simulate anaerobic digestion that happen, for instance, in digesters (Makinia & Zaborowska, 2020). Furthermore, the hydraulic model determines the mixing patter (e.g. Completely stirred tank reactors (CSTR) or pug flow), and interactions between process and compounds (e.g. connection between units as bioreactors and clarifiers) by means of the combination of differential equation base on mass balances. On the other hand, simulation protocol is a stepwise methodology that enables simulation success mainly in the characterization and calibration phase (Rieger et al, 2012).

4.1.2. WASTEWATER SIMULATORS

Many simulators allow users to link various tanks or unit processes together according to the wide-plant setup (e.g. from anoxic to aerobic tank for nitrification), and hereafter, to simulate the wide-plant performance under different operating and environmental conditions. With aid of a simulator unexpert users can enhance plant operation by understanding system responses when changing control variables (Melcer, 2004). There are many simulator categories to perform wastewater simulation that depend on the level of complexity, user programming expertise, and level of education on the wastewater branch. The two most accepted simulation categories are general purpose and specific wastewater simulators.

Specific wastewater treatment simulators are divided into two types: open structure and closed structure. In the latter, the user does not require too much programming knowledge (minimal user training), since the simulator is an icon-based approach to connecting process to unit blocks, users also specify initial conditions, components, physical, biological, and kinetic properties of wastewater systems by means of Pop-Up windows that allows the model parameters modification (Meijer & Brdjanovic, 2012). Those closed structure simulators enable the understanding of the process by changing the control variables and analyzing the system responses (Melcer, 2004). Some examples of closed structure programs are, but not limited to: BioWin (EnviroSim, Canada, 1990 introduced), GPS-X (Hydromantis, Canada, 1991), EFOR (DHI, Denmark, 1990), SIMBA (IFAK, Germany, 1994), STOAT (WRc group, United Kingdom, 1994), WEST (Hemmis/DHI, Belgium/Denmark, 1998), SUMO (Dynamita, France), DESASS y EDAR (Spain) (Makinia & Zaborowska, 2020).

4.1.3. SIMULATION PROTOCOLS

A simulation protocols (or guideline) is an organized, proven (recorded pass experience) and smart stepwise procedure to reduce the complexity of a simulation project of wide-plant models, and bring highlights on model calibration to succeed with the simulation (Makinia & Zaborowska, 2020). In fact, simulation protocols have been developed to familiarize novice designers and stakeholders with a practical procedure to reduce conflicts between operational and plant design information (Meijer & Brdjanovic, 2012). For example, Rieger et al. (2012) suggests the simulation process of a continuous AS plant for nitrogen removal that was carried out by checking the sludge production and following the next stepwise procedure: first biokinetic parameters, then clarifier performance by settling parameters, nitrification by tracking alkalinity levels and ANO inhibition, denitrification by influent and recycled characteristics, and finally the oxygen transfer by mass transfer parameters. Additionally, different to domestic wastewater simulation, industrial applications must present detailed information of waste material after the production process, in the project definition stage, which is of paramount relevance and aid to understand the inflow characterization, efficient data collection, model development (also extensions) and scenarios analysis (Rieger et al., 2012). On simulation protocol the general simulation tasks are divided into several sub-tasks such as: Objectives and purpose, configuration of treatment process (plant layout), data gathering (for calibration), calibration (model correction, fine tuning, or curve fitting), validation (model checking), and finally, simulated scenarios. For more information about calibration protocols readers are invited to review Table 3.27 from Chen et al. (2020), and chapter 6 of Makinia & Zaborowska (2020).

4.2. THEORETICAL FRAMEWORK

At next it will be present more details about the liquid line simulation, SBR systems, SBR simulation, available simulator for SBR systems, and main characteristics to take in account when dealing with calibration protocols.

4.2.1. LIQUID LINE SIMULATION

As stated before, a plant-wide simulation focusses on the liquid line that consists of influent, bioreactor, hydraulic, oxygen transfer, heat transfer, and sedimentation models. It will present an especial emphasis on bioreactor models since it is the core of biological process and presents the most complex parameter variability according to the industrial wastewater application for the SBR system matter of study. For the remaining models, continuous AS or large-scale systems, it is suggested to read chapter 3 of Makinia & Zaborowska (2020).
Mass balance equations are the basis of any wastewater model description. Thus, transport (physical process: Multi reactor flow scheme, connection, recirculation, excess sludge removal, solids separation) and conversions (bio-chemical process, transformation of non-linear differential equations, and conservations principles of COD, P, and electric charges as ions) should be couple or related together. The former does not change the chemical structure of all materials, while the latter does, and both describe the concentration changes (state change) over time (Gujer & Henze, 1991). Transport and conversion processes are also called micro-kinetics and can be easily studied in the laboratory. When comparing full-scales system, the major differences lie in the transport process rather than the conversion process (Chen et al., 2020).

- **BIOREACTOR MODEL SIMPLIFICATIONS**

A model is a simplification or utile representation of reality but never the exact reality, thus, models take in account only the most important parts of reality to represent it, and thus, model success depends on the expectation of the modeler while representing the reality (Lopez-Vazquez et al., 2017). In that sense, bioreactor models make simplifications to accomplish the realty representation of biological and physicochemical processes that are undertaken in wastewater treatment by means of in size-, time-, and microorganisms' detail-scale.

The size-scale of the reality representation is usually analyzed either small or macro scale. There are some approaches that represent the small size of inner process in the wastewater such as computational fluids dynamic (CFD), a field that is out of the scope of this investigation, for further research read Karpinska & Bridgeman (2016) for more information. On the other hand, in conventional ASM (bioreactor model) the size scale is based on assumption of whole well mixed reactor (CSTR) and not on small scales, e.g., simplification of sludge mass rather than floc scale, because the small size is not relevant enough and highly time consuming to represent the whole reactor behavior (Lopez-Vazquez et al., 2017).

Time scale is also simplified from reality, this dimension is usually analyzed in wastewater treatment either steady- or dynamic-state, which are selected according to the nature (origin of wastewater) and variable objectives (removal parameter target) (Lopez-Vazquez et al., 2017). Steady-state analyses variables that change in time but without changing load and flow patterns of influent feed, and hence the change in concentration is close to zero ($dC/dt=0$), while dynamic-state analyses time dependent variation ($dC/dt\neq0$) with switching load and flow inputs (Qasim & Zhu, 2018). One of the big challenges in wastewater treatment is that state variables differ in scales of times from few seconds to several days as explain by Casellas et al. (2008), if the temporal variable objective is daily changes that happened too slow as ammonia in the digester or too fast as chemical precipitation in the reactor, steady-state condition is suitable for the simulation. By the contrast, if the variable objective in time is daily changes of nitrate and nitrite in the reactor, which change rapidly (but not as fast as chemical precipitation), the suggested time scale to select should be dynamic simulation (Lopez-Vazquez et al., 2017). According to Meijer, & Brdjanovic (2012) steady state modeling is used for retrofitting designs or flat domestic sewers analysis, since daily average concentration and flows are used, while dynamic modeling is suitable for steep domestic sewers, or process control design, operational troubleshooting, specific effluent discharge, etc.

From the simulation point of view, the microbiological scale is referred to as the mathematical representation scale of the AS, i.e., the ASM type, which is selected from the objective of the simulation. This means that the objective of simulation is not always set for representing the whole and detailed reality as ADN or genes scales but obtaining a good relationship between recorded dates and simulations. This approximation is accomplished on ASM by simple entities or surrogate organisms such as heterotrophs or nitrifiers that define the level of mathematical modelling organization. There are different types of microbiological scales or approaches such as black-box (empirical models), gray-box (biokinetic or mechanistic or steady-state models), and crystal-box (metabolic models or dynamic models) (Chen et al., 2020).

Biokinetics models such as activated sludge models (e.g. ASM1, ASM2d, among others) are built on the conceptualization (idea) of physical and biological mechanisms for surrogate microorganisms (e.g. OHO, ANO) that transform materials in the systems, and assume the microbial cell as a black box, but not the whole reactor as in black box models. Biokinetics models should be calibrated and validated against real data due to the conceptualization of the methodology to probe its reliability (Van Loosdrecht et al., 2015). In these models, sludge composition, microbial dynamic and chemical changes are represented by processes as hydrolysis, fermentation, ordinary heterotrophic organisms (OHO), autotrophic nitrifying organisms (ANO) growth, decay of OHO and ANO (Hauduc et al., 2013). Moreover, the functioning of biokinetic models is based on hypotheses of biological processes and interactions (e.g. cell growth or maintenance, and depredation respectively) that are

represented by mass balances and mathematical expressions, both depict the physical behavior of the system (Qasim & Zhu, 2018; Chen et al., 2020).
To handle this bunch of differential mathematical equations and also to differ and isolate transport from transformation (conversion), a matrix format facilitates the recognition of the stoichiometric and kinetic reactions with the regarding switching functions to turn on or off some processes as environmental conditions change (Gujer & Henze, 1991; Melcer, 2004). The matrix also presents microbiological processes as microorganisms growth, decay, hydrolysis, etc., mostly by saturation type- or enzymatic switching functions (e.g. hyperbolic Monod) to determine which processes are either activated or deactivated according to the environmental conditions, e.g. OHO aerobic growth is activated in the presence of S_s and S_{O2} and take the form of $S_S/(k_S+S_S)$ and $S_O/(K_{O,H}+S_O)$ respectively, and for OHO anaerobic growth is deactivated in the presence of S_{O2} and takes the form of $K_{O,H}/(K_{O,H}+S_O)$. This form of kinetics is adopted for numeric convenience and better approximations, rather than for mechanical accuracy (Gujer & Henze, 1991). Lopez-Vazquez et al. (2017) broadly recommends the use of biokinetics models for nitrogen removal. However, these types of models do not correctly represent the kinetic analysis under transient conditions, for example for oxygen-limited conditions, such as in industrial applications without buffer influent tanks (Chen et al., 2020).

• INDUSTRIAL WASTEWATER SIMULATION

ASM are mostly biokinetic and metabolic models, and have been developed mainly for municipal wastewater systems, but they are also used as a starting point to industrial model developments since many reactions and process from industrial applications occur also in domestic wastewater (Gernaey et al., 2004). The main different to use ASM in industrial effluents is paying attention to wastewater characterization, biological (kinetics and stoichiometry parameters) and physicochemical process that negatively impacts the overall system performance (Melcer, 2004; Casellas et al., 2008). Different from domestic wastewater, industrial wastewater must be thoroughly studied on industrial kind and plant specific approach since wastewater composition changes between industrial applications and between the same activity. Those effluents are highly dependent on the production scheme that exert variation with time and used materials due to different experiences and habits in the production scheme (Orhon et al., 2009).

For industrial applications ASM can be modified, selecting the model structure and complexity, gathering experimental data, adding mathematical model formulation (new reaction and process to the general matrix, only when needed), and finally calibrating and validating the model (Melcer, 2004). The structure and complexity are set mostly by the scope of simulation and additional contaminant of interest according to the process and regulatory requirements, in general AS models should contain sludge production, oxygen demand, dynamic oxygen response, effluent concentration of specific contaminants, and organic volatilization components. Specific contaminants such sulfur could present specific sulfur oxidizing bacteria that demand additional oxygen requirements, while volatile components in forms of COD could be limiting for heterotrophic bacteria growth and pollutant gases of releasing concern. Another important issue could be acute nitrification inhibition by industrial wastewater (Gernaey et al., 2004), as well as toxic chemicals that create microorganisms' inhibition and should also be taken into account in the ASM models (Orhon et al., 2009). Moreover, gathering experimental data is required to model calibration for better response to the specific industrial wastewater application, after calibration more experimental data should be collected and so on. Therefore, is highly recommended to reviewing plant operating data and treatment examples of similar industrial wastewater composition since characterization serves as effluent parameter limitation informing which contaminant are potential to remove or not, and which other could cause inhibition (Orhon et al., 2009).

Melcer (2004) suggests the use of ASM1 or ASM2 for food industry wastewaters, since share a huge similarity with domestic wastewater, always paying too much attention to the appropriate characterization and fractionation. For petroleum refinery industries this author suggests the use of ASM1 with some special modifications in phenolic COD utilization, acetate uptake as a third type of soluble readily biodegradable substrate (S_A) founded in the OUR profile studies in Coen et al. (1998), volatilization of volatile organic compound, switching function for inhibition, adsorption of COD, and growth and decay of sulfur oxidizers. Gernaey et al. (2004) cited some works on cheese industrial effluent using ASM3+BioP reaction from the TUDP model, also adding Mg^{2+} switching function for Mg^{2+} limited kinetics. Besides, those authors cited the treatment of pharmaceutical industry with ASM1 modifying a decrease into the soluble biodegradable organic substrate (S_S) due to the recalcitrant nature of contaminants (S_I).

Orhon et al. (2009) present a straightforward methodology for the biodegradation assessment to characterize industrial wastewater pointed out the importance of the COD fractionation especially for particulate inert (non-biodegradable) COD fraction (X_I) that should be hydrolyzed (X_S) prior to uptake by microorganisms. Moreover, the author highlights the importance of respirometry test (dissolved O_2 concentrations Vs time plots) for the assessment of stoichiometric and kinetics coefficients. This author also suggested to prior replace or remove other contaminants such as micropollutants from the manufacturing process intending to reduce the toxic and inhibitory effect on the effluent treatment. For many other good practices on industrial wastewater management, it is highly recommended chapter 6 of Orhon et al. (2009). Additionally, the report of Reijken et al. (2018) is strongly suggested for cellulose hydrolysis in the paper industry, Waki et al. (2018) for the swine wastewater treatment, Bentancur et al. (2021) for the pulp mill, as well as the book of Orhon et al. (2009) for textile on chapter 9 and leather tanning on chapter10. Rieger et al. (2012) for simulating some industrial wastewater such as soy sauce and petrochemical sites, and finally, examples from Brdjanovic et al. (2015) book for oil refinery, tannery, and pulp mild industrial effluents.

4.2.2. SBR SYSTEMS

SBR system consist of filling, reaction, settling, drawn and idle phases, its flexibility in operation, low construction and maintenance cost enables good performance and flexibility when treating high strength nutrient effluent (carbon, nitrogen and phosphorus) in transient conditions that cause several operational problems such as industrial wastewater (Lobo et al. 2016), as landfill leachates, hypersaline, tannery, brewery, dairy, among others industrial applications (Mace & Mata-Alvarez, 2002; Chen et al., 2020). Besides, many experiments could be performed by using SBR system, for instance, as shown by Kim et al. (2005) for the fate of tetracycline (an antibiotic) in activated sludge process. Different to continuous flow systems SBR present constraints and advantages that requires different design considerations such as the incorporation of a variable-volume simulation, cyclic operation, and several phases in each cycle in succession (Orhon et al., 2009). Another difference is that AS is preferred when treating large amounts of wastewater e.g. domestic effluents (Casellas et al., 2008), while SBR system are mostly used on industrials application since SBR consumes more than 60% of expenses during automatic operation than AS systems (Chang et al., 2000).

- **OPERATION AND MECHANISM OF NUTRIENT REMOVAL**

The SBR operation system begins with the fill phase, followed by reaction or process (with aeration and/or stirring), settling, which is influence by the sludge volumetric index (according to Chang et al. (2000)), then with drawn or decant phase and ends with idle phase. This cycle is repeated over and over again as presented in Figure 1.

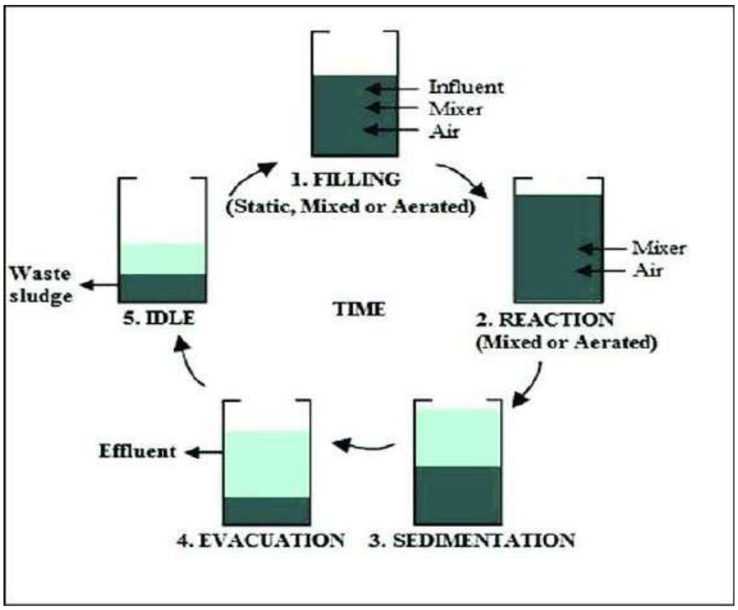

Figure 1. SBR operative phases.
Source: Singureanu & Woinaroschy (2019).

The way in which wastewater is transformed in the SBR system is by means of variation of the environmental condition in the reacting phase, e. g., changing the availability of oxygen (aerobic (S_{O2}>0), anoxic (S_{O2}=0 and S_{NO3}>0) and anaerobic (S_{O2}=0 and S_{NO3}=0) phases), soluble organics (e.g. BOD or COD), and keeping microorganisms from previous cycles, which are present in the form of VSS, similar to the continuous AS process. Control of environmental conditions drives selection, enrichment, and activation of different types of microorganisms in a single sludge bio community (e.g. OHO, nitrifiers, PAOs or GAOs) that enhance the treatment process (Oles & Wilderer, 1991; Filali-Meknassi et al., 2004). For instance, Oles & Wilderer (1991) cited that growth of heterotrophic bacteria (OHO) depends on the feeding pattern, i.e., the fast fill strategy (pulse feed, common in SBR systems) produce a higher maximum growth of heterotrophic bacteria value, than uniform substrate supply pattern (step feed, common in AS). However, the cell production yield is inversely affected by fast fill SBR pattern. Therefore, it is essential to optimize the order and duration of the SBR phases to maintain a better bio community of microorganisms (Casellas et al., 2008). Furthermore, Orhon et al. (2009) stated that sludge settleability varied with different fill and react rations and conditions.

Biological nutrient removal is achieved in SBR systems by changing periods of operational cycles such as fill, react (including adjustment of anaerobic, anoxic, and aerobic environmental conditions), settle, drawn and idle phases (Filali-Meknassi, 2004; Corominas, 2006). Similar as activated sludge systems for carbon removal high BOD/COD ratio is required, for nitrogen removal low N/COD ratio and the react phase in SBR systems is set to anaerobic and anoxic (denitrification) and aerobic conditions (nitrification), for phosphorous removal low NO_3/COD and high VFAs/COD ratios are suggested. In case where carbon is limiting for denitrification process, influent feeding (e.g. raw or anaerobic wastewater), external carbon strategies are recommended e.g. methanol, acetate, ethanol, and waste or industrial by-products (Filali-Meknassi et al. ,2005).

4.2.3. SBR SIMULATION

Simulation facilitates the operation of wide-plants, especially when the processes can be carried out autonomously as in the case of the SBR system. Simulations are also performed intending to design new units as suggested by Orhon et al. (2005), or improving existing systems before on-side implementation, and hence, reducing expenditures of experimentation (Oles & Wilderer, 1991; Casellas et al., 2008). When simulating, some biological conversion cannot be considered by the modeler, according to the simulation objectives. For example, a modeler could decide to turn off biological conversion that takes place during settling, draw and idle phase, intending to optimize the computational resources, producing that the concentration of the end of a cycle is remains the same for the next cycle, i.e. the previous stage feeds the next stage (Orhon et al., 2009).

- **SBR SIMULATORS**

There are a wide range of simulators from general purpose and specific wastewater treatment, every simulation has its own graphic user interface, different reactor types, but also different way to manage and control the SBR simulations. Thus, it will be present as follows general characteristics of SBR simulators for wastewater engineering treatment.

Closed structured programs provide predefined blocks for complex WWTP, but the user has no high degree of freedom for changing the kinetic and stoichiometric processes. Most of the simulators bring free tutorials available on YouTube platform. For instance, SIMBA ® software integrates the complexity of the SBR phases and conditions (e.g. transitions) by means of an operative condition matrix (programable SBR control) and the Petri net (programable block control) that turn on or off those external operative conditions. Phases/states such as filling, mixing, aeration, settling, drawn and idle are performed by the signal of the operative condition panel, which is a matrix for the SBR control, that activates with a value of 1 or deactivate with a value of 0 pumps, stirs, and aerators. While the Petri net are programmable blocks that manage states (e.g. aerating) and transition conditions (e.g. idle). States are turned on or off, and transitions allow time delay and external operation between phases and are also subjected by external conditions. When all the conditions are met SBR operates (Ifak Magdeburg, 2020). Another SBR simulator is WEST Software, which also provided tailored programs which facilitated the changes of operational conditions of the SBR process (Larrea et al., 2007).

GPS-X ® software (Hydromantis, Hamilton, Canada) allows to simulate the treatment of municipal and industrial SBR systems, which facilitates dynamic modeling as well as sensitivity analysis (Filali-Meknassi et al., 2004). This software involves various libraries for selection of the mathematical models (according to the type of wastewater to be treated), and the configuration of nutrient removal either C, or N or P. In this software SBR simulations are achieved by means of simple and advanced reactor configurations. The former present a fixed order of operations and phases, same time, and unique sequencing, while the latter allows to include more flexible characteristics for more complex systems as intermittent cycle extended aeration system (ICEAS) and cyclic activated sludge systems (CASS). This software allows flexibility of simulations, and code is customizable in GPS-X by programming ACSL or Phyton lines for no sequencing and sophisticated phases of treatment. This simulator brings the possibility of time shifting configuration for multiple SBR systems in parallel operation to delay the beginning of the SBR cycle (Snowling, 2020).

BIOWIN ® software is a use-friendly Windows-based package founded on modeling principles of IAWQ models that ties together biological, chemical, and physical process models that are undergone in the influent, primary settling, biological, side stream, anaerobic digester, physicochemical-process. This software reduces the extensive knowledge of influent characterization of activated sludge models since the modeler can use actual measured data directly as input parameters (e.g. TSS, COD. BOD_5, TN, TP) and BioWin will accept this data and translate it to ASM model parameters or fractionations (e.g. X_I, X_S, S_S, S_I, S_F, etc.). BioWin version 6.2 allows users to simulate the next available SBR system types: single-tank, SBR with prezone tank (buffer tank), and SBR with two prezone tank reactors.

- ## SBR MATHEMATICAL BIOREACTOR MODEL

As follows it will present some implications of SBR system simulations for transport and transformation relations based on mass balances, as well as simplification for size-, time- and microbiological-scales.

Based on mass balance equations transport and transformation process are related. To exemplify it substrate consumption (C) and microbial growth (X) mass balance expression will be presented from SBR systems (Oles & Wilderer, 1991). Where C_O and V_O represent the initial substrate concentration and static (initial) reactor volume.

$$\frac{d_C}{d_t} = \frac{Q*(C_O - C)}{V_O + Q*t} - r \quad \textit{Equation 1}$$

$$\frac{d_X}{d_t} = \frac{-Q*X}{V_O + Q*t} + r \quad \textit{Equation 2}$$

As shown before, those equations differ from continuous AS processes, since the exchangeable volume (V_t=Q*t) varies with time during filling and drawn phases. When the SBR system is full, then influent (Q) is equals to zero (Q=0), and the substrate consumption and microorganisms' growth are described by the process transformation rates (r) (Oles & Wilderer, 1991). As stated before, the transport description changes according to the reactor type (first term at the right term of the equations) and remains similar for the transformation rates independent of the reactor type (r, second term at the right term of the equations).

SBR and intermittently aerated reactors present inherent dynamics (time scale-approximation) of pollutants transformation, thus mostly they are not well represented by steady-state models (Rieger et al., 2012). i.e. concentration of components, such as particular readily biodegradable substrate, NH_4^+, NO_3^-, and NO_2^-, change during each SBR cycle, and hence SBR should be simulated as dynamic state rather than a steady-state process. Dynamic states system is strongly suggested by Ky et al. (2001) due to the high effectiveness in the calibration process of a cheese factory wastewater with SBR systems. However, some authors suggest that under constant inflow feed and composition dynamic systems tend to reach a "quasi steady-state" or also called "pseudo steady-state" condition. For instance, Orhon et al. (2009) suggested that SBR system reaches cyclic pseudo steady-state condition, under constant influent and operational conditions after 2 SRT, were considered to equalize short-term variations. Ky et al. (2001) suggested 3 SRT to pseudo steady state. BIOWIN 6.2 SBR user notes suggest not only tracking 3 or 4 SRT but also viewing the TSS response due to the difficultness of SRT calculator in SBR systems. Rönner-Holm et al. (2006) found steady-state conditions in the SBR system after 140-200days of operation. While Casellas et al. (2008) has set an establishment condition (pseudo steady state) at 100 days. On the other hand, time step-approximation of simulation is another important variable to consider since loss of pollutants response are difficult to analyze. Filali-Meknassi et al. (2004) proved 0.001d, 0.003d and 0.005d for time steps during simulation of SBR for slaughterhouse effluents from the meat industry and concluded that lower values present no important changes in the final results but higher values difficult the visualization of the idle and purging phases.

In conventional ASM the size scale-approximation is based on assumption of whole well mixed reactor (or CSRT) and not on small scales. Which means that size scale approximation includes the whole completely mixed system (henze et al., 1987).

The microorganisms scale-approximation depends mainly on the nutrient removal target, for instance, for carbon removal much attention should be paid to heterotrophic microorganisms with black box or biokinetic models. Biokinetic are suitable for carbon and nitrogen removal and some industrial applications such as meat industry, and metabolic or crystal-box models for carbon, nitrogen, and phosphorus, as well as for a wider range of industrial application.

- **SBR SETTLING MODEL**

As in continuous AS systems settling tanks provide solid-liquid separation by solids clarification, thickening and storage. TSS in SBR system of domestic effluent is sometimes neglected from simulation studies, but in some industrial effluent is important due to sensibility for filamentous bulking bacteria growth due to nutritional disbalances.
TSS is modeled either by means of empirical equations or by the solid flux theory calculations. The solid flux theory is one of the most applied settling model approaches in AS systems. This theory states that during settling the flocculent suspension presents a distribution of different settling zones, which have certain solid-handling capacity, and that the clarification process is driven by gravity settling and solid wastage underflow forces. Those forces are expressed mathematically as liner function of two terms: solid concentrations, and settling and underflow velocities (Makinia & Zaborowska, 2020). Flux theory has been developed 1-D (dynamic models) and 2D (hydraulic) settling models. A common approach to solve the continuity equation is by discretizing the clarifier in horizontal layers of equal height, while sludge concentration is assumed to be constant. The occurrence of biological process in the secondary clarifier is also possible but is most relevant for large scale continuous AS systems, since arising of nitrogen gas would arise some sludge particles (Makinia & Zaborowska, 2020).

For SBR system another approach is presented by BioWin 6.2 that divided the discretized layers in sub cells. The software must solve a flow balance to determine how flow moves through the entire cells number, in all direction possible. For calibrating the settling model, users are prompted to adjust the up-flow fraction of sludge transport to calibrate the potential of flow pathway transport.

4.2.4. CALIBRATION

Treating different industrial applications have demonstrated that influent fractionation (from data characterization) and ASM parameters are not universal, even between the same industry, and thus, both must suffer adjustments and estimations that are called calibration (Makinia & Zaborowska, 2020). Thereby, calibration is defined as an adjustment to enhance the good of fitness (best-fit set) between predicted variables output (simulations) and a certain set of actual measured data (reality) within an acceptable criterion (Gernaey et al., 2004; Meijer & Brdjanovic, 2012; Makinia & Zaborowska, 2020). Some degree of calibration is required to accurately predict system performance characteristics such sludge production, effluent composition (e.g. Nitrification, Denitrification), oxygen requirements, internal concentration dynamics, among others (Gernaey et al., 2004; Melcer, 2004). Calibration is the most time-consuming stage of any simulation project and should be carried out with thorough attention especially when parameters are selected from literature (Brenner, 2000).
Methods for determining influent wastewater characteristics and ASM parameters for calibration can be divided into two main categories: direct measurements using analytical techniques ("standard methods") and bioassay methods (e.g. respirometric analysis).

- **DATA CHARACTERIZATION (INITIAL CONDITIONS)**

Data characterization (influent characteristics) is determined mostly by means of analytical techniques that requires extensive measurement campaigns and lab-scale experiments, and is from paramount importance since potential error on flow measurements, sampling and laboratory analysis can lead to an uncertain data quality and unjustified adaptation of the model parameters (Makinia & Zaborowska, 2020). Data characterization plays an important role in the context of industrial wastewater since those effluents present a special fractionation in comparison with domestic wastewater.

Wastewater characteristics refers to the partitioning of influent organic material into soluble/particulate and biodegradable/inert portions (components) from carbon, nitrogen and phosphorous mostly, e.g., influent total nitrogen into ammonia (inorganic) and organic nitrogen and so on. Also, other parameters are considered such as nutrient balances ratios (as COD/N, COD/P), pH, buffering capacity (alkalinity), etc. (Orhon et al., 2009). This influent characterization is mostly determined based on filtration methods to discretize particulate from soluble components e.g. slowly degradable COD (X_S, which is adsorbed or entrapped in the solid phase). To dig deeper into the general influent characterization components readers are suggested to review table 6.9 from Makinia & Zaborowska (2020) that explains the influent fractionation of wastewater according to the STOWA guidelines. Meijer & Brdjanovic (2012) explain in chapter 7 how is the influent fractionation by the STOWA guidelines performed and exemplify in chapter 8 the fractionation stepwise procedure.

- **CALIBRATION PROCEDURE**

ASMs parameter adjustment can be meet by two model calibration procedures: System engineering (e.g. dynamic sensitivity analysis) and process engineering (ad hoc' tuning, based on modeler expertise), where the former relies purely on mathematical optimization algorithms, and the later understanding the process, model structure and "trial and error" adjustments (Gernaey et al., 2004). The system engineering approach is problematic due to the complexity of unidentifiable variables of many non-linear equations, for instance, the dead-regeneration concept, while process engineering requires a considerable level of expert knowledge.

In process engineering calibration parameters are adjusted one by one, based either on modeler expertise or static sensitivity analysis (where is defined which parameter should kept under control), and following predefined (rational) stepwise procedure of calibration protocols until reasonably fit or acceptance criteria is achieved regarding measured data (Rieger et al., 2012; Makinia & Zaborowska, 2020). According to Meijer & Brdjanovic (2012) with aid of protocols the complex calibration stage becomes a reproducible exercise beginning by default parameters simulations, additional parameters adjustment based on the application, and mass balance for checking measured data.

4.3. CONCEPTUAL FRAMEWORK

When there are no good results among simulation values and experimental data (e.g. commonly with sludge wastage rates), this usually indicates that the system required either a specific modification of the biological parameter, proper influent characterization, by means of new data gathering campaigns, or physicochemical process considerations (Melcer, 2004; Rieger et al., 2012). Due to the large number of possible biological parameters to modify Andreottola et al. (1997) and Makinia & Zaborowska (2020) suggested that the problem should be dividing in subproblems (subsets) by the metabolic base as: Heterotrophs, hydrolysis, nitrification, phosphorus removal, settling and stoichiometry (yields, fractions. etc.), which is the way in which parameters within a software are organized. But always remembering that the "better" simulation is achieved when the less and basic parameters are changed (Artan et al., 2002). There are some parameters that are dependent on the influent characteristics such as: COD fractions, maximum growth rate of nitrifiers, one example of an independent parameter is the maximum growth rate of heterotrophs, which also depend on the feed patter and load. It is known that one parameter is independent when little variation from waste to waste is shown (Henze et al., 1987).

4.3.1. SBR INDUSTRIAL WASTEWATER CALIBRATION

Denitrification rate should be set up with a switching function since nitrification rate depends on the aerobic or anaerobic conditions due to the electron acceptor requirements. Oles & Wilderer (1991) suggest a switching function that depends on oxygen concentration, nitrates, and $K_{O,H}$. They also found that the maximum growth of heterotrophic bacteria was 11d^{-1} for SBR systems, while for continuous system this value is as low as 1.5 d^{-1} (Oles & Wilderer, 1991). Switching functions are used when simulation produces unrealistic values that could be reduced by the limiting switching functions (Oles & Wilderer, 1991).

4.3.2. SBR MEAT INDUSTRY WASTEWATER CALIBRATION

Andreottola et al. (1997) have studied pre-screened piggery wastewater using a bench scale SBR system for biological nitrogen removal. The calibration step was proved based on sensitivity analysis for NH_4^+-N, NO_3-N and NO_2-N variables by means of 2 track studies for calibration phase and 2 for validation phase. Authors have added a nitration kinetic switching function to the used ASM1. 13 parameter values between rates, coefficients, and factors, which slightly differ from domestic applications. Additionally, a piggery effluent was treated in a SBR by Tilche et al. (2001) based on a past study of Andreottola et al. (1997), the process has been modelled and calibrated to enhance the good-of-fit evaluations, allowing 98% of COD, N and P removal by adding a switch function that simulates the toxic effect of ammonia on the nitratation step in MATLAB-SIMULINK platform. Influent characterization, kinetic and stoichiometric parameters were analyzed by respirometric bioassays. Through simulation the aeration time changes from 2h to 1.5h.

4.3.3. PARAMETERS FOR RENDERING CALIBRATION

Nowak et al. (1996) have investigated meat rendering effluent (7000mg DOQ/L and 1100 mg TKN/L) in continuous AS with high NO_2^- and low phosphorus concentrations (0.2mg PO_4^{3-}/L, which lead into phosphorous deficiency that is required for nitrobacter microorganism). Authors have found a yield Y_{PO43-} of 0.016 gP/gCOD, X_{S1} of 0.03 and X_{S2} of 0.002 gP/g COD, half saturation K_{PO43-} for ammonia oxidizers in rage of 0.01-0.05 mgP/L, $K_{i-PO43-}$ for nitrite oxidizers of 0.2 mgPO_4^{3-}-P/L; μ_{max} of 1.8 d^{-1} and b at 0.06 d^{-1} of ammonia oxidizers; K_{I-NO2} of 1.2 mgNO_2/L for denitrification.

Nakhla, Liu & Bassi (2006), have treated meat rendering wastewater in continuous AS have found substrate consumption rate of 1.47-4.86 mg COD/mg VSS-d; μ_H 0.45-2 d^{-1} and b of 0.05 d^{-1}; K_S of 17.7-61.3 mg COD/L, Y of 0.135-0.416 mg VSS/mg COD. In this document are also suggested correction of modelling for biomass growth by Haldane (inhibition) model and hydrolysis by Monod's models and k, K_s, Y, K_i and K_H parameters are presented. Also, authors stated that the high oil and grease caused 57-70% of degradation rate reduction in apparent biomass soluble COD.

5. MATERIALS AND METHODS

The methodology will follow the recommendations from IWA task group on good modelling practices (GMP) presented in the unified protocol for using ASM by Rieger et al. (2012), one of the most extensive consensuses on wastewater simulation protocol that clumps together protocols such as BIOMATH, STOWA, HSG, WERF, among other guidelines (Makinia & Zaborowska, 2020). This simulation guideline was evaluated in more than 100 domestic wastewater plants and upgraded industrial effluents as a soy sauce plant that was composed of bean processing, brewing, and bottling (Rieger et al, 2012). Gather data were used from the master thesis of Rodriguez et al. (2011) that aimed to evaluate experimentally the removal of carbon and ammonia-nitrogen efficiency of a SBR pilot system for the wastewater treatment of a rendering plant in Amaga, Antioquia, Colombia.

5.1. PROJECT DEFINITION

The meat industry sector is composed of agriculture (livestock or intensive animal farming) and industrial activities like slaughtering, packing, transport, preservation, marketing of primary products, and meat rendering (Woodard, 2006). Meat rendering transforms waste material (by-products) from meat industry activities to useful products such as: animal feed additives like meat and bone meal, blood meal, hydrolyzed feather meal, among other protein meal, as well as raw material for animal feed supplements (livestock, poultry, aquaculture, and pets), soaps and rustproofing paints. According to Meeker & Hamilton (2006) after slaughtering up to ⅓ to ½ of each produced animal is not consumed by humans, and thus, by-products as blood, paunch, leather, hide, fat, bones, etc, have a huge potential to be reused on a circular economy way.

5.1.1. SITE DEFINITION

Data for this study were taken from the rendering protein recovery plant: Agropecuaria San Fernando S.A (AGROSAN, yellow dot in Figure 2) from Amaga (blue dot in Figure 2), Antioquia, Colombia (06°03'N, 75°41'O), which is located at 1496m MSL, and mean temperature at 21°C.

Figure 2. Rendering plant location.
Source: Own elaboration based on software Google Earth Pro (2023).

The rendering company produces meal and fat products for animal-feed from meat by-products as viscera, feathers, blood, tallow, bone, and fat, which originate from cattle and pigs' slaughterhouses, chicken slaughter farms, and the meat industry sector. The company offered 7 products: Meat meal, blood meal, bone meal, chicken viscera meal, hydrolyzed feather meal, chicken oil, and industrial tallow.

5.1.2. PRODUCTION PROCESS

The process begins with coarse by-products pre-breaking and grinding, afterwards materials (e.g. viscera) are washed for manure removal. Then, is followed by material hydrolysis in the cooker batch systems (i.e. by steam contact) that sterilize, break molecular bonds, and separates and realizes lipids. The solid phase then goes through a drying, pressing and grinding process to finally obtain visceral, meat, bone, and hydrolyzed feather meal. While the liquid phase goes through a centrifugation process, where high melting fats, emulsifying (fine grinding), and liquids are separated from solid remnants and then washed out to obtain lipids such as oil or industrial tallow. Unlike the previous products, prior to centrifugation, for blood meal production a coagulation process is carried out at a high temperature, then the materials are conveyed through a centrifugation process that separated the solid and liquid phases. Finally, the gathered liquid phase (the condensate) from the centrifugal step, which stays at high temperatures, condensates in the wet scrubber, also known as a vapor washing, that decreases its temperature (cooling process).

5.1.3. ANALIZED SBR WASTEWATER

The entire rendering plant generates an average flow of 5.52 l/s (476.928m^3/d), which are divided into four types of influents (Figure 3): housekeeping (1.7 l/s), condensate (2.5 l/s), plasma (0.8 l/s) and domestic wastewater (0.52 l/s). The major source of housekeeping effluent is produced from raw material washing, followed by equipment cleaning (e.g. cookers, mixers, grinders, and emulsifiers) and from machinery, floor, and container cleaning operations. On the other hand, condensate wastewater is produced from stick wastewater (liquids and solid materials), after being in a gaseous state in the centrifugal step (cyclone). In this study only the Housekeeping (Figure 3-1) and condensate (Figure 3-2.1) effluent will be a matter of study, and thus the boundary condition is represented by the red rectangle on Figure 3, i.e. plasma (Figure 3-3) and domestic (Figure 3-4) influent will not be analyzed, as presented by the cross red marks.

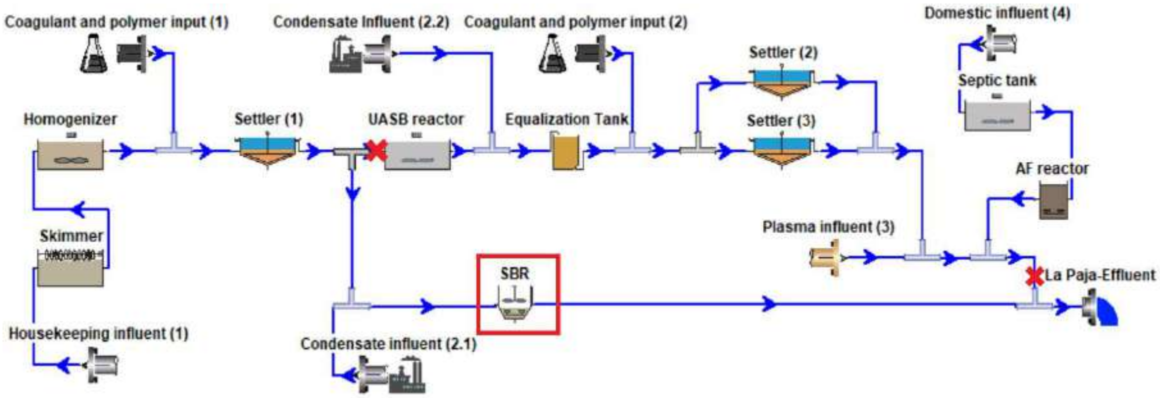

Figure 3. Liquid line production scheme of the whole rendering plant and SBR location, the SBR system treats the pretreated Housekeeping (1) and Condensate (2.1 and 2.2) influent on a differential load basis. The red square depicts the control volume of analysis.

Source: Own elaboration using BioWin-6.2 software ®.

From the total housekeeping (1.7 l/s), and condensate wastewater (2.5 l/s), only 0.025 l/s were analyzed in the SBR system since this is the maximum hydraulic load capacity of the SBR system. The half volume of reaction capacity of the SBR is equals to 0.733m^3 per cycle (skin color portion in Figure 4) and the system will treat 3 cycles in one day, which is equals to 2.19m^3 of volume capacity per day (or 0.025l/s).

- **DIFERENTIAL OVERLOADING STAGES**

The meat rendering facility, matter of study, combine the housekeeping and condesate wastewater in an existing UASB, but this system did not meet the pollutant standards specially for nutrients removal such as nitrogen, and thus, the new SBR system must be analyzed to remove nitrogen from this industrial effluent. Additionally, the SBR system operates for eight different overloads stages, i.e. changing the percentages of housekeeping and sticking wastewater in a lumped matrix. Initially, the system was fed with a composition of 100% to housekeeping procedures and 0% stick wastewater. Then, the housekeeping wastewater is reduced, and the stick wastewater is increased progressively, and so on, until reaching the eighth differential stage, compound of 0% housekeeping and 100% condensate wastewater, as presented in Table 1.

Table 1. Operational overloading stage of the SBR system with housekeeping and stick wastewater.

Stage	Time of operation (d)	Mix ratio	
		Housekeeing wastewater (%)	Condensate wastewater (%)
I	0-21	100	0
II	22-43	100	0
III	44-77	100	0
IV	78-98	90	10
V	99-154	80	20
VI	155-189	50	50
VII	190-231	30	70
VIII	232-252	0	100

Source: Own elaboration based on Rodriguez et al. (2011).

5.2. DATA COLLECTION

Data collection and reconciliation consists of SBR physical parameters, cycling, existing data collection (State/Total approach), data analysis and processing, and influent fractionation (Fraction approach/Driven function). From the simulation point of view, data analysis, processing, completion, and influent fractionation are extremely necessary for the right calibration stage.

5.2.1. SBR PHYSIC PARAMETERS

The fiberglass SBR system had 2.92m^3 of volume capacity, a controlled PLC system that turns-on or -off the equipment parts as: The submerged aerator, pump, and stirring system. The pre-settling (coarse settling tank, or buffer tank) and the reactor tanks were connected by means of an elbow tube that transported the solids from one to another tank by communication vessels. The influent had a 1” PVC pipe with a downward elbow to discharge the wastewater in the pre-settler compartment. While the effluent is withdrawn first by a 25mm PVC tube and coupled then to a 1” PVC pipe that discharges the effluent. Each compartment had two 2” PVC purge pipes, with shutdown valves in the SBR bottom. The separating inner wall was 0.08m thick and 1.3m high. At next, will be explained the pumping, aeration, automation equipment, and SBR dimensions.

The SBR system was equipped with a NOVA180 pump (220-240 V/50 Hz) that conveys the influent, and effluent, while the underflow is activated and controlled by a shutdown valve. This is an automatic operation device for turbid and fiber-free water and is equipped with a float switch for automatic on/off control. The aerator AQUA200 (220-240, V/50Hz, 0,3HP, 330W, 1.5A) was used to blow air into the treatment. The pump body, head and propeller are wrapped by a techno polymer for thermal motor protection. The system was operated under a programmable logic controller (PLC) (ATB a 110-230V~50/60Hz, 1600 VA IP65), the PLC device controls a maximum of one: pump, aerator and stirring system. The controller is compound of a display, four buttons and two led light signals. The display can record the operative data in a log-storage format.

Figure 4 shows the diagram of the SBR system, as well as the diameters of the inlet (1”), outlet (1”) and sludge wastage pipes (2”), thickness of the reactor (0.08m) and diameter of the control cover (0.9m). The SBR system has a total surface area of 2.24m^2, maximum volume capacity of 5.61m^3 (delimited by the white, dark yellow, skin, and brown color spaces Figure 4), utile volume of 2.92m^3 (without the white portion), 1.46m^3 of reactor volume (the skin and brown portion), and 0.733m^3 of stationary volume (brown space).

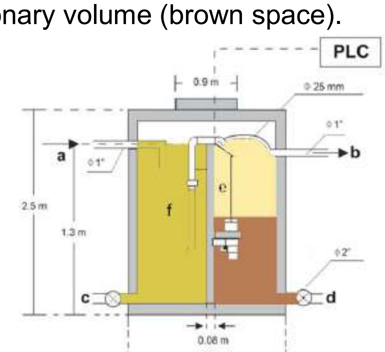

Figure 4. SBR system, dimensions of (a) inlet, (b) outlet, (c & d) purge valves, (e) suction tube for filling the SBR through communicating vessels, (f) coarse particle separator and homogenizer. Source: Rodríguez et al. (2011).

5.2.2. SBR CYCLING OPERATION

The cyclic operation is formed by filling, reaction, sedimentation, drawn and idle (Figure 5), three times in the day an 8h cyclic is repeated over and over again. The filling stage lasts 35min, in which every 2h of the reaction phase one third of filling pulse is pumped into the system (0.244m^3). As follows, six hours of reaction phase consisting of 8min of intermittent aeration and 15min of stirring without aeration. The underflow is carried out 15min before the aeration ends. Finally, the remaining 2h the sedimentation is carried out, as shown below in Figure 5. The decanting phase (5min) was very fast because a pump performed the procedure.

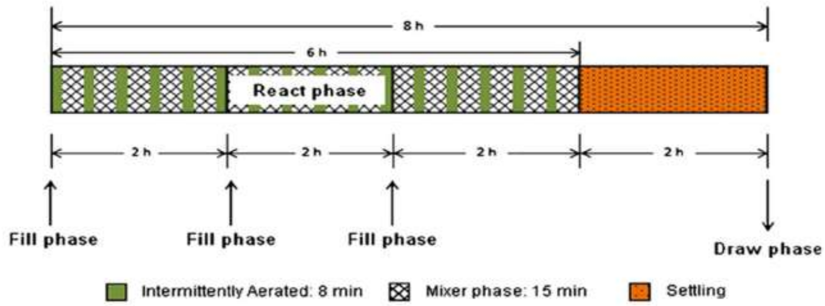

Figure 5. Schematic diagram of the SBR operation cycles.
Source: Rodríguez et al. (2011).

5.2.3. EXISTING DATA COLLECTION

As follows it will be presented the analytical techniques, and state variables from the input, sludge, and effluent (yield) data. The original state variables for this project were gathered by Rodríguez et al. (2011) for a series of 50 daily data samples taken over 8.4 months at the meat by-products plant. The load conditions of the washing and concentrated wastewater of the plant were changed through mixing rates and the averaged mixed composition in Table 1.

- **ANALYTICAL TECHNIQUES**

In 2008 the wastewater samples were collected, preserved, and transported to the research group GDCON (Grupo Diagnostico y Control de la Contaminación) from the Universidad de Antioquia. Analytical techniques are shown in Table 2 for the determination of contaminating parameters on input data, pre-settling tank, reactor tank, and effluent are presented below based on standard methods 16th edition from APHA et al. (2005).

Table 2. Analysis techniques for the determination of investigated parameters.

Type of phase	Parameter	Unid	Methodology	Source
Liquid phase (influent, effluent, underflow)	BOD_5	mg/L	5210 B	Standard Methods [21]
	COD_T	mg/L	Closed reflux (colorimetric method - 5220 D)	
	COD_F	mg/L	Closed reflux (colorimetric method - 5220 D)	
	N-TKN	mg/L	2540 F	
	N-NH_4^+	mg/L	ion chromatography (2540 F)	
	N-NO_2^-		ion chromatography (2540 F)	
	N-NO_3^-	mg/L	ion chromatography (2540 F)	
	PO_4^{3-}	mg/L	ion chromatography (2540 F)	
	SO_4^{2-}	mg/L	ion chromatography (2540 F)	
	pH	-	potentiometric (4500-H^+ B)	
	Temperature	°C	2550 B	
	DO	mg/L		
	Conductivity	mS/cm		
Solid phase (Biomass)	TS	mg/L	Gravimetric and dried at 103-105°C (2540 B)	Standard Methods [21]
	VT	mg/L	Gravimetric and dried at 550°C (2540 C)	
	TSS	mg/L	Gravimetric, microfilter, and dried at 103-105°C (2540 D)	
	VSS	mg/L	Gravimetric, microfilter, and dried at 550°C (2540 E)	
	SVI	mg/L		Standard Methods [195]
	SV	m/h		

Source: Own elaboration based on Rodríguez et al. (2011)

The original set of data of Influent and effluent is composed by the next series of analytical parameters: COD, BOD_5, NH_4^+-N, NO_2^--N, NO_3^--N, PO_4^{3-}, SO_4^-, pH, Temperature, conductivity, and sludge composition by TS, VS, TSS, VSS, SVI index. The FOG parameter was not recorded, and thus, it will not take into account for this simulation project.

- **ORIGINAL INPUT DATA**

Table 3 presents the inflow composition of stage II from the industrial effluent. The composition of stage II mostly composed by housekeeping activities shows that carbon and nitrogen nutrients are still high in proportion to domestic wastewaters, which is expected for industrial effluents. The COD/TN ratio in this case is equal to 18, which is a high and favorable value that suggested biological wastewater treatment. Values like Sulfur (S), Alkalinity, Calcium and Magnesium will be explained in numeral 5.2.4 data processing (missing data completion).

Table 3. Influent composition-Analytical results for stage II.

PHASE	DATE (d)	TCOD (mg/L)	CODF (mg/L)	BOD5 (mg /L)	NH4+ (mg/L)	NO2- (mg/L)	NO3- (mg/L)	PO4-3 (mg/L)	SO4- (mg/L)	pH	T (°C)	conductivity (uS/cm)	TSS (mg/L)	VSS (mg/L)
PSEUDO-STEADY STATE	0	6566.67	5511.11	5340.00	364.34	0.02	1.02	223.87	42.71	6.46	24.60	2.04	740.00	680.00
STABLE RESPONSE	23	10383.33	4425.00	4202.30	534.70	0.02	1.28	45.91	100.40	6.57	25.50	4.12	2170.00	930.00
	28	7391.00	2502.30	1473.33	534.70	0.02	0.80	< L.D	168.57	6.60	26.50	1.99	1400.00	1270.00
	35	7505.43	2419.65	1529.54	522.65	0.02	0.93	0.00	132.87	6.32	0.00	3.01	2019.00	1154.87
	43	6940.00	2703.10	1106.67	522.03	0.02	0.00	< L.D	24.68	6.00	24.70	2.33	770.00	710.00

Source: Own elaboration based on Rodriguez et al. (2011).

The sludge composition presented in Table 4 that is originated from the domestic WWTP "San Fernando", the first of the three WWTP located in the Aburra valley, Antioquia, Colombia. The SSV/TSS ratio is equal to 85%, which is a typical value for domestic wastewater. The sludge volume index (SVI) was 142ml/g (moderate settleability) that is an "acceptable" to form a good sludge blanket in continuous AS and SBR systems (Olsson & Newell, 1999). However, in countries like The Netherlands this value of SVI over 120 ml/g is commonly consider as a bulking sludge volume index (Chen et al., 2020).

Table 4. Initial sludge composition and SVI index of San Fernando sludge sample.

Type of phase	Parameter	Unid	Value
Solid phase (Biomass)	TSS	mg/L	1265
	VSS	mg/L	1075
	VSS/TSS	-	0.85
	SVI	mg/L	142.97
	SV	m/h	3.36

Source: Own elaboration based on Rodriguez et al. (2011b).

Total data effluent of SBR system treatment is present in Table 5. In this case, and different from influent, all the possible state variables are presented to compare during the calibration process.

Table 5. Effluent composition-Analytical results.

PHASE	DATE (d)	TCOD (mg/L)	CODF (mg/L)	BOD5 (mg/L)	NH4+ (mg/L)	NO2- (mg/L)	NO3- (mg/L)	PO4-3 (mg/L)	SO4- (mg/L)	pH	T (°C)	conductivity (uS/cm)	TSS (mg/L)	VSS (mg/L)
PSEUDO-STEADY STATE	0	2233.33	1673.30	1177.78	341.28	0.61	0.60	40.62	11.40	6.99	25.10	2.65	630.00	600.00
STABLE RESPONSE	23	2300.00	802.30	675.00	229.50	0.02	0.60	2.00	164.76	7.73	31.50	5.21	693.30	533.00
	28	1006.67	602.30	340.00	256.56	0.02	0.79	2.00	174.99	7.70	29.00	2.87	750.00	680.00
	35	1294.21	709.56	384.32	267.32	0.02	0.64	2.00	171.76	7.65	0.00	3.60	799.00	598.00
	43	840.00	803.10	206.67	309.02	0.02	0.32	2.00	144.39	7.79	26.60	2.86	420.00	400.00

Source: Own elaboration based on Rodriguez et al. (2011).

5.2.4. DATA ANALYSIS AND PROCESSING

Prior to simulations it is suggested data analysis to define the period of analysis of simulation, filter out possible errors, evaluate the raw data, and prove data quality and reliability by the respectively methods: Graphics, outlier detection, sanitary checks(pre-checks), mass balances calculations (data reconciliation), among others. This data analysis will be presented for the HKWW, and for the CWW the same process is followed but not presented.

For right BioWin influent and STOWA fractionation processing input missing (gap) data must be completed, because BioWin prompts state variables (total approach) like TKN, TP, Alkalinity, Calcium and Magnesium, and other additional fraction as S_A that are required for the STOWA fractionation, which were not sampled in the data collection campaign, and therefore, those variables must be approximated (supposed) from similar studies to full fill the input feed data.

- **INPUT MISSING DATA COMPLETION**

Housekeeping missing data will be approximated from slaughterhouse wastewater due to the similarity in composition, in both cases activities such as carcasses washing to remove manure, washing-up of equipment, and that trucks and blood waste are mixed in the collecting channels. However, for the condensate missing data Metzner & Temper (1990) suggest do not take as a reference the slaughterhouse wastewater since the manure contain differ between them and will not be comparable. Therefore, missing condensate data will be taken from another rendering condensate wastewater as presented next.

- **APROXIMATIONS FOR BOTH HOUSEKEEPING AND CONDESATE INFLUENT**

TN is computed as the addition of the organic (e.g. TKN) and inorganic nitrogen species (e.g. NO_3^- and NO_2^-). Consecutively, the TKN value is calculated as the addition of nitrogen in biomass, total organic nitrogen, and ammonia. The biomass nitrogen is neglected from the NTK computation due to the small number of microorganisms at the influent for both housekeeping and condense wastewater. While the organic nitrogen will be computed as 16% of the total protein content (also for both effluents), which is the theoretical ratio suggested by Mariotti et al. (2008) and used in the specific rendering studies of Hansen & West (1992) and Brennan et al. (2021). The protein content was measured during the samples campaign of Rodriguez et al. (2011), therefore, the NTK was computed as 16% of the protein content plus the NH_4^+ concentration.
Missing housekeeping effluent will be adopted from a slaughterhouse effluent. According to the study of Filali-Meknassi et al. (2004) treating slaughterhouse effluent (5098 mgCOD/L, 370 mgTKN/L and 87 mgTP/L), the PO_4^{3-} content from TP is equals to 52.8% (i.e. TP is 1.89 times the PO_4^{3-} concentration or 46 mgPO_4^{3-}/L), and the alkalinity concentration was 585mg $CaCO_3$/L (5.85 mmol/L). On the other hand, in the study of Hansen & West (1992), authors present that rendering cleaning effluent is composed of 26 mgCa^{+2}/L, and 7mg Mg^{+2}/L. Finally, Ng et al. (2022) suggested that the S_A value (in form of VFAs as acetate) was found to be around 330mg Acetic acid/L, i.e., the S_A/COD ratio could be found as the division of 500mg Acetic acid/L divided by 31200mg COD_T/L.
From the full physicochemical characterization study of a rendering condensate effluent by Brennan et al. (2021) (10813mg COD/L, 1630mg TKN/L, 51mg TP/L), the missing data of the actual rendering plant will be adopted. Brennan et al. (2021) found that the PO_4^{-3} content from TP is equals to 41% (i.e. TP is 2.44 times the PO_4^{3-} concentration or 21 mg PO_4^{3-}/L), also found a sulfur concentration of 10 mg S/L, 10.9mg Ca^{+2}/L of calcium, and 0.8mg Mg^{+2}/L of magnesium. On the other, hand Hansen & West (1992) founded for rendering condensate effluent a concentration of <4mg of PO_4^{3-}/L, <1 mg Ca^{+2}/L, <1mg Mg^{+2}/L, which is a typical value for this kind of effluents. Nakhla et al. (2003) have found 5200mg $CaCO_3$/L of alkalinity in rendering wastewater (52 mmol/L). Finally, Brennan et al. (2021) also found that 1519.7 mg Acetic acid/L of $S_{A,}$ (in form of VFAs as acetate) could be divided by 10813mg TCOD/L to compute the S_A/COD ratio.

5.2.5. INFLUENT FRACTIONATION

BioWin software offers the possibility to feed the influent model with analytical data by the "Influent specifier" option. However, an extensive measured data campaign is required to identify soluble and particulates, degradable and nondegradable components not only for carbon species, but also for nitrogen and phosphorous ones, which is not the case for this study. As an alternative, Influent fractionation was carried out following the fractionation methodology of the Dutch Foundation of Applied Water Research (STOWA) protocol that were acquired during the short course (2022) in the IHE institute, the Netherlands, this protocol is also available in Makinia & Zaborowska (2020) table 6.9. Additionally, in the book of Melcer (2004) are available general inflow familiarization and fractionation nomenclature and meaning. Nitrogen and phosphorous fractions (e.g. INS_A, iPS_A, etc) are suggested in Roeleveld & Van Loosdrecht (2002). At next on Table 6, it will be presented the final fractionation for Default, pseudo-steady-state, HKWW (Stage II), and CWW (Stage VIII) that were completed with missing data founded in the literature as presented in numeral 5.2.4

Table 6. BioWin influent fractionation of pseudo-steady-state, HKWW, and CWW.

BioWin Fraction	DEFAULT (Default)	PSEUDO-STEADY STATE (High.Ss)	HKWW (FA)	CWW (FA)
1 (Ss)	0.1600	0.7996	0.3282	0.7857
2 (Sa)	0.1500	0.1758	0.4445	0.1802
3 (Xsp)	0.7500	0.9500	0.9500	0.9500
4 (SI)	0.0500	0.0397	0.0219	0.0434
5 (XI)	0.1300	0.0696	0.5206	0.0713
6 (Fcel)	0.5000	0.9500	0.9500	0.9500
7 (SNH4)	0.6600	0.8716	0.9046	0.9527
8 (XS*iNXS)	0.5000	0.0158	0.0163	0.0008
9 (SI*iNSI)	0.0200	0.0044	0.0021	0.0006
10 (N/COD ratio)	0.0700	0.0700	0.0700	0.0700
11 (SPO4)	0.5000	0.5291	0.2323	0.4098

Source: Own elaboration.

5.3. PLANT MODEL SET-UP.

This step describes the plant model layout, and the general parameters for the SBR system, and pre-running simulation with default parameters to check the hydraulic model and prepare the albums (charts, or diagrams in BioWin), before any formal simulation. Additionally, it will present the reliability assessment of this first attempt at simulation to avoid bias in the other simulations.

5.3.1. PLANT MODEL LAYOUT

With the aid of predefined blocks of the BioWin simulator (i.e. model elements) the plant layout is defined as shown in Figure 6. Predefined blocks as influent, SBR reactor, effluent (decant) and sludge sink were selected from the main toolbar menu. The WAS tank is only a strategy to check the SRT but is not strictly necessary for performing the SBR simulations.

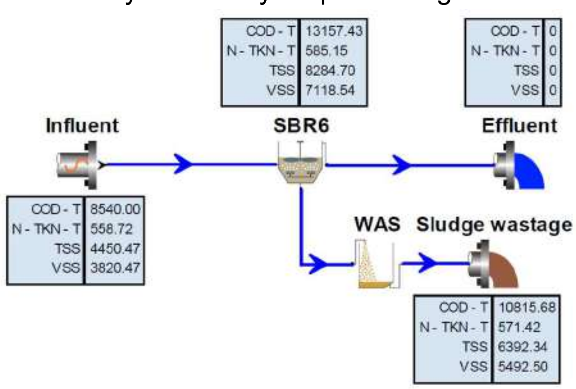

Figure 6. SBR Flowsheet for the Meat By-products plant.
Source: Own elaboration based on BioWin-6.2 software ®

5.3.2. GENERAL PROJECT

The liquid-line description of the current project is based on the mass balances equation managed by the BioWin software that couples together physical process (i.e. transport) and bio-chemical process (i.e. conversion) to describe concentration changes over time.

- **BIOWIN ASDMi**

The microbiological scale (conversion) was defined as the general BioWin Activated Sludge/anaerobic Digestion Model (ASDM) that has more than 50 state variables, and 80 process expressions. BioWin not only simulates activated sludge and anaerobic digestion process, but also models sulfur, chemical precipitation reactions, pH and alkalinity, and Industrial components. The Activated sludge process is compound by growth and decay processes of the next biomass groups: Ordinary heterotrophic (for COD removal and denitrification), methylotrophic (for denitrification using methanol under anoxic conditions), ammonia oxidizing (ammonia gas and ammonium ions, for Nitrification), nitrite oxidizing (for Nitrification), anaerobic ammonia oxidizing (for Nitrification), phosphorus accumulating (Biological phosphorous removal), sulfur oxidizing and reducing biomass. All the biomass groups beginning with a base rate expression (usually the specific maximum growth rate) than is altered (increasing or decreasing) by Monod kinetic and stoichiometry, environmental conditions (D.O, NO_2 or NO_3), nutrient limitations (switching functions of ammonia, phosphate, calcium, magnesium, and ions) and pH limitations.

- **HYDRAULIC MODEL**

The hydraulic model (transport) is selected as continuous stirred-tank reactor (CSTR) as size-scale approximation (whole approach). This model is composed of an influent and two effluents: the decant and sludge sinks as presented in Figure 6.

- **SIMULATIONS OPTIONS**

Due to the dynamic (time-scale) nature of the SBR system pseudo-steady state should be reached before the simulation analysis to avoid vias in effluent results. This state is achieved either around 2 SRT, according to Orhon et al. (2009), or by viewing the establishment of the TSS response in the TSS Vs time graph. Table 7 shows the time of simulation in days, in the way in which the influent must have to be customized in the BioWin influent block to consider the SBR cycled variation, and the simulation phase of calibration either for pseudo-steady-state or stable response. Table 7 shows a value of -39 days that corresponds to the span of time of pseudo-steady-state establishment (2 times SRT) that indicates simulation starts 39 days before the project recording data. Finally, the simulation data interval is set as 5 min for both pseudo-steady state condition, and stable response periods.

Table 7. Simulation points for pseudo-steady-state, stage II, and stage VIII for the calibration of HKWW and CWW respectively.

WASTEWATER TYPE	PHASE	TIME (d)	COMMENT
HOUSEKEEPING	PSEUDO-STEADY STATE	(+39)	Initial polutlant load (2SRT)
	STABLE RESPONSE	23	Pollutlant load change
		28	Pollutlant load change
		35	Pollutlant load change
		43	Pollutlant load change
CONDESATE	PSEUDO-STEADY STATE	178	Initial polutlant load (2SRT)
	STABLE RESPONSE	238	Pollutlant load change
		240	Pollutlant load change
		247	Pollutlant load change
		252	Pollutlant load change

Source: Own elaboration

- **SETTLING MODEL PARAMETERS**

BioWin uses a modified Vesiling model with maximum compactability and clarification switch (Envirosim, 2021). For the simulation purposes the next settling parameters were set as default: maximum Vesilind settling velocity, Vesilind hindered zone settling, clarification switching function, specified TSS concentration for height calculation, maximum compactability constant, maximum compactability slope were respectively of 170 m/d, 0.37L/g, 100mg/L, 2500mg/L, 1500mg/L, 0.01L/mg respectively. The non-reactive option (analysis of ASM during settling to take into account denitrification) is chosen for this study since the pilot SBR system is too small and there is not notable stagnant zones in the reactor.

5.3.3. OPERATIONAL SBR CONDITIONS

The operational conditions are configurated by the SBR dimensions, itinerary setting, aeration, temperature, SRT, influent rates, and sink streams. In relation with SBR dimensions, the minimum decant level (liquid hold-up) was selected as 50% of the reaction tank (0.73m^3, brown portion of Figure 4). The itinerary (cycle) setting was set up as: 8h of cycle length of duration, mix until settling at 6h and draw effluent starting at 7:55h (i.e. 5min at the end of the cycle). Decant flow is computed by the software according to the drawn timespan and the minimum decant level (50%). The aeration method is DO setpoint approach (instead of airflow input), which is set as intermittent itinerary aeration option, i.e., 1.1mg O_2/L for 8min aeration and 15min aeration off over and over again, until 360 min (6 hours), and with a density of diffuser equals to 1. The Diffuser density was set as 0.1% to avoid high rate of aeration that overpassed the set D.O concentration. The operative average temperature value was fixed as 21°C in the Project/Plant/Liquid Temperature option. While the SRT was set as 30 days to promote the growth of nitrifying bacteria (Rodríguez et al., 2011). Three loads from influent flow rates of 0.24333m^3 (⅓ of 0.73m^3) are delivered to the SBR tank at times 0, 2, 4 hours, which means that every 2 hours an incoming flow of 10.01m^3/d is pumped during 35min, similar as scheduled by Oles & Wilderer (1991) and Corominas (2006). This incoming stream is repeated every 8h cycle. Moreover, the HRT is equal to 16h, where the total volume is 1.46m^3 and the inflow is 3 times 0.73m^3/d.

There are two types of sink streams, decant and underflow rates. Decant flow rate (effluent drawn) is set by default calculation by the BioWin simulator software. The program subtracts the current liquid and the minimum decant volume (50% V_R) and computed the necessary flow to discharge the subtraction volume. In this case, the subtraction is 210.24m^3/d in 5min (0.73m^3 drawn volume). It is important to recognize that the lower time of the drawn phase, the shorter settling time occurs, and therefore the lowest TSS effluent concentration will be removed. On the other hand, the underflow rate is related to the SRT, and in a SBR system is computed as the Filled initial volume percentage times the reactor volume divided by the wasted volume times the cycle number (SRT=(%fill*V_r)/(V_w*m)). When the wastage volume is too small and cannot been pumped by the pumping equipment, the wastage sludge is removed every day or even days and not in each cycle (Envirosim, 2021). In this case, the SRT were equals to 30d, 1,46m^3 is the total reacting volume, and 3 times (cycles) the reactor should be filled up, then 0.0487m^3/d or 0.0162m^3/cycle will be wasted as underflow from the mixed liquor volume during the last phase of mixing. To configure the underflow rate in BioWin is than simple as the total reaction volume (V_r) divided by the SRT (0.0487m^3/d), i.e., the last 15min (from 5.75 to 6 hours) of the reacting phase the underflow rate is equal to 0.049m^3/d and the software computes the wastage per cycle (0.0162m^3/cycle).

5.3.4. PRE-RUNNING SIMULATIONS

The pre-running is a quick scan to check the hydraulic model before the pollutants analysis based on default influent and parameters, i.e., after the hydraulic checking, the system set-up is ready to simulate, and thus, it is accepted to perform the first simulation with default parameter (e.g. for HKWW). Additionally, issues related to inflow, underflow, aeration, and albums for plotting results, are also adjusted in the pre-running stage. Pre-running simulations are compound of pseudo(quasi)-steady-state and stable response. The former is set with the selected "seed values option", initiated 60 days before the "Stable response" on stage II and VIII. While the latter is reaching the pseudo-steady state (60 days), the influent load is changed according to the pollutants load presented in
Table 7 and for the HKWW and CWW.
The pre-running configuration is set by means of the the influent characterization of the BioWin software, which is set as total variable approach that is changed in the "Editing influent" window in the influent block. As presented in Table 8, HKWW data are rearranged in the way that users must enter the input data in the BioWin software, and using the state variables (total approach), CWW is not necessary in this case since the hydraulic model is proven only one time. For this pre-running simulation stage, NTK was approximated as the measured NH_4^+, TP as the measured PO_4^{3-}, and finally the Alkalinity, calcium and magnesium parameters were assumed as default BioWin values (domestic wastewater). For this first default simulation attempt there is no missing data change since simulations will perform with default values.

Table 8. Influent composition of housekeeping effluent from the meat by-products plant on Stage II.

PHASE	DATE (d)	TCOD (mg/L)	NTK (mg/L)	TP (mg/L)	S (mg/L)	NO3- (mg/L)	pH	Alkalinity (mmol/L)	ISS (mg/L)	Calcium (mg/L)	Magnesium (mg/L)
PSEUDO-STEADY STATE	0	6566.67	364.34	223.87	10.00	0.12	5.91	50.00	435.00	80.00	15.00
STABLE RESPONSE	23	10600.00	534.70	45.91	10.00	0.73	5.93	50.00	1386.00	80.00	15.00
	28	6306.67	534.70	< L.D	10.00	1.94	6.94	50.00	1200.00	80.00	15.00
	35	8973.33	522.65	0.00	10.00	0.00	6.77	50.00	670.00	80.00	15.00
	43	8540.00	522.03	< L.D	10.00	1.14	6.96	50.00	630.00	80.00	15.00

Source: Source: Own elaboration based on Rodriguez et al. (2011).

5.3.5. GRAPHICAL INFLUENT PERFORMANCE ANALYSIS

To get insight on how to differentiate the simulation response by means of the influent fractionation strategy, it will carry out the graphical performance (effluent) analysis. Thus, three simulation scenarios will be run: Simulations with (1) original inflow (but no missing data) and default influent fractionation, (2) fractionated inflow with the STOWA protocol and (3) average fractionation inflow with STOW protocol for the four points of the HKWW on stage II and four points of the CWW on stage VIII (
Table 7). Those simulation scenarios will be compared to each other, considering the pseudo-steady-state and stable response.

5.4. CALIBRATION

Influent fractionation and default parameters are not enough for most of the industrial applications and acceptable good-of-fit evaluations; thus, calibration and validation are still required. In this project, the process engineering approach is adopted for the calibration as a method to enhance the good of fitness between predicted variables and measured data for the effluent response. The calibration for industrial wastewater will be based on the compilation of past simulation experiences of Melcer (2004), Orhon et al. (2009), Meijer & Brdjanovic (2012), and Rieger et al. (2012) for COD and N removal. The authors have proven that little changes in the influent fractionation, and parameters presented in Figure 7, produces high sensitivity in other parameters response, and thus, the most sensible parameters will be analyzed for this nitrogen removal application. Macronutrient fractions (e.g. S_S, iNs_S, iPx_S) and kinetic parameters (e.g. $\mu_{H,Max}$, $\mu_{AUT,Max}$) are usually obtained from empirical respirometric tests. However, for this project those parameters will be estimated by means of static sensitivity analysis. Finally, the J^2 coefficient will be adopted for the validation to present the change in model efficiency between calibration and validation steps.

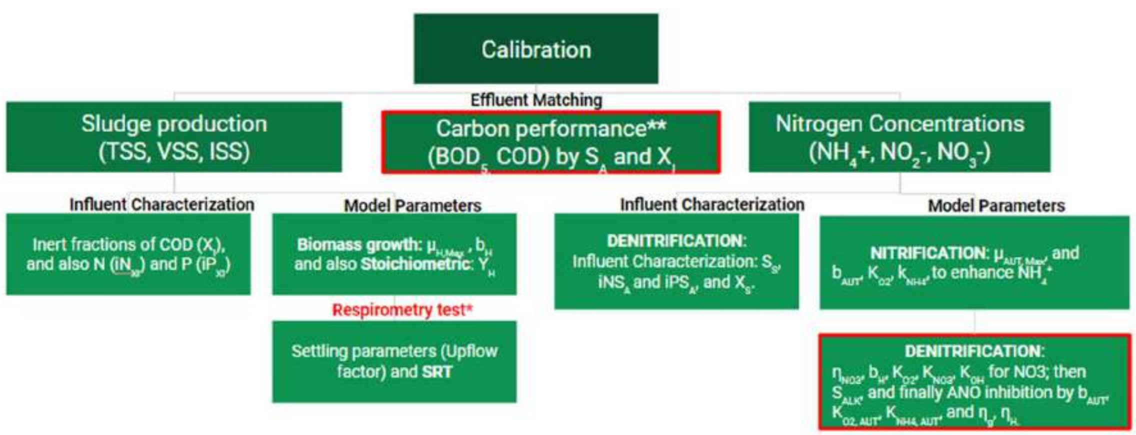

Figure 7. Suggested compiled calibration procedure.
Source: Source: Own elaboration based on the adaptation from Melcer (2004), Orhon et al. (2009), Meijer & Brdjanovic (2012) and Rieger et al. (2012).

5.4.1. SENSITIVITY ANALYSIS

Although fractions, parameters, and ratios from Figure 7 presented the higher sensitivity for industrial applications according to the literature, the current calibration was first analyzed by means of the static sensitivity analysis, following the calibration procedure from Figure 7 (results of sensitivity analysis for HKWW are shown in attachment 10.2). Static sensitivity analysis is the modification of one parameter while the others were kept constant, i.e. every sensitivity analysis was performed reducing and augmenting the suggested fraction, parameter, or ratio value. For the whole sensitivity analysis simulation was performed under the completed fractionated influent (5.2.4) rather than default influent.

5.4.2. CALIBRATION PROCESS AND SCENARIOS

Parameter tuning is not only important in the calibration step, also the stepwise procedure of the calibration, plays a huge role in the simulation results. Thus, the first set of effluent variables to be calibrated is sludge production (such as TSS, VSS, ISS), followed by carbon performance (BOD_5, COD, which is optional), and finally nitrogen concentrations (NH_4^+, NO_2^-, NO_3^-). In all cases influent fractions and model parameters were adjusted parallel to the sensitivity analysis on attachment 10.2 to enhance the effluent fine-tuning process. This ordered procedure is suggested from the highest to the lowest uncertainty parameters (Meijer & Brdjanovic, 2012; Rieger et al., 2012). The carbon performance is not usually analyzed and suggested by the aforementioned authors since it's accepted to count with stated variables as TCOD, COD_S and COD_{AC}, and BOD_5, at least for the STOWA protocol. However, in this specific simulation study the COD_{AC} was not recorded in the sample campaign, leading to an additional analysis of the COD_{AC} influence in the carbon performance.

According to Envirosim (2021), in an SBR system the fraction modifications produce high variables changes, and thus, long term simulations should be performed to allow system stabilization. Therefore, all the sensibility analysis will be presented simulating from the pseudo-steady state until the finalization of the four measure points for stage II, i.e. days 23, 28, 35, 43 (
Table 7). Finally, It is noted that for other simulation exercises, the next calibration scenarios may vary depending on data availability and the nature of the wastewater.

- **CALIBRATION OF HOUSKEEPING WASTEWATER (HKWW)**

a) SLUDGE PRODUCTION MODIFICATIONS

It was observed during the sensitivity analysis (attached as annex 10.2.1) that in all scenarios the simulated values were higher than the observed ones, suggesting that the model requires additional fine tuning on fractions and model parameters. Therefore, observed TSS at the effluent ((1) **Observed_SRT30**) will be compared against the next four realistic simulation scenarios: (2) **Default_SRT30**: Default fractionation and parameters for SRT equals to 30d as presented in numeral 5.2.5**.** and Table 6, (3) **FA_SRT30**: Fractionated Average (FA) influent composition for SRT equal to 30d as mentioned in numeral 5.2.5 and Table 6 for HKWW; (4) **FA_Low.P.Mod_SRT30**: FA influent and low parameter modifications (explained at next) for SRT equals to 30d, (5) **FA_High.P.Mod_SRT30**: FA influent and High parameter modifications (detailed below on Table 9) for SRT equals to 30d. Finally, also against the next two non-realistic scenarios: (6) **High.S_S_P.Mod_SRT30**: High S_S fraction that corresponds to the pseudo-steady-state influent fractionation, low parameter modification for SRT equals to 30d as mentioned in numeral 5.2.5**.** and Table 6, for pseudo-steady-state, and (7) **High.S_S_SRT1**: High S_S fraction and SRT equals to 1d. The last two scenarios present high biodegradable fraction (High S_S) that was not founded by the STOWA protocol but suggested according with the simulation analysis.

Table 9. Sludge production and nitrogen model parameters modification from slaughterhouse wastewater based on literature recommendations.

Parameter	Abbreviation	Units	Value			Source
			Low	High	Reference	
Max. OHO biomass growth rate	μ,max	1/d	0.5	15	10	(Andreottola et al.,1997)
aerobic OHO Decay constant	bH	1/d	0.1	0.062	0.03	
hydrolysis rate constant	KH	1/d	0.5	5	5	(Filali-Meknassi et al., 2005)
anoxic hydrolis factor	KH	1/d	0.05	2.8	0.28	(Andreottola et al.,1997)
Max. AOB biomass growth rate	μ,max	1/d	0.3	5	0.36	(Andreottola et al.,1997) (Filali-Meknassi et al., 2005
AOB Decay constrant	bAut	1/d	0.3	0.017	0.2	(Filali-Meknassi et al., 2005)
Saturation coefficient for Oxygen AOB	KO2	mg O2/L	0.001	0.1	0.01	
Saturation coefficient for (Substrate) Ammonia AOB	KNH4	mg NH4/L	0.1	0.5	0.2	

Source: Own elaboration based on literature recommendations

b) NITROGEN PERFORMANCE MODIFICATIONS

Model parameter modification will be carried out only for scenarios 4, and 5, to analyze the nitrogen performance. Additional to the model parameters mentioned in numeral a) from HKWW calibration on 5.4.2, ammonia oxidizing parameters were changed as next. For scenario (4) **FA_Low.P.Mod_SRT30**: The maximum growth rate of autotrophic bacteria to 0.09d^{-1}(0.9d^{-1} default), and aerobic decay rate to 0.05d^{-1} (0.17 d^{-1} as default) from the list (Table 9). For scenario (5) **FA_High.P.Mod_SRT30**: Maximum growth rate of ordinary heterotrophic bacteria to 5d^{-1} (0.9d^{-1}default), and aerobic decay rate to 0.017d^{-1} (0.17 d^{-1} default) as presented on Table 9. As presented before, the idea is to simulate low and high extremes from mean suggested value to identify the trend on the modification and following the suggestion on literature for slaughterhouse wastewater (Table 9).

- **FINAL HOUSEKEPING WASTEWATER SIMULATION.**

According with the HKWW calibration results and following the recommendation of Andreottola et al. (1997) and Filali-Meknassi et al. (2005) for slaughterhouse effluents, the HKWW will run under the next model parameters modifications: hydrolysis constant rate of 0.5 d^{-1}, anoxic hydrolysis factor of 0.05 d^{-1}, Max. OHO biomass growth rate of 0.5d^{-1}, aerobic OHO Decay constant of 0.1d^{-1}, Max. AOB biomass growth rate of 0.36 d^{-1}, AOB Decay constant of 0.2d^{-1}, Saturation coefficient for Oxygen AOB of 0.01mg O2/L, and Saturation coefficient for Ammonia AOB of 0.2 mg NH_4^+/L.

5.4.3. CALIBRATION OF CONDENSATE WASTWATER (CWW)

- **SLUDGE PRODUCTION AND NITROGEN PERFORMANCE MODIFICATIONS**

Similar as for HKWW, it will be analyzing the next simulation scenarios for CWW, taking into consideration final sludge production and nitrogen modifications: (1) **Observed_SRT30**: Observed TSS at the effluent, this measured data will be compared against the next four realistic simulation scenarios: (2) **Default_SRT30**: Default fractionation and parameters for SRT equal to 30d as presented in numeral 5.2.5 and Table 6, (3) **FA_SRT30**: Fractionated Average (FA) influent composition for SRT equal to 30d as mentioned in numeral 5.2.5 and

Table 6 for CWW; (4) **FA_Low.P.Mod_SRT30**: FA influent and low (minimum) parameter modifications (explained on Table 10) for SRT equal to 30d, (5) **FA_High.P.Mod_SRT30**: FA influent and High (maximum) parameter modifications (explained below) for SRT equals to 30d. Finally, the next two non-realistic scenarios due to the high biodegradable content (High S_S), which was not founded by the STOWA protocol but suggested according with the simulation analysis: (6) **High.S_S_P.Mod_SRT30**: High S_S fraction that corresponds to the pseudo-steady-state influent fractionation, low parameter modification for SRT equals to 30d as mentioned in numeral 5.2.5 and Table 6 for pseudo-steady-state, and (7) **High.S_S_SRT1**: High S_S fraction and SRT equal to 1d.

Table 10. Sludge production and nitrogen model parameters modification from rendering wastewater.

Parameter	Abbreviation	Units	Value			Source
			Low	High	Reference	
Max. OHO biomass growth	µ,max	1/d	0.1	3	0.45-2	(Nakhla & Bassi, 2006)
OHO Decay constant	bH	1/d	0.1	0.01	0.05	
Hydrolisis rate constant	KH	1/d	0.1	1	0.21-0.66	
Half-saturation concentration (Substrate)	Ks	mg COD/L	10	100	17.7-61.3	
Yiel of OHO biomas to substrate	Y,OHO	mg VSS/mg COD	0.1	0.5	0.135-0.416	
Max. AOB biomass growth	µ,max	1/d	0.5	2.5	1.8	(Nowak et al., 1996)
AOB Decay constrant	bAut	1/d	0.1	0.01	0.06	
Half- PO4- saturation for AOB (nitrosomonas)	K, AOB(PO4)	mg PO4/L	0.01	0.1	0.01-0.05	(Nowak et al., 1996)
Half- PO4- saturation for NOB (nitrobacter)	K, NOB(PO4)	mg PO4/L	0.1	0.3	0.2	

Source: Own elaboration based on literature recommendations

- **FINAL CONDENSATE WASTEWATER SIMULATION.**

According with the CWW calibration results, and following the suggestion of Nakhla, Liu & Bassi (2006) and Nowak et al. (1996) for rendering effluent facilities, the CWW will be run under the next model parameters modifications: hydrolysis rate constant of 0.44 d^{-1}, Max. OHO biomass growth rate of 1.23d^{-1}, aerobic OHO Decay constant of 0.05d^{-1}, Half-saturation concentration of 39.5 mg COD/L, Yield of OHO biomass to substrate of 0.28 mg VSS/mg COD, Max. AOB biomass growth rate of 0.5d^{-1}, and AOB Decay constant of 0.1d^{-1}, Half- PO_4^{3-} saturation for AOB of 0.08 mg PO_4^{3-}/L, Half- PO_4^{3-}- saturation for NOB of 0.2 mg PO_4^{3-}/L. Also, the CWW was analyzed by MAE and RMSE criteria for the good-of-fit evaluation in the next section.

5.4.4. NUMERICAL ASSESSMENT

The extent of discrepancies between predicted and observed data will be assessed by means of the next performance methodologies (Table 11): MAE (mean absolute error), RMSE (root mean squared error) for calibration and MAPE (mean absolute percentual error) for calibration, and J^2 (Janus coefficient) for validation by means of the MSE (mean squared error) results.

The MAE quantifies the average magnitude of model errors between predicted and observed values (or accuracy), without considering their direction (Makinia & Zaborowska, 2020), the MSE measures the average squared difference between predicted and observed values. It penalizes larger errors more than smaller ones due to the squaring of differences, while the RMSE is the square root of MSE and provides an estimate of the standard deviation of prediction errors (overall agreement) (Hauduc et al., 2015). In both cases, because its optimal value is zero, the good-of-fit asses should be the lowest possible. While MAE provides a direct measure of error, it is expressed in the same units as the observed data. This can make it challenging to assess the error's significance, especially when comparing models applied to different datasets with varying scales. To address this, researchers often convert MAE into a percentage of the observed values, known as the MAPE. This transformation standardizes the error measure, allowing for easier comparison across different datasets and models. Finally, The model performance is evaluated by means of R-4.0.2.®, packages “zoo” and “hydroGOF” and function “gof” for MAE, MSE, RMSE, while MAPE is computed by means of library “MLmetrics” and function “mape_value”.

Validation will be performed using the J^2 coefficient, since this evaluation indicates the change in model efficiency between calibration and validation steps (Rieger et al., 2012), this value is computed for instance by means of MSE values of calibration and validation stages as presented in Table 11.

Table 11. Goodness-of-fit evaluation of a model performance.

Stage	Evaluation Criteria	Formula
Calibration	Mean absolut error (MAE)	$\frac{1}{n}\sum_{i=1}^{n}\lvert y_{i,obs} - y_i\rvert$
	Root mean square error (RMSE)	$\sqrt{\frac{1}{n}\sum_{i=1}^{n}(y_{i,obs} - y_i)^2}$
	Mean absolute percentual error (MAPE)	$\frac{1}{n}\sum_{i=1}^{n}\frac{\lvert(y_{i,obs}-y_i)\rvert}{\lvert y_{i,obs}\rvert}$
Validation	Mean square error (MSE)	$\frac{1}{n}\sum_{i=1}^{n}(y_{i,obs} - y_i)^2$
	Janus coefficient (J^2)	$\frac{\frac{1}{n\_val}\sum_{i=1}^{n\_val}(y_{i,obs} - y_i)^2}{\frac{1}{n\_cal}\sum_{i=1}^{n\_cal}(y_{i,obs} - y_i)^2}$

n: Total number of experimental data points for the output variable y
$y_{i,obs}$: Observed (measured) data at point i
y_i: model prediction at point i
n_cal and n_val: Total number of measurements used in the calibration and validation periods, respectively.
Source: Own elaboration based on modifications from Makinia & Zaborowska (2020).

5.5. SIMULATION OF DIFFERENTIAL OVERLOAD

To determine the maximum ratio of HKWW and CWW that must be combined to treat the rendering facility and comply with the local discharge limits, empirically the SBR system operates under eight different overloads stages (Table 1), i.e. changing the percentages of housekeeping and stick (condensed) wastewater in a lumped matrix. With aid of the influent data completion, model parameter, at next it will be presented the differential overload of HKWW and CWW simulation for the whole project.

5.5.1. INFLUENT DATA COMPLETION

The total influent composition of both HKWW (stage I, II, III) and CWW (stage VIII) is already known, even the input missing data, as mentioned on numeral 5.2.4. But missing data from stage IV to VII is Unknown, thus, the missing data was pondered according to the percentage of differential overload (weighted average fashion). For instance, the Calcium content of any data belonging to stage V is computed as the calcium concentration for HKWW times 0.8 (80% of overload) plus the calcium concentration of CWW times 0.2 (20% of overload), and everything divided by 1 (or 100%).

5.5.2. INFLUENT DATA FRACTIONATION

Similar for missing data completion, the fractionation of the differential overload data was weighted between housekeeping and condensate wastewater according to the overload ratio. For instance, the inert soluble COD fraction of stage VI is computed as the S_I fraction of stage II (HKWW) times the overload percentage (50%) plus the S_I fraction of stage VIII (CWW) times the overload percentage (50%), and everything divided by 1 (or 100%). Table 12 summarizes the fractionation results of the differential overload project.

Table 12. BioWin Fractionation Input for differential load of wastewater. Fractions are ordered according to the BioWin input prompt.

FRACTION/ COMPOSITION	PSEUDO-STEADY STATE	STABLE RESPONSE Housekeeping (%) / Condensate Wastewater (%)							
		STAGE I	STAGE II	STAGE III	STAGE IV	STAGE V	STAGE VI	STAGE VII	STAGE VIII
	100%/0%	100%/0%	100%/0%	100%/0%	90%/10%	80%/20%	50%/50%	30%/70%	0/100%
1 (Ss)	0.7874	0.3282	0.3282	0.3282	0.3739	0.4197	0.5569	0.6484	0.7857
2 (Sa)	0.1785	0.4445	0.4445	0.4445	0.4181	0.3917	0.3124	0.2595	0.1802
3 (Xsp)	0.9500	0.9500	0.9500	0.9500	0.9500	0.9500	0.9500	0.9500	0.9500
4 (SI)	0.0176	0.0219	0.0219	0.0219	0.0241	0.0262	0.0327	0.0370	0.0434
5 (XI)	0.1090	0.5206	0.5206	0.5206	0.4757	0.4307	0.2959	0.2061	0.0713
6 (Fcel)	0.9500	0.9500	0.9500	0.9500	0.9500	0.9500	0.9500	0.9500	0.9500
7 (SNH4)	0.9605	0.9046	0.9046	0.9046	0.9094	0.9142	0.9286	0.9383	0.9527
8 (XS*iNXS)	0.0007	0.0163	0.0163	0.0163	0.0147	0.0132	0.0085	0.0055	0.0008
9 (SI*iNSI)	0.0001	0.0021	0.0021	0.0021	0.0020	0.0018	0.0014	0.0011	0.0006
10 (N/COD ratio)	0.0700	0.0700	0.0700	0.0700	0.0700	0.0700	0.0700	0.0700	0.0700
11 (SPO4)	0.4098	0.2323	0.2323	0.2323	0.2500	0.2678	0.3211	0.3566	0.4098

Source: Own elaboration

5.5.3. MODEL PARAMETER CONFIGURATION

Based on the calibration results of HKWW and CWW (attached as annex) the model parameters modification is also weighted proportional to the differential overload, i.e., the hydrolysis rate constant of stage VII is computed as the K_H of stage II (HKWW) times the overload percentage (30%) plus the K_H fraction of stage VIII (CWW) times the overload percentage (70%), and everything divided by 1 (or 100%). Table 13 summarizes the modification on model parameters of the differential overload project.

Table 13. BioWin fractionation input for differential load of the housekeeping and rendering wastewater. Parameters were found to present the highest sensitivity on the calibration.

MODEL PARAMETER	PSEUDO-STEADY STATE	STABLE RESPONSE								
		STAGE I	STAGE II	STAGE III	STAGE IV	STAGE V	STAGE VI	STAGE VII	STAGE VIII
	100%/0%	100%/0%	100%/0%	100%/0%	90%/10%	80%/20%	50%/50%	30%/70%	0/100%
μH,max	0.5000	0.5000	0.5000	0.5000	0.5730	0.6460	0.8650	1.0110	1.2300
bH	0.1000	0.1000	0.1000	0.1000	0.0950	0.0900	0.0750	0.0650	0.0500
KH	0.5000	0.5000	0.5000	0.5000	0.4940	0.4880	0.4700	0.4580	0.4400
μAut,max	0.3600	0.3600	0.3600	0.3600	0.3740	0.3880	0.4300	0.4580	0.5000
bAut	0.2000	0.2000	0.2000	0.2000	0.1900	0.1800	0.1500	0.1300	0.1000

Source: Own elaboration

5.5.4. GOOD-OF-FIT OF MODEL PERFORMANCE

Similar to HKWW and CWW, differential overloading will be assessed by means of MAE and RMSE for calibration, and J^2 for validation.

- **MODEL PERFORMANCE ASSESSMENT**

Differential overload simulation was already calibrated changing the influent fractionation (numeral 5.5.2) and modifying the model parameters values (numeral 5.5.3). The model performance is evaluated by means of R-4.0.2.®, packages “zoo” and “hydroGOF” and function “gof” for MAE, MSE, RMSE, while MAPE is computed by means of library “MLmetrics” and function “mape_value”.

- **VALIDATION ASSESS**

The J^2 coefficient is computed by means of MSE values of calibration and validation stages, as presented in Table 11. For the validation of the differential overload analysis, one point of each simulation stage was used (8 in total) presented in Table 14. Those points were not used for the calibration step.

Table 14. Validation of measured and simulated effluent concentration, that were not considered on the calibration phase.

DATE (d)	MEASURED DATA				SIMULATED DATA			
	TSS (mg/L)	COD (mg/L)	BOD (mg/L)	NH4 (mg/L)	TSS_FracAverPMod	COD_FracAverPMod	BOD_FracAverPMod	NH4_FracAverPMod
9	470.00	2706.67	1053.30	336.99	7537.15	13058.96	3067.27	352.07
28	750.00	1006.67	340.00	256.56	9166.18	13988.16	3583.39	554.91
65	190.00	540.67	201.70	233.91	7750.08	12204.31	2730.81	481.30
84	54.00	874.00	50.67	174.61	7959.96	10344.00	2605.16	685.47
114	1140.00	1083.33	366.67	318.42	11277.36	19977.22	6860.66	596.30
175	70.00	190.67	35.00	194.39	4536.57	8677.39	2603.22	459.89
205	392.12	366.67	292.75	431.67	2025.09	3933.33	1332.58	666.77
240	2.20	401.54	178.69	251.54	1084.82	2150.86	993.31	583.02

Source: Own elaboration

6. RESULTS AND ANALYSIS

6.1. DATA COLLECTION

6.1.1. DATA ANALYSIS

Only organics, nutrients, and solids were matter of data analysis since those parameters are called for attention by the national standards. Grease and oil are also required but data was not available. Data analysis will be presented next only for HKWW (stage II), and for the CWW the same process was performed but not presented.

- **GRAPHIC METHOD**

The graphic method was the selected methodology to define the period of simulation, i.e. in which period the system presents a stagnant concentration (steady state) at the influent (continuous line) and effluent (dashed line). In this sense, stage II of simulation, which ranges from day 22 to 43 (Table 7) are highlighted in the red box on Figure 8, Figure 9 and Figure 10. Stage II presents a steady-state experimental response for organics (TCOD, COD_S, BOD_5), Nutrients (NH_4^+, NO_x^-, and PO_4^{3-}, and low steady response for solids but more stable than for stage I and III, which are also 100% HKWW ratio. The soluble/Total COD ratio is less than 0.5 indicating that most of the carbon is present in particulates form and that the coagulant step and grease and fat removal is not working completely well. The BOD_5/Total COD ratio indicates that in the calibration period less than 20% of the total carbon belongs to the biodegradable fraction, indicating the complexity in availability in readily biodegradable carbon.

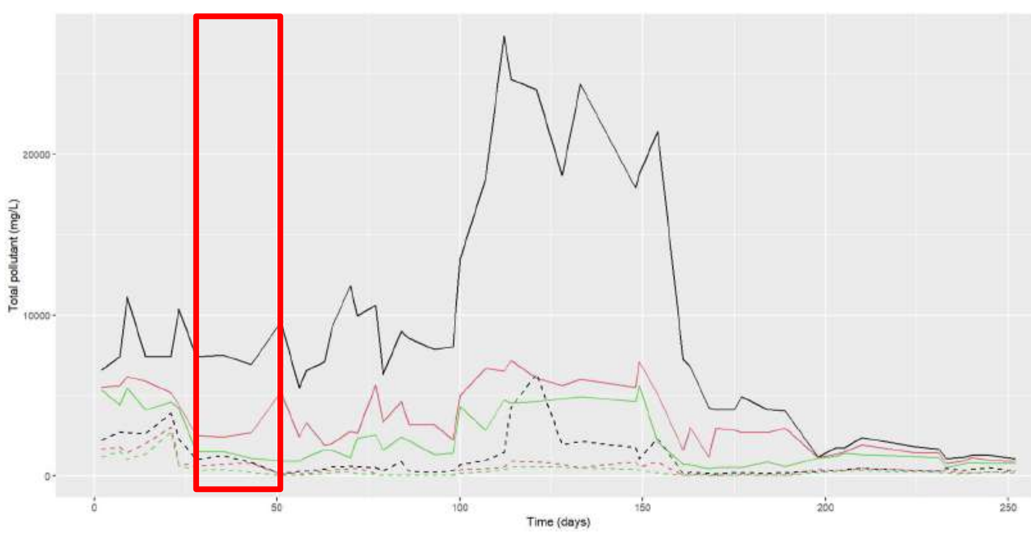

Figure 8. TCOD (black), COD_S (red), BOD_5 (green) Vs time of operation (days) for influent in continuous line and effluent in dashed line.

Source: Own elaboration based on software R-4.0.2.®, packages "ggplot2" and function "ggplot".

On the other hand, the nutrient species present a similar steady-state patron in the influent and effluent, even in the presence of carbon overloading with the condensate wastewater. As NH_4^+ and PO_4^{3-} lines are present in Figure 9, there is not enough removal of nitrogen and phosphorus.

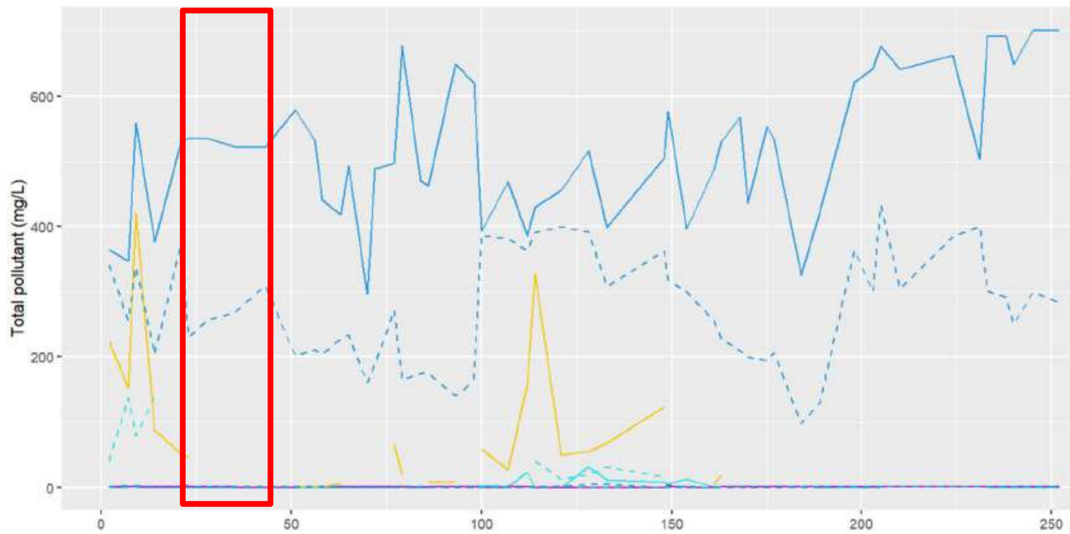

Figure 9. NH_4^+(Dark blue), NO_2^-(Light blue), NO_3^-(Pink), and PO_4^{3-} (Dark yellow) for influent in continuous line and effluent in dashed line

Source: Own elaboration based on software R-4.0.2.®, packages "ggplot2" and function "ggplot".

Although the solid analysis presents that there is not actually a steady-state pattern on the influent solid's concentration for Stage II, but neither for stage I nor III. There is a steady-state pattern at the effluent as expected since after stage 1 the system reaches the microorganisms establishment, and the settling conditions remain the same in the SBR system non-depending on the feed load pattern.

Analyzing the differential loading data, there is a shift in stages 5 and 6, where the Inert solids (ISS) are larger than the volatile solids (VSS) presenting an overload condition that tends to contain large amounts of inorganic materials. In general, the whole effluent suspended solids.

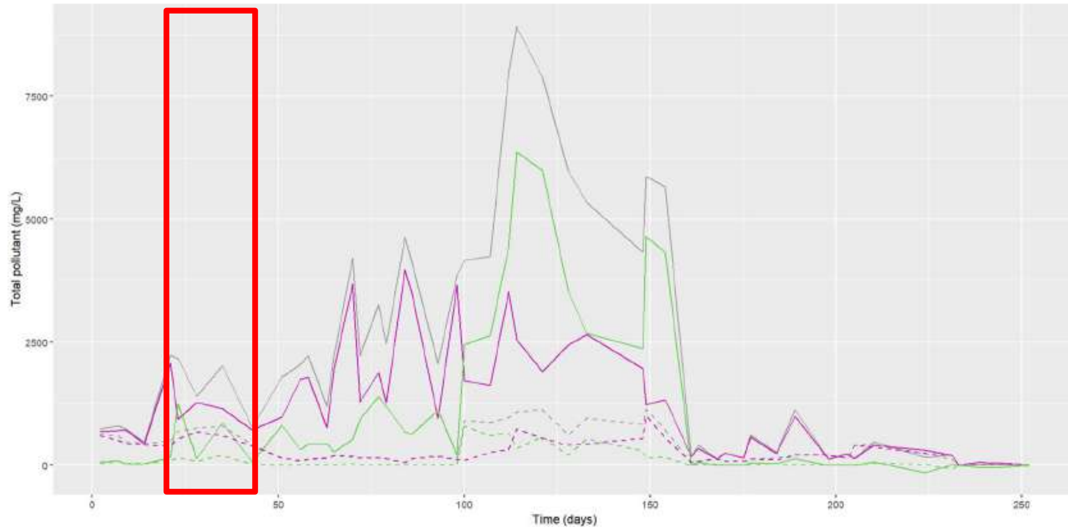

Figure 10. TSS (gray), VSS(magenta), ISS(light green) for influent in continuous line and effluent in dashed line.
Source: Own elaboration based on software R-4.0.2.®, packages "ggplot2" and function "ggplot".

- **OUTLIER DETECTION**

In Figure 11 is presented the outlier detection of organics parameter as TCOD, COD_S, and BOD_5 by means of box and whiskers plots for both influent (I suffix, Figure 11) and effluent (E suffix, Figure 11) on stages I, II and III or from 0 to 77 days of simulation, (
Table 7). Stages I to III are selected to analyze the acclimatation stage and microorganism's establishment under the same feed pattern, i.e., stages I and III also contain 100% housekeeping and 0% condensate wastewater.

As seen in the plot of Figure 11, influent and effluent data are skewed to the left and the most dispersion is present to right values. Only BOD_5 from effluent present an outlier on sample point of 2718.3mg DBO_5/L that belongs to the last measured BOD_5 data from stage I, suggesting simulating with data from stage II where parameters present the closest steady-state condition, without affecting the simulation period.

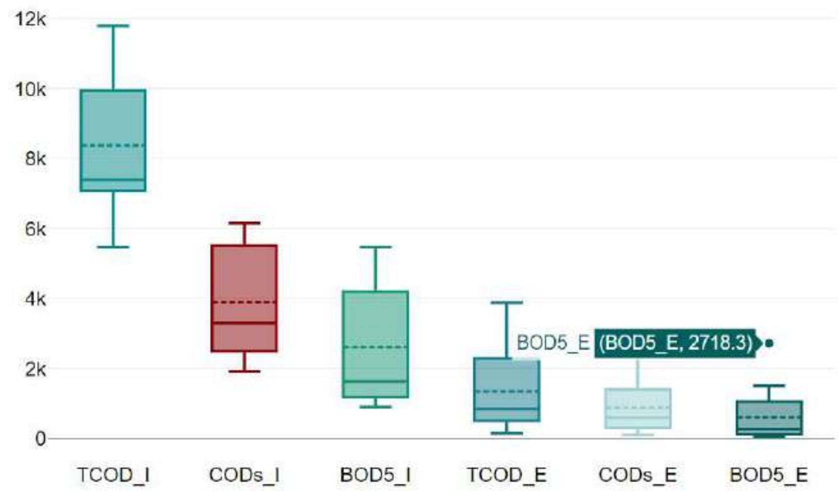

Figure 11. Outler detection of organics (COD, BOD_5 and CODs) for influent (I) and effluent (E). Source: Own elaboration based on online statistics calculator DATAtab (2023).

On the other hand, Figure 12 presents nutrients outlier analysis for NH_4^+, NO_2^- , NO_3^-, and PO_4^{3-}. In this case the variables NO_X^- present the lowest dispersion and outlier points. However, this parameter will be neglected in the influent but thoroughly analyzed in the effluent simulations results. The value 420.51mg/L of PO_4^{3-} (influent) belongs to stage I, as well as 377.86 for NH_4^+(effluent), and suggesting simulating on stage II where parameters present the closest steady-state condition.

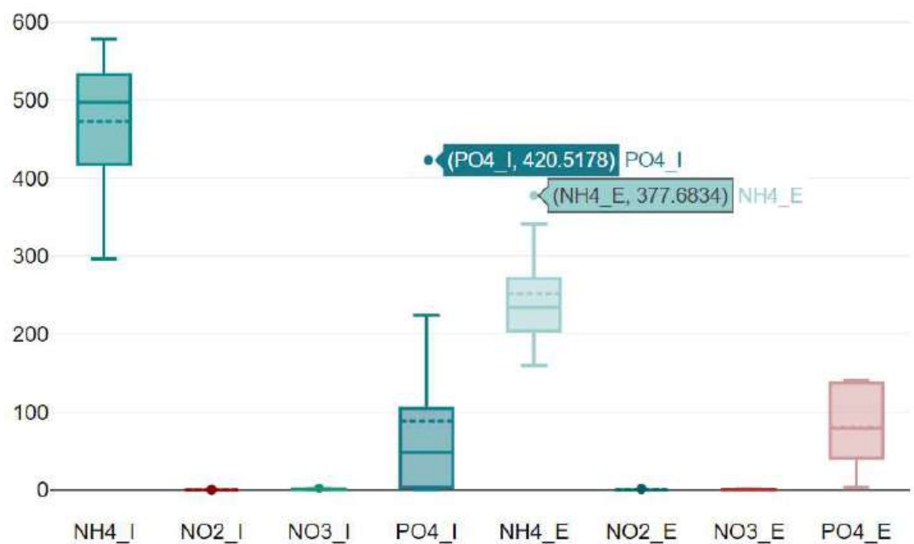

Figure 12. Outler detection of nutrients (NH4+, NO2- , NO3-, and PO_4^{3-}) for influent (I) and effluent (E). Source: Own elaboration based on online statistics calculator DATAtab (2023).

The only outlier points for the solids analysis (Figure 13) is the concentration of volatile suspended solids from the Stage III of analysis (3690mg VSS/L), value that also lay out of the period of simulation analysis (stage II).

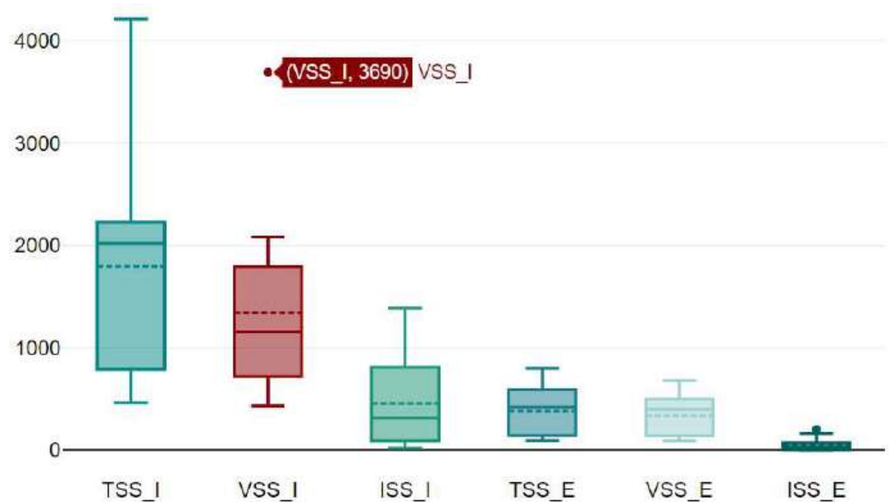

Figure 13. Outler detection of suspended solids (TSS, VSS and ISS) for influent (I) and effluent (E). Source: Own elaboration based on online statistics calculator DATAtab (2023).

- **SANITARY CHECKS**

Sanitary (plausibility) checks, which are applied only for influent analysis, as TN=TKN+NO_3^- +NO_2^- for nitrogen, TKN>NO_X^- on nitrogen species; NH_4^+>NO_3^-, and TP=PO_4^{3-} for phosphorus species were possible to check latter after data completion. In Figure 11, Figure 12 and Figure 13 it's seen that $COD_{S,}$ and BOD_5 values are lower than TCOD ones as expected, as well as NO_X^- species that are lower than NH_4^+. TSS and VSS after stage VI present some inconsistencies thus creating some noises in the ISS calculation that is required for the total influent approach that uses BioWin software.

6.1.2. DATA PROCESSING

The influent missing data completion, in the calibration phase, was carried out based on the requirements of the STOWA characterization protocol (e.g. S_A) and fraction parameters to feed the BioWin Software (e.g. TKN, TP, Alkalinity, Ca^{+2}, Mg^{+2}). As follows, it will present the housekeeping and condensate missing data completion.

- **TOTAL COMPOSITION OF MISSING DATA**

Table 15 for housekeeping and
Table 16 for condensate wastewater contain approximations for variables as alkalinity, sulphur, calcium and magnesium in the way in which BioWin prompted the total composition inflow that were described in numeral 5.2.4 (data processing and influent assumptions).

Comparing Table 15 and
Table 16, it is seen that the HKWW contain a higher carbon, phosphorus, sulfur, ISS, calcium, and magnesium concentrations, while condensate (stick) contains higher NTK, pH, and alkalinity, who "preliminary" suggest a possible mixing of matrices to enhance its individual treatment. Due to the advance decomposition state and hydrolysis of the transformed materials in the production process for both HKWW and CWW, the concentration of the oxygen influent is approximate to be zero (0 mg DO/L).

Table 15. Completed housekeeping influent composition-Analytical results for stage II.

PHASE	DATE	CODT (mg/L)	NTK (mg/L)	TP (mg/L)	S (mg/L)	NO3- (mg/L)	pH	Alkalinity (mmol/L)	ISS (mg/L)	Calcium (mg/L)	Magnesium (mg/L)
PSEUDO-STEADY STATE	0	6566.67	418.03	423.11	68.80	0.12	5.91	11.70	435.00	26.00	7.00
STABLE RESPONSE	21	10600.00	596.43	86.78	68.80	0.73	5.93	11.70	1386.00	26.00	7.00
	26	6306.67	574.63	< L.D	68.80	1.94	6.94	11.70	1200.00	26.00	7.00
	33	8973.33	565.05	0.00	68.80	0.00	6.77	11.70	670.00	26.00	7.00
	41	8540.00	558.72	< L.D	68.80	1.14	6.96	11.70	630.00	26.00	7.00

Source: Own elaboration.

Table 16. Completed Condensate influent composition-Analytical results for stage VIII.

PHASE	DATE	CODT (mg/L)	NTK (mg/L)	TP (mg/L)	S (mg/L)	NO3- (mg/L)	pH	Alkalinity (mmol/L)	ISS (mg/L)	Calcium (mg/L)	Magnesium (mg/L)
PSEUDO-	178	1070.00	729.89	5.07	16.55	0.43	9.15	104.00	42.00	10.90	0.80
STABLE RESPONSE	238	1173.33	721.01	5.56	25.28	0.55	9.26	104.00	42.00	10.90	0.80
	240	1280.00	685.89	6.07	16.03	0.80	10.11	104.00	50.00	10.90	0.80
	245	1266.67	720.89	6.00	9.59	0.85	9.87	104.00	37.50	10.90	0.80
	252	1066.67	751.45	5.05	10.89	0.85	8.99	104.00	40.00	10.90	0.80

Source: Own elaboration.

6.1.3. INFLUENT FRACTIONATION

Figure 14 and Figure 15 shows visually the incoming characterization (fraction approach) of carbonaceous, nitrogen, and phosphorus substrates that were fractionated from state variables (total approach) of Table 15 and
Table 16 for housekeeping and condensate wastewater respectively (an even more detailed of fractionation of HKWW is found as annex on Table 17, Table 18, Table 19 and Table 20), using the nomenclature of the unified protocol (Rieger et al., 2012), and based on the actual measurement and similar studies assumptions.

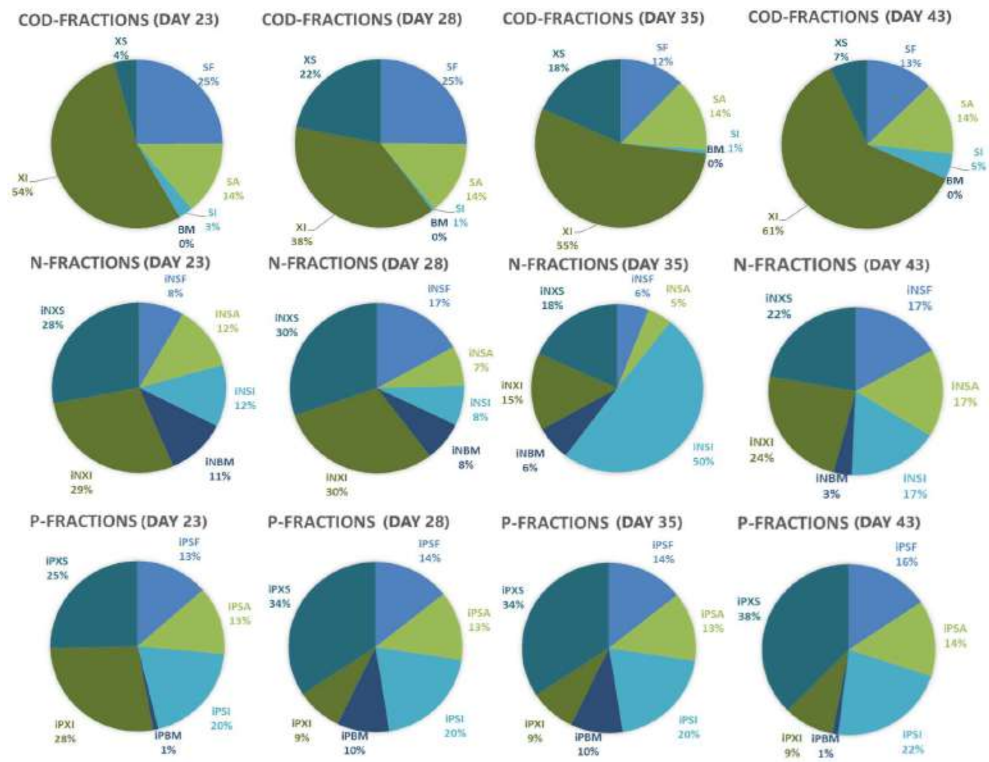

Figure 14. Inflow COD, N and P fractionations for soluble and particulate components of HKWW of stage II.
Source: Own elaboration.

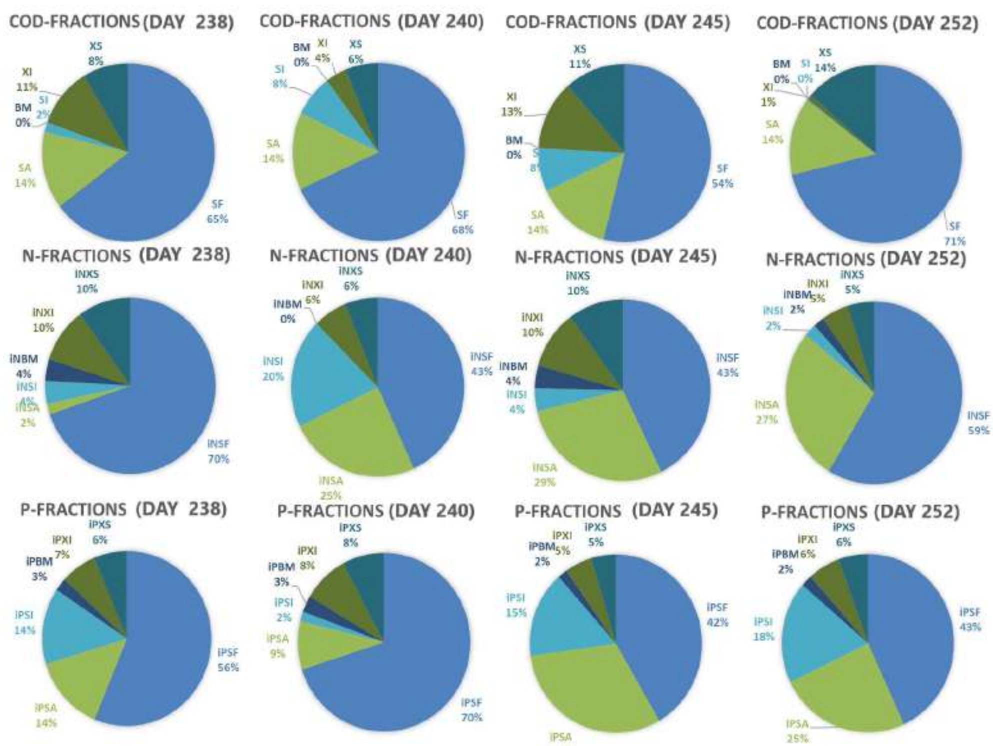

Figure 15. Inflow COD, N and P fractionations for soluble and particulate components of CWW of stage VIII.

Source: Own elaboration.

Different to municipal wastewater, industrial wastewater (i.e. HKWW and CWW) present negative values for X_S fraction when fractionating in the STOWA protocol that must be fixed by tunning the k constant, and Y_{BOD} yield parameters of the BOD model. The common range of the constant k from the BOD model is between 0.15 and 0.6 d^{-1} of domestic wastewater. It was found that if BOD_U is higher than S_S ($BOD_U > S_S$), thus, to avoid the negative X_S values, the k value should be out of the suggested domestic upper limit of k (i.e. 0.8). But, when BOD_U is lower than S_S ($BOD_U < S_S$), which is mostly the case for the HKWW, the k value should be out of the lower domestic limit of k (e.g. 0.13). In general, for housekeeping wastewater the k and Y_{BOD} are 0.13d^{-1} and 0.2, while for the condensate wastewater are 0.90d^{-1} and 0.25 respectively. After the fine tuning of the Xs, the TCOD balances close correctly.

In general, the biggest COD fraction for HKWW was X_I (up to 51%), follow by 33% of S_s (57% of S_F and 43% of S_A), 14% of X_S and 2% of S_I, while for CWW the COD fraction were 80% of S_S (where up to 82% was S_F and 18% was S_A), 10% of X_S, 7% of X_I and 3% of S_I for the CWW. Roeleveld & Van Loosdrecht (2002) suggest common values for N- and P-fractions on domestic wastewater. However, for industrial applications those parameters should be tuned until matching with the TKN and TP state variables, as suggested by the STOWA protocol (Meijer, & Brdjanovic, 2012). In general, the nitrogen fractionation is 92% of ammonia, around 6% of organic particulate nitrogen, and 2% of organic soluble nitrogen for HKWW, while for CWW is 95% of ammonia, around 2% of organic particulate nitrogen, and 3% of organic soluble nitrogen. On the other hand, 23% and 40% of the phosphorous content in the influent HKWW and CWW belong to the orthophosphates, while the remaining is present in form of organic phosphorous for untransformed cell materials. Finally, Table 6 summarizes the BioWin input fractionation base on the STOWA protocol for the HKWW (stage II), and CWW (stage VIII). Base on the last findings, although the COD/N or COD/P ratio are analyzed the CWW present worst ratios for the biological process, CWW is more "biodegradable" than the HKWW based on the amount of S_S, and nutrients availability.

6.2. PLANT MODEL SET-UP.

6.2.1. PRE-RUNNING SIMULATIONS

The simulation analysis with default values of influent, without data completion, and default parameters is performed to check the hydraulic model before the pollutants analysis. Thus, it will present at next the HKWW hydraulic model checking.

- **PSEUDO-STEADY-STATE AND HYDRAULIC MODEL VERIFICATION**

The simulation starts 60d before the first simulation point (day 21) to ensure the pseudo (quasi)-steady state. However as seen in Figure 16 the biomass establishment was reach at 7-12d, when the TSS settled down in the SBR system, this value is less than the 2 times SRT suggested by Orhon et al. (2009) (i.e. 60d for this study). The pseudo-steady-state simulation is important since during this time span high numerical variation occurs in TSS production (as presented in the starting period on Figure 16), as well as in the air input, and nutrient prediction. From this simulation period the BioWin system warns that more than 10% of effluent nitrogen is stripped as ammonia due to the high load of nitrogen.

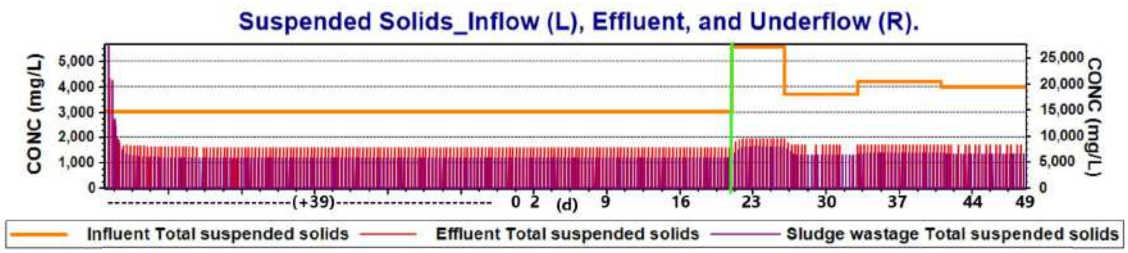

Figure 16. Solids chart: The chart presents the inflow total suspended solid concentration at the left axis; the effluent and underflow stay at the right axis. The green line divides the pseudo-steady state at the left side, from the stable response at the right.
Source: Own elaboration running the BioWin software ®.

Figure 17 presents the sludge retention time (SRT) for the pre-running simulation. As expected, the SRT is around 30d with some notable increase after every inflow change (after the green line on Figure 17). Those changes could be attributed to the rapid microorganism's growth due to the augmentation of available degradable carbon.

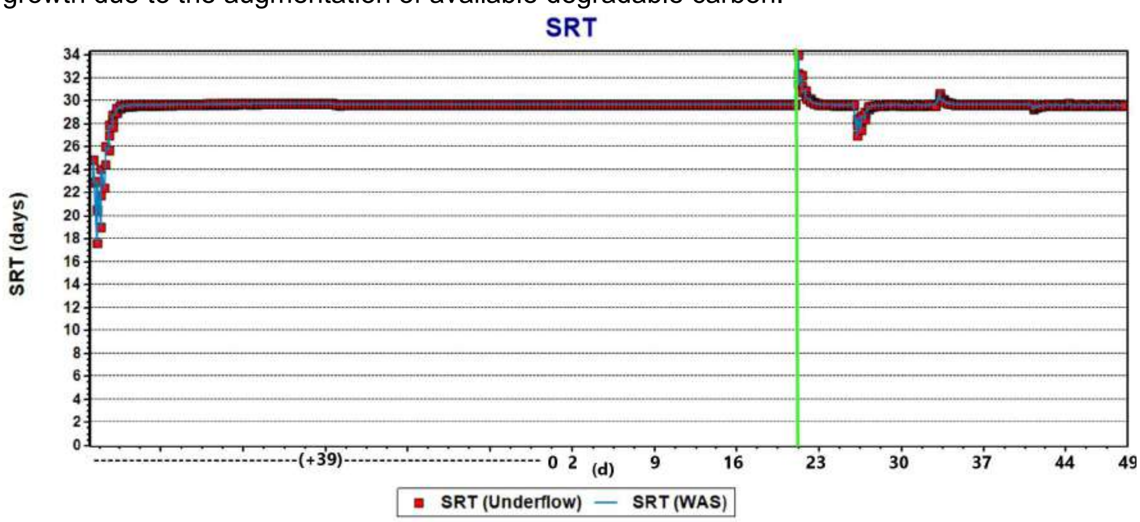

Figure 17. SRT chart: Sludge retention time (sludge age) during HKWW analysis (Stage II).
Source: Own elaboration running the BioWin software ®.

- **STABLE SBR RESPONSE**

The hydraulic model was verified with the "Check hydraulic data" option, to avoid overflows or excessive sludge wastage. Therefore, this first attempt helps to adjust the underflow value to prevent washout. Finally, the album for presentation of output results was corrected to aid in understanding of the SBR configuration. Much attention should be paid in this point, since the checking of the hydraulic model could be "ok" according to the Software, but the simulation could present sludge washout (when the concentration of TSS Vs time decreases rapidly and approaches close to zero). From this simulation period the system also warns for more than 10% of effluent nitrogen is stripped as ammonia, and low phosphorus concentration as a limited condition, which means that the microorganism growth is reduced by at least half due to the lack of influent phosphorus.

Figure 18 presents the inflow, drawn and underflow for the stable response of simulation of HKWW on stage II. Figure 18–1 shows the general simulation results for the pseudo-steady-state at the left side, and the stable response period at the right side. Due to the difficulty of visualization of the flow chart, to check little variation, and better understanding on the liquid line, the in-process Flow chart is presented (Figure 18-2), this graph shows the process of the last simulation day. Figure 18-2 presents three cycles per day with three influent loads (dashed gray line), the underflow (purple line), and the effluent (red line) in the last 5min of each cycle.

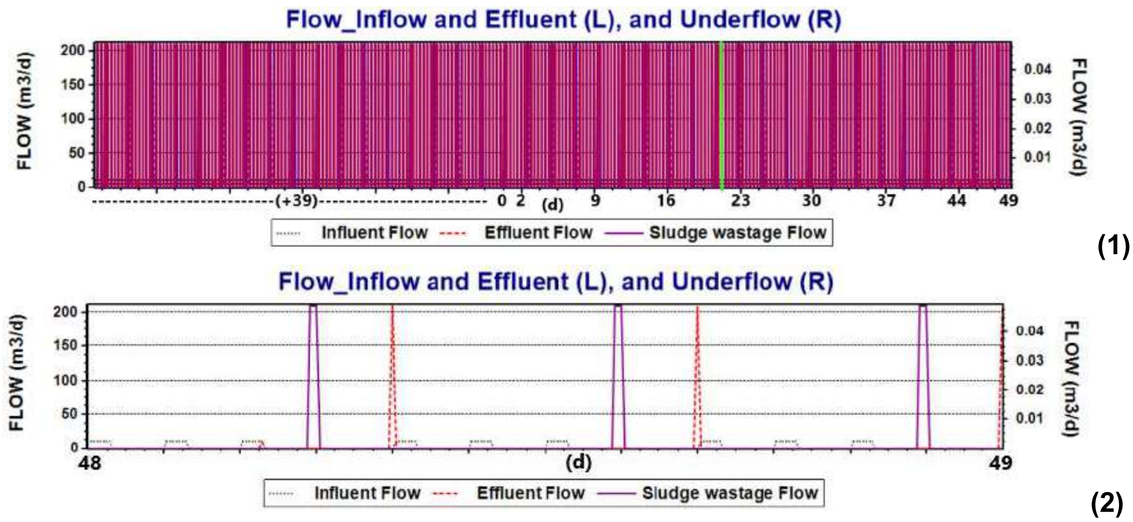

Figure 18. Flow chart: (1) Hydraulic checking of stage II. (2) In process of the last simulation day. Influent flow at the left axis (L), while the effluent and underflow stay at the right axis (R). Source: Own elaboration running the BioWin software ®.

According to Figure 19-1, the maximum liquid depth is 1.3m and the lower liquid depth was around 0.65m (blue line), i.e., the SBR never overpast the maximum hydraulic (liquid) capacity of 1.46m^3 but interchange the liquid volume until the lower limit of 0.733m^3 that is the red line. As mentioned before, Figure 19-2 present the in process of the last simulation day to check small variation of liquid and volume changes. As seen the system presents three inflow purges and three stagnant periods, and after the three-inflow load per cycle, the system reaches the maximum capacity of 1.46m^3 or 1.3m high.

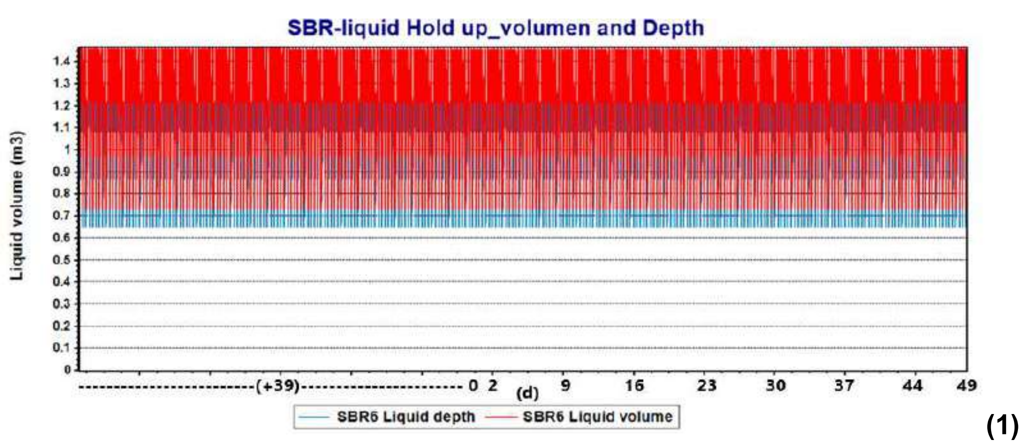

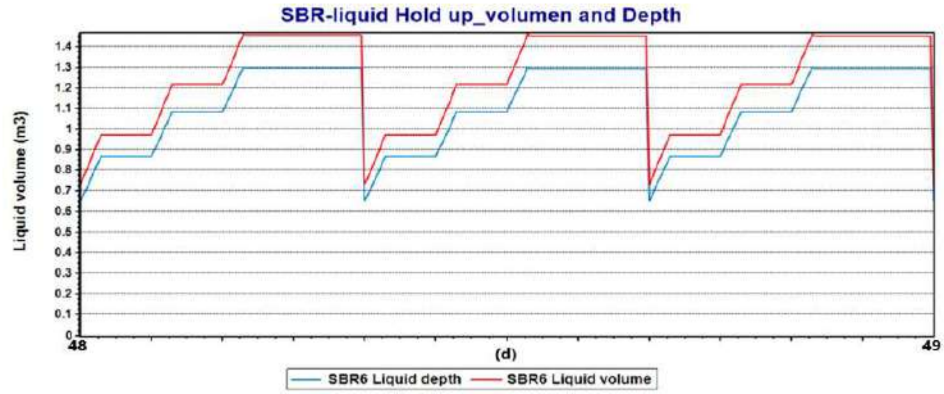

(2)

Figure 19. SBR hydraulic chart: (1) liquid volume and depth of SBR for stage II. (2) In process of the last simulation day.
Source: Own elaboration running the BioWin software ®.

During the pre-running simulations, it is also important to probe the aeration system response. Figure 20-1 presents that the D.O for the whole simulation is set as 1.1mg O_2/L, and Figure 20-2 (last simulation day) presents the differential aeration, which last 8min of activated aeration, and then stops the next 15min over and over again until 360min (6 hours). Also, it is presented the sedimentation period where no oxygen is supplied to avoid sludge breaking during the settling phase.

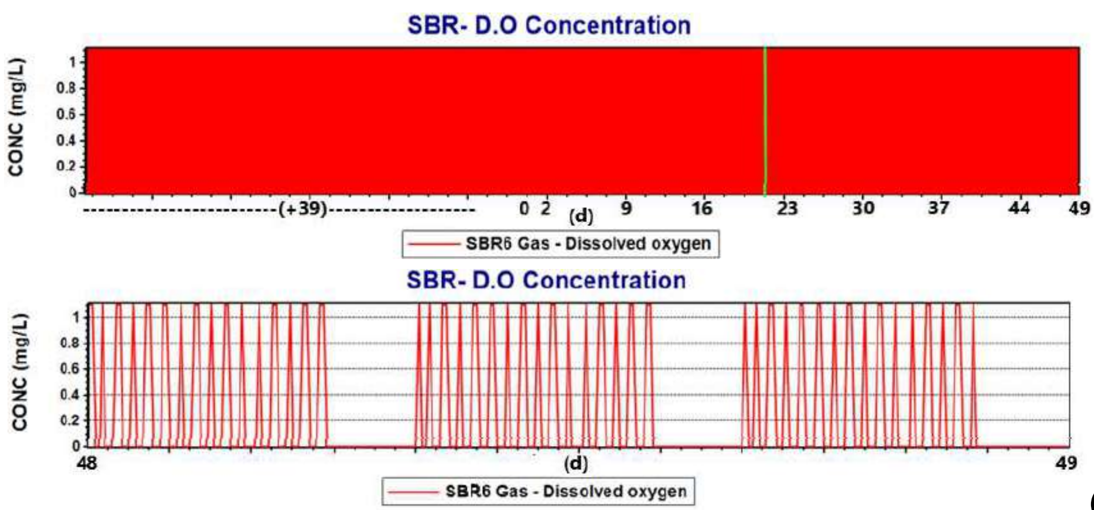

(1)

(2)

Figure 20. D.O chart: (1) control of DO during satage II, and (2) Inprocess of the last simulation day.
Source: Own elaboration running the BioWin software ®.

6.2.2. GRAPHICAL INFLUENT PERFORMANCE ANALYSIS

- **HOUSEKEPING WASTEWATER (HKWW)**

As follows, it will present the effluent comparison of TSS, COD, BOD, and NH_4^+ for measured data (observed, big green dots), against the data simulation of default influent (light blue lines), fractionated influent (dark blue line), and average fractionated influent (dashed dark green line) with the STOWA protocol.

As a result, all the simulated scenarios present a similar TSS response (Figure 21-1). From the process point of view, the observed TSS at the effluent have reached values of only 5800mg/L, overpassing the 200mg TSS/L allowed by Colombian standards (50mg/L for the World Bank). The SVI was greater than 450ml/gr in the four days of sampling control, i.e., this high SVI suggests that the pilot SBR was not allowing good sedimentation, probably due to bulking reason because of nutrient deficiency, and the remaining fat and oil contain that was not correctly removed.

Simulated COD and BOD response (Figure 21-2 and Figure 21-3 respectively) shows closer fit regarding observed values for the fractionation scenario than for the default or average fractionated scenarios. The main difference between the fractionated or average fractionated and default inflow scenarios, analyzing the COD effluent response, is that the former contains a higher biodegradable concentration (SS) than the latter, this SS difference leads an increase in the amount of active OHO biomass that transforms the biodegradable (Ss) COD. In the case of the BOD concentration is better represented by the average fractionation inflow than the other scenarios. Besides, from the measure data point of view, the observed COD and BOD_5 performance data neither comply the standards (900mg COD/L a 450mgBOD/L respectively for Colombia and 250mg DQO/L, 50mg DBO/L for the World Bank) since the observed COD and BOD_5 was higher than 11000mg/L and 2500mg/L respectively.

For the ammonium response the simulated fractionation and average fractionation case reproduces worse fitted values than those for the default influent simulations, meaning that the influent fractionation is not enough to represent the similarity between observed and simulated data in terms of nitrogen concentrations, and thus, additional model parameter should be fixed before running the final simulation. Ammonium was the variable that best represent the nutrient removal from the four main studied variables. Furthermore, contrasting observed NH_4^+ values for the influent (range from 522 to 534mg/L) and effluent (range from 229 to 309 mg/L), during the simulation period, the actual SBR system do not nitrify and denitrification completely due to the ammonium, nutrients, pH, and oxygen inhibition.

As seeing in Figure 21, the fractionation and average fractionation inflow scenarios shows relatively same results for all the control performance variables (effluent TSS, TCOD, BOD_5, NH_4^+), suggesting that calibration could be realized by the average fractionation instead of changing the fractionation for every simulation control point and also because the observed data and simulation present a steady-state of the nutrient response. Therefore, the HKWW will be simulated with the average fractionation to analyze the in-process behavior.

- **CONDESATE WASTEWATER (CWW)**

Similar as presented for HKWW at next it will be presented the effluent comparison of TSS, COD, BOD, and NH_4^+ for measured data (observed, big green dots) of CWW, against the simulation of default influent (light blue lines), fractionated influent (dark blue line), and average fractionated influent scenarios (dashed dark green line).

In this case, the TSS response was better represented by the average fractionation, followed by the fractionation inflow as seen in Figure 22-1. However, the overall system performance is critical considering that the average TSS response is equals to 5.59mg TSS/L which indicated that this matrix is facing solids wash out. Similarly, the COD and BOD (Figure 22-2 and Figure 22-3) present the same response pattern as for HKWW, the better fighting was reached with the average fractionated inflow. The effluent COD and BOD is equals to 389.7mg COD/L and 167.98 mgBOD/L values that overpass the national regulations of 900mg COD/L a 450mgBOD/L respectively and for slaughtering houses as a frame reference of standards (250mg DQO/L, 50mg DBO/L for the World Bank).

Finally, the ammonium effluent response was similar as for HKWW, since the default fractionation present better finetune regarding observed data, suggesting that better parameter calibration should be realized to increase the accuracy of actual system representation. Ammonium was the variable that best represents the nutrient removal from the four main studied variables. Different to the HKWW, the simulated ammonia concentration responses present the closest finetune with measured data, but still overestimate.

The fractionation and average fractionation inflow shows relatively same results for all the control performance variables (Figure 22), suggesting that calibration could be realized by the average fractionation, and because the observed data and simulation present a steady state of the nutrient response. Therefore, CWW will be also simulated with the average fractionation to analyze the in-process behavior.

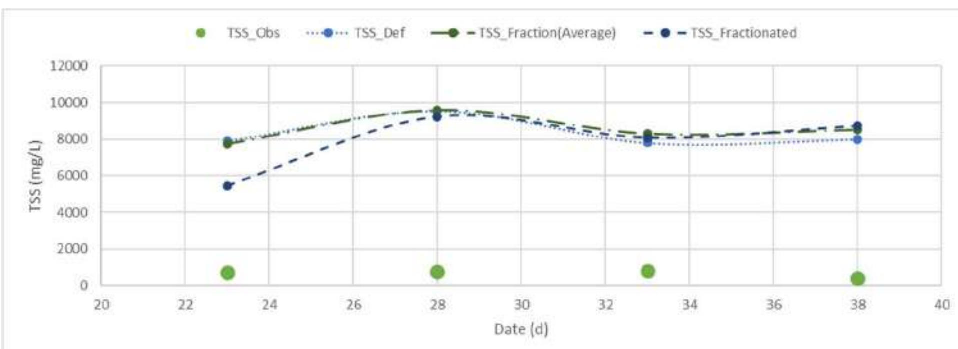

(1)

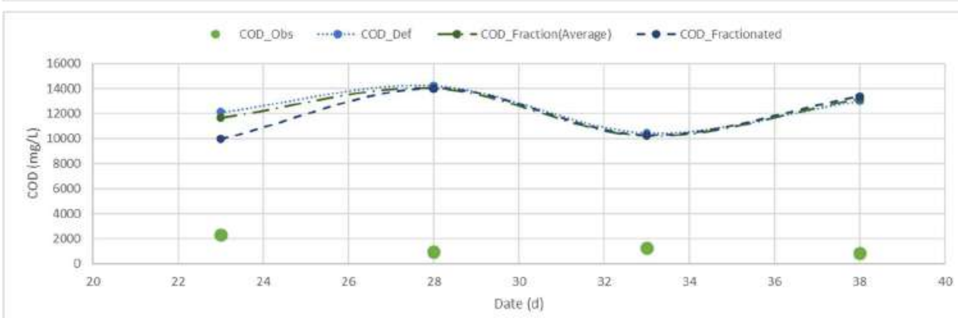

(2)

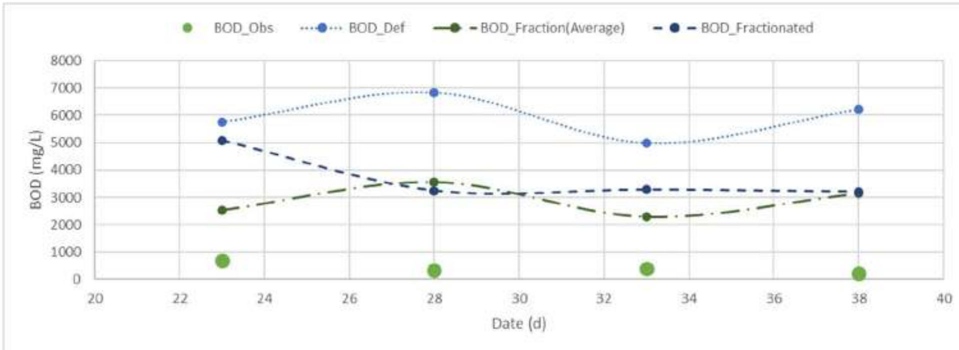

(3)

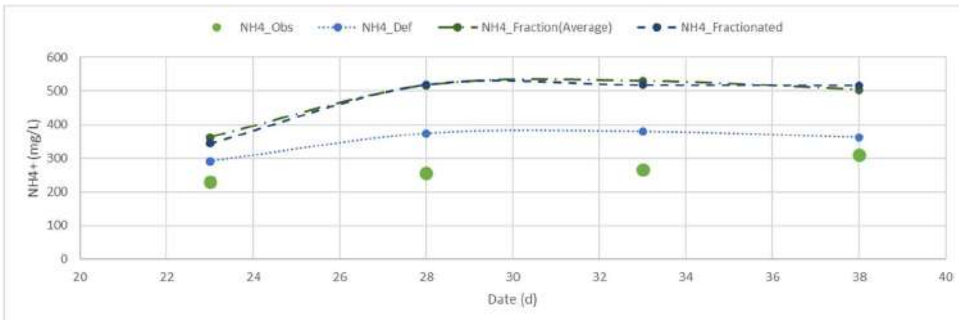

(4)

Figure 21. Track study for measured data (points) and corresponding simulated results (continuous line) on stage II of (1) TSS, (2) COD, (3) BOD_5 and (4) NH_4^+ concentrations for housekeeping wastewater.

Source: Own elaboration.

Finally, it is highlighted that condensate wastewater present a clear and better good-of-fit regarding to the fractionated input than the default one, suggesting that for this water matrix the fractionation present an enhancement in the matrix simulation and understanding.

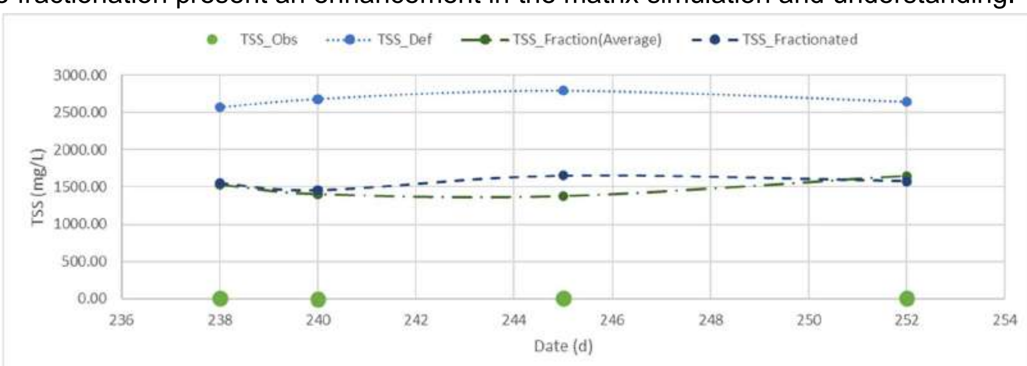

(1)

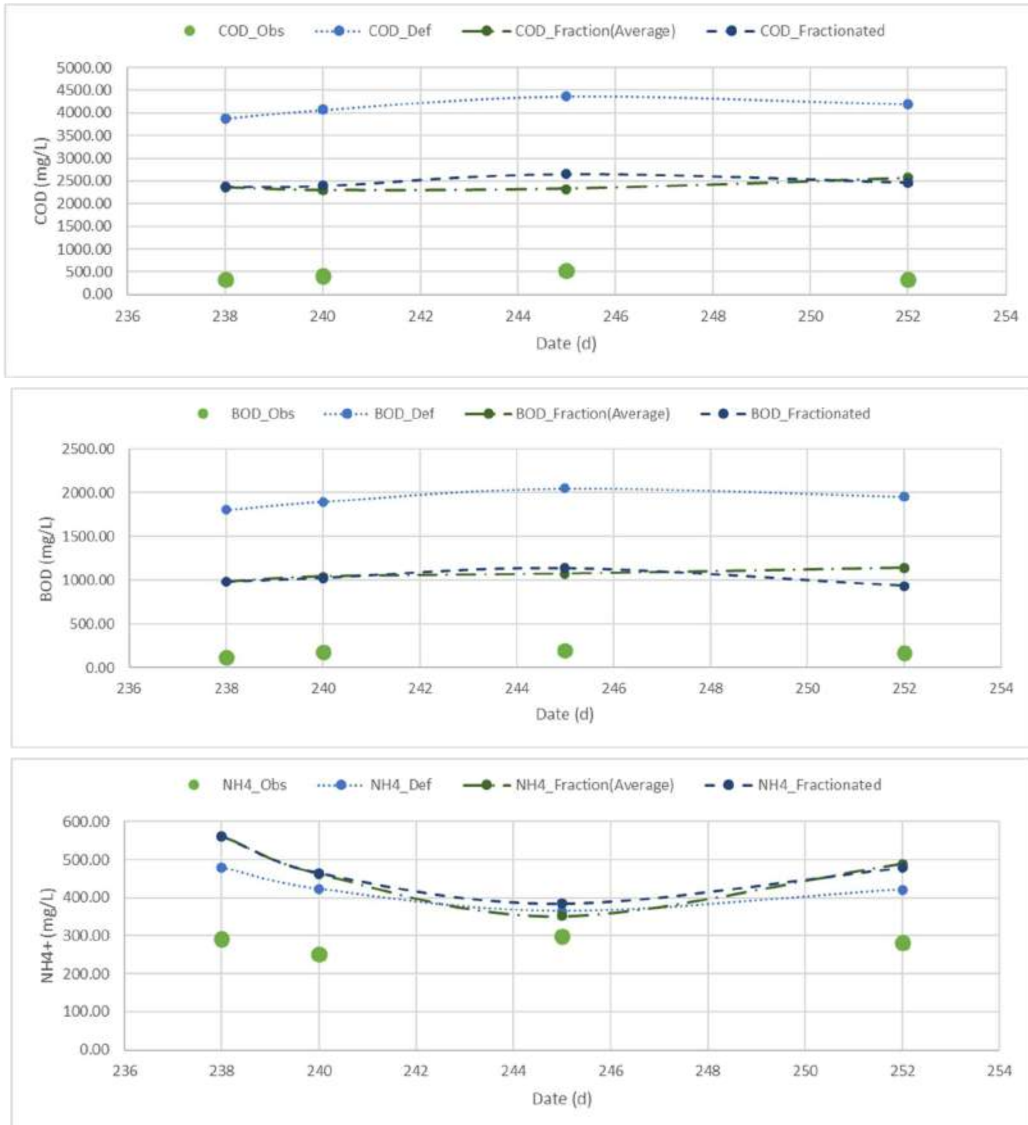

(2)

(3)

(4)

Figure 22. Track study for measured data (points) and corresponding simulated results (continuous line) on stage VIII of (1) TSS, (2) COD, (3) BOD_5 and (4) NH_4^+ concentrations for Condensate wastewater.

Source: Own elaboration.

6.3. CALIBRATION

6.3.1. CALIBRATION PROCESS FOR HKWW

- **SLUDGE PRODUCTION MODIFICATIONS FOR HKWW**

As presented in the Figure 23, scenarios 2, 3, 4, and 5 reproduce same TSS effluent results with a mean value of 8000mg TSS/L, scenario 3 are skewed to the right, even though all of them over reproduces TSS response in comparison with observed mean value of 665mg TSS/L.

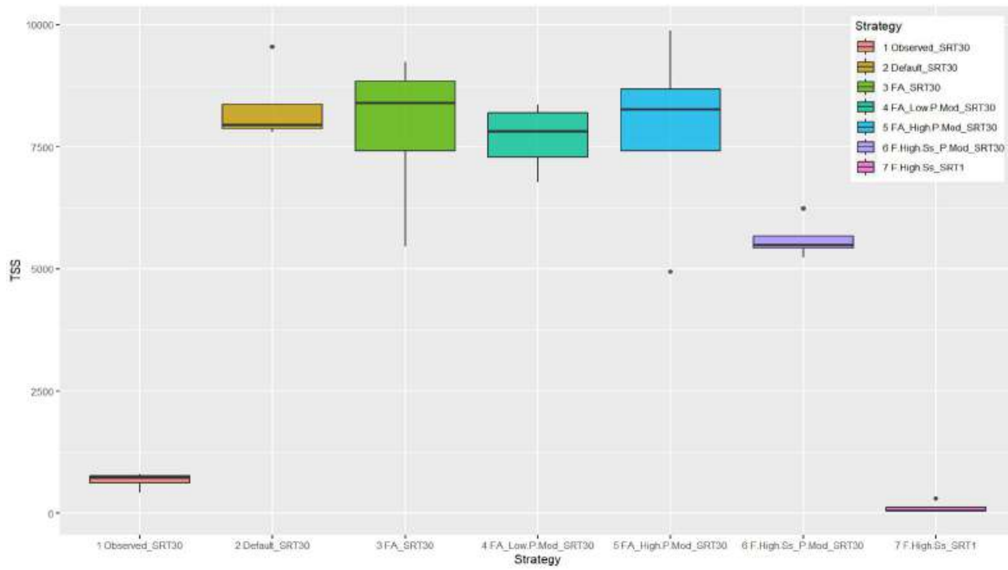

Figure 23. Observed and simulated strategies for TSS calibration.
Source: Own elaboration using software R-4.0.2.®, packages "ggplot2", and function "ggplot".

Analyzing scenario 3 on detail, which was the lowest TSS from the four realistic simulation scenarios (Figure 24), it was found that the pseudo-steady-state influent fractionation is characterized by high S_S content, and thus, during this period the TSS response is lower (around 5000mg TSS/L) than the four simulation points of stage II (8000mg TSS/L on average), which confirms that high S_S produce low values of TSS at the effluent. Additionally, it was found when the ISS increases the VSS decrease proportionally to keep 8000mg/L (mean value) of total suspended solids.

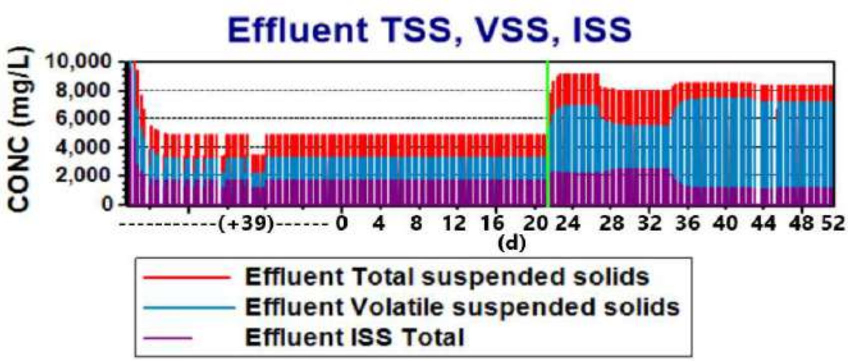

Figure 24. Effluent TSS concentration for scenario 3 FA_SRT30 scenario on stage II.
Source: Own elaboration running the BioWin software ®.

Analyzing scenario 6 on detail, which contains an unrealistic overestimated biodegradable COD fraction (high S_S). Additionally, coupling together high S_S fraction and low parameter modification, the simulated average TSS response is around 3000mg TSS/L for the pseudo-steady-state period (left side of Figure 25), and 5000mg TSS/L for stage II (right side on Figure 25). This phenomenon occurs due to two possible reasons: the dramatic phosphorous reduction at the influent or the fractionation change at the influent. The phosphorus was proven ones again, but the change in the fractionation presents a marked reduction in the TSS effluent response. Since the change in the fractionation from stable response, which occurs after the establishment condition (pseudo-steady-state, left side of Figure 25) is characterized for low the F_{BS} fraction, the TSS response increase (Stable response, right side of Figure 25).

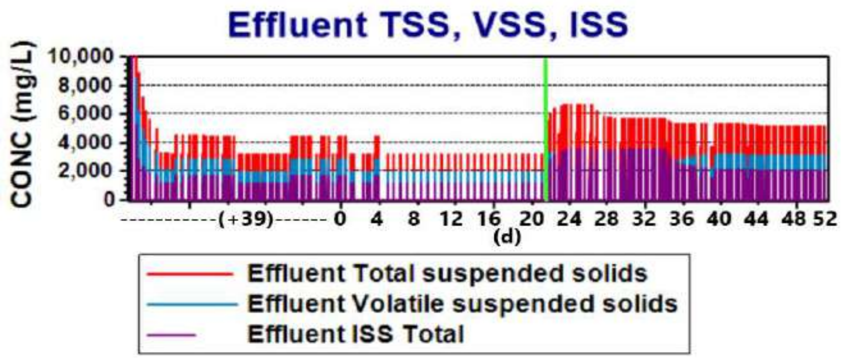

Figure 25. Effluent TSS concentration for scenario 6 High.SS_P.Mod_SRT30 on stage II. Source: Own elaboration running the BioWin software ®.

Simulation scenario 7 also contains an unrealistic overestimated biodegradable COD fraction (high S_S), and SRT equals to 1d. As presenting by Figure 26 both pseudo-steady-state and the four simulation points of stage II present lower sludge production. As seen in Figure 26, the scenario 7 was run with SRT of 1d which is an unrealistic operative condition, since the SRT in the pilot SBR was set as 30d and the S_S fractionation is calculated from the STOWA protocol (not suggested by the literature). Therefore, Figure 26 presents a detailed analysis of TSS response effect while changing the SRT variable.

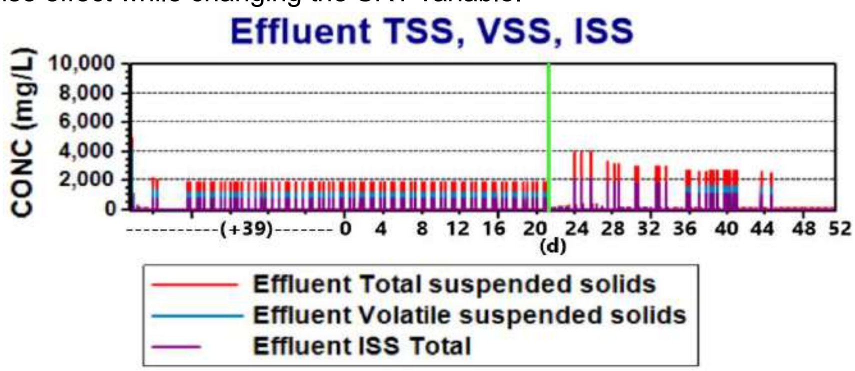

Figure 26. Effluent TSS concentration for scenario 7 High.SS_SRT1 on stage II. Source: Own elaboration running the BioWin software ®.

Figure 27 shows that only SRT equals 1d (scenario 5, Figure 27) present the high data dispersion, and biggest changes, but it does not necessarily imply that the mean value (around 4000mg TSS/L, as mean value) of this simulation scenario present the better fit with measured data. Only when SRT=1d and High S_S are couple together, the system response present closer results. The main issue with accepting the unrealistic fractionation is the lack of methodology to reply with another wastewater analysis and is an unrealistic operative condition.

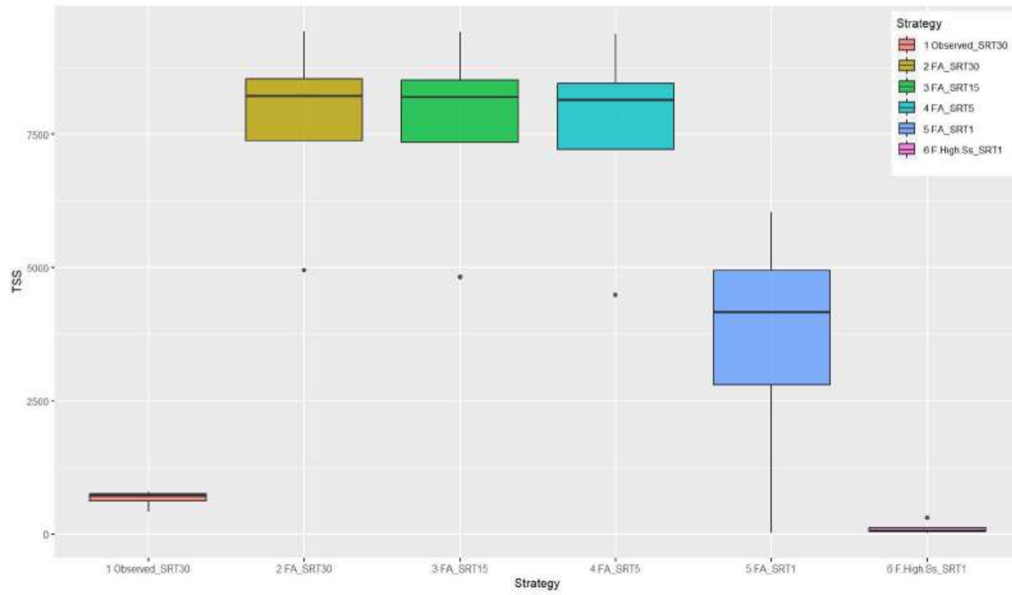

Figure 27. Observed and simulated strategies for TSS calibration based on SRT analysis on Stage II (HKWW).
Source: Own elaboration using the software R-4.0.2.®, packages "ggplot2", and function "ggplot".

- **CARBON PERFORMANCE FOR HKWW**

Carbon calibration is not too common in the GMP methodology, since carbon is the main driving force, and is, from the technical point of view, it is already considered from the fractionation of any influent. Although the analysis of S_S and X_I fraction do not present significant insights on carbon species responses presented in attachment 10.2.2, at next it will be present the effect of the seven simulation scenarios from the sludge production described in numeral a) from calibration of HKWW on 5.4.2 .
Although TCOD of all simulation scenarios are far from the observed data (strategy 1), result present an enhancement in the prediction of TCOD at the effluence since the mean value is reduced with the strategy 4 and 5. As happened for the sludge production analysis, the unrealistic strategies are the ones that present the better fitting results.

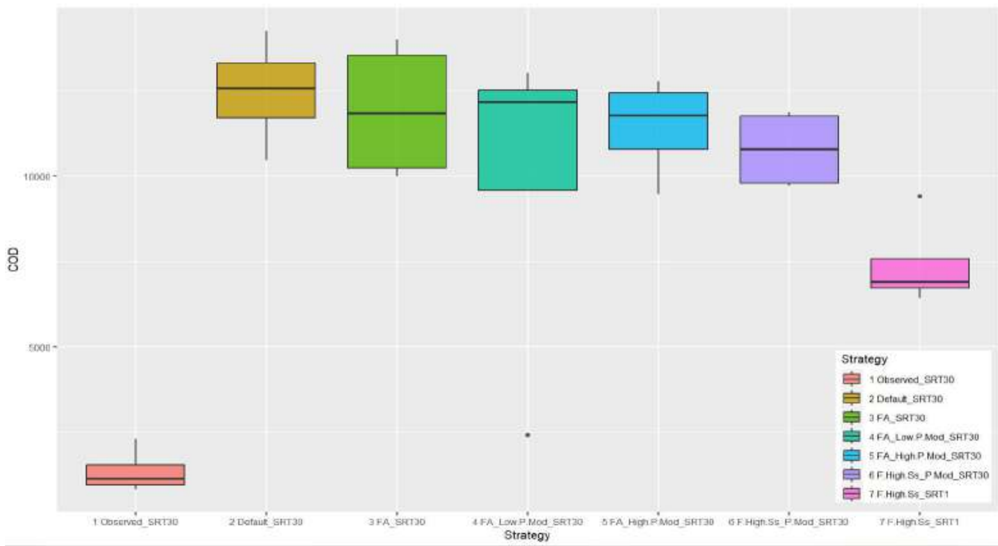

Figure 28. Observed and simulated strategies for TCOD calibration based on SRT analysis on stage II (HKWW).
Source: Own elaboration using the software R-4.0.2.®, packages "ggplot2", and function "ggplot".

BOD was also analyzed, in this case scenarios 3, 4, 5 that includes the STOWA fractionation present better BOD results than the unrealistic scenario 6 with high S_S fractionation. This finding suggests that the closest TCOD and BOD is reproduced by use of the STOWA fractionation, as expected.

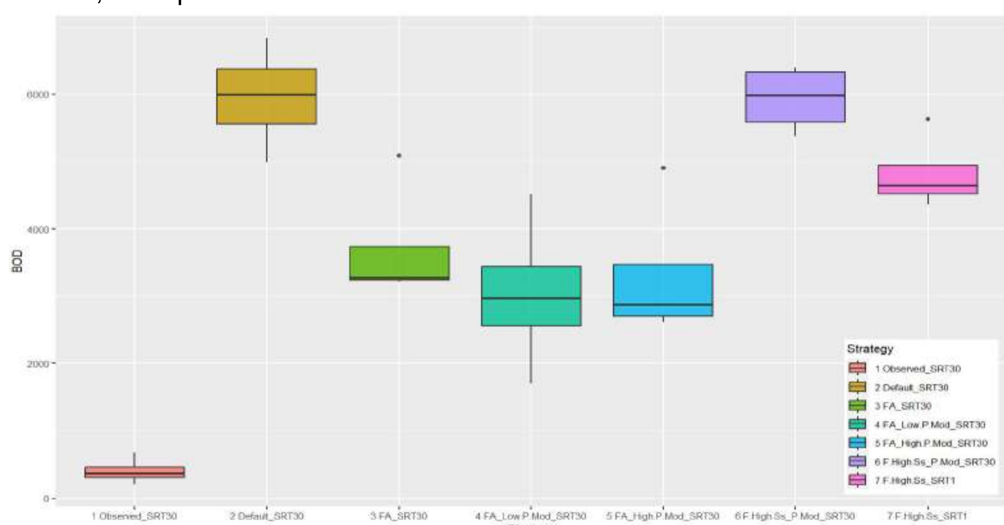

Figure 29. Observed and simulated strategies for BOD calibration based on SRT analysis on HKWW (stage II).
Source: Own elaboration using the software R-4.0.2.®, packages "ggplot2", and function "ggplot".

- **NITROGEN PERFORMANCE FOR HKWW**

Scenarios 3, 4, 6, and 7 do not present a relative change on the ammonium description and thus are discarded from this analysis. On the other hand, Figure 30 shows that the default fractionation (scenario 2) and increased model parameters (scenario 5) reproduce the closest values to observer NH_4^+ at the effluent. However, the effect of TSS response must be also considered, and thus scenario 5, it is the most suitable for describing the ammonium response. In conclusion, model parameter of scenario 4 is the most appropriate for describing the OHO behavior, but for better representation of the nitrogen species at the effluent, model parameters modification of scenario 5 are suggested.

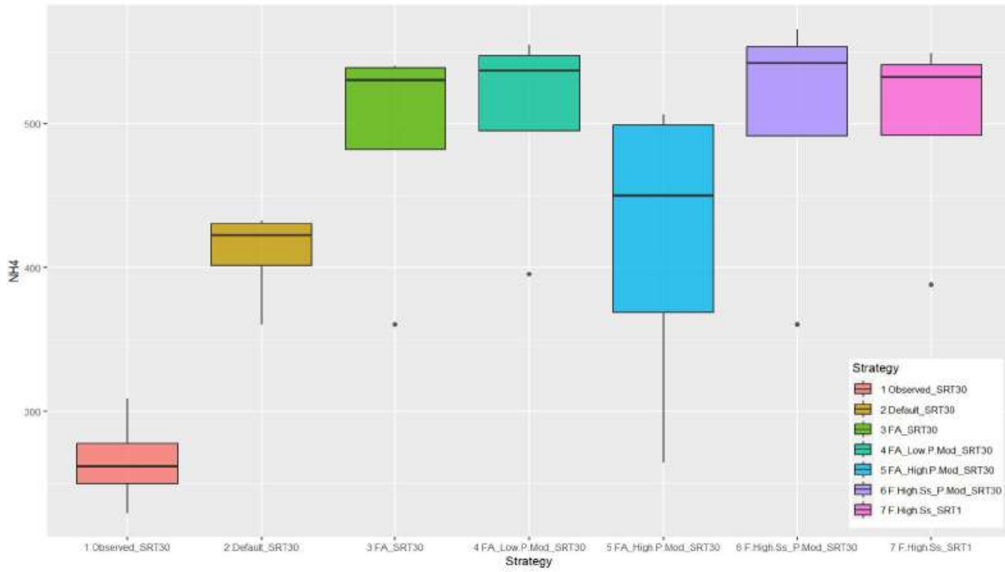

Figure 30. Observed and simulated strategies for TN calibration based on SRT analysis on stage II (HKWW).

Source: Own elaboration using the software R-4.0.2.®, packages "ggplot2", and function "ggplot".

6.3.2. FINAL HOUSEKEPING WASTEWATER SIMULATION

After the previous hydraulic load checking on numeral 6.2.1 and considering that the maximum hydraulic capacity of inflow is constant and set as 0.733m^3/d, nutrient loads will be also analyzed. Figure 31 shows that the pseudo-steady state is run until day 21 (left part of green line), a then the four nutrient step loads are presented one after another. Additionally, Figure 31 shows that the highest nutrient load for the HKWW is the carbon input (purple line Figure 31), which is compound of 51% of X_I and only 33% biodegradable (where up to 57% was S_F and 43% was S_A) based on the STOWA protocol results on numeral 6.1.3. Then carbon is followed by nitrogen, in this case the nitrogen is 92% soluble ammonia, the rest is present in its organic forms. Finally, 23% of phosphorus is present in soluble orthophosphates and the rest in organic P.

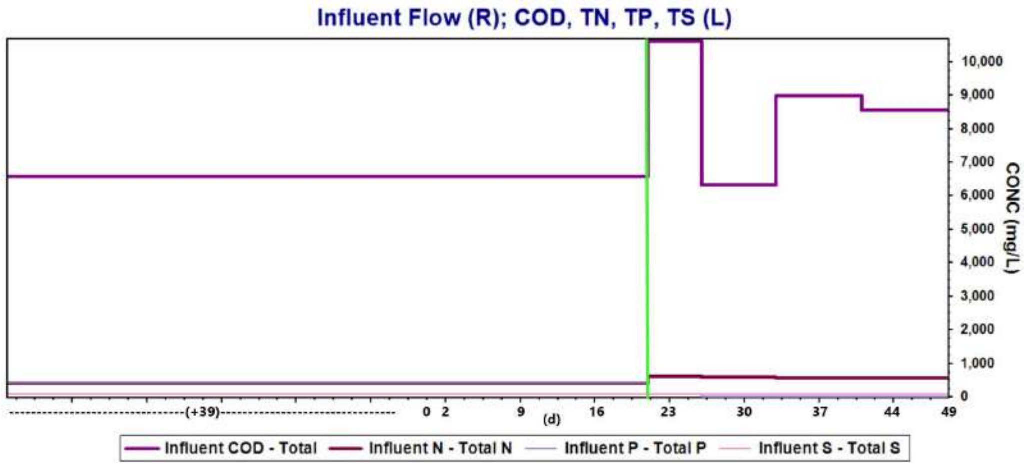

Figure 31. Flow/Nutrient chart: Influent flow (R for right axis) and nutrient concentration (L for left axis) stable stage II.
Source: Own elaboration running the BioWin software ®.

Apparently, the nutrient load response in the SBR system (Figure 32-1) behaves almost the same as the inflow presented in Figure 31, which indicates low transformation by the system, but analyzing the in process is recognizable that an small transformation of the COD is taking place in the SBR system, as well as for nitrogen and phosphorous but in a even small scale (comparing the delta from the initial and the last concentration). On the other hand, sulfur concentration is not transformed at all. The unfortunately small transformation of COD is caused mainly by the phosphorus deficit (purple line on the right side of Figure 32-1), since after the decrease of inflow P concentrations the COD concentration increased by the overload of carbon, which limits the OHO growth in 50% or more. When the BOD removal is ineffective, like in this case due to the high amount of FOG, the heterotrophic bacteria are numerous and out-compete autotrophic bacteria. This fact is proven by the extent of OHO microorganisms (red line on Figure 32-4) and reduction on the carbonaceous OUR values especially after the pseudo-steady state.

On the other hand, the low nitrogen removal is the result of ammonia and pH inhibition of ANO (autotrophs), and high oxygen concentrations. The high amount of unconverted ammonia produces an inhibitory and toxic environment for ANO microorganisms, that reduces its growth rate (Orhon et al., 2009). Additionally, the low pH (around 6 on Figure 33) cause inhibition of autotrophs, which requires a pH range between 6.5 and 7 (Brønd & Sund, 1994), and damage the nitrification process (i.e. inhibits more of 50% autotrophic growth rates) since the acid pH influences ammonium specie become the dominant, which is well known for inhibit nitrifying microorganisms. Finally, the high oxygen concentration is the consequence of the high intermittent aeration that increases the oxygen transfer coefficient (KLa), and thereafter, the oxygen concentration (Larrea et al., 2007). The high intermittent aeration is a good aeration strategy from the KLa point of view, if considering that at high temperature the KLa coefficient is even higher than for low temperatures. However, this oxygen excess inhibits the ANO growth that requires anoxic conditions rather than full aerated conditions. This fact is proven by the non-existence of ANO microorganisms (Figure 32-4) and low OUR values for nitrification (Figure 32-2). The excess of oxygen also affects the heterotrophic denitrification, which requires an even lower oxygen concentrations to force OHO to use NO_2 as electro receptor rather than O_2, in the hypothetical case that nitrites were high enough to develop the denitrification. These findings are also proven by the non-existence of ANO (dark blue lines on Figure 32-4), ADNO and its oxygen uptakes rates, who are not growing and accumulating in the system, although the SRT was set to 30d trying to keep them for enhancing the nitrogen removal.

After every overload of COD (red lines on Figure 32-1) the sludge production increases too, because of the high X_I COD fraction of the influent and the low reproduction of new cells (VSS on Figure 32-3).

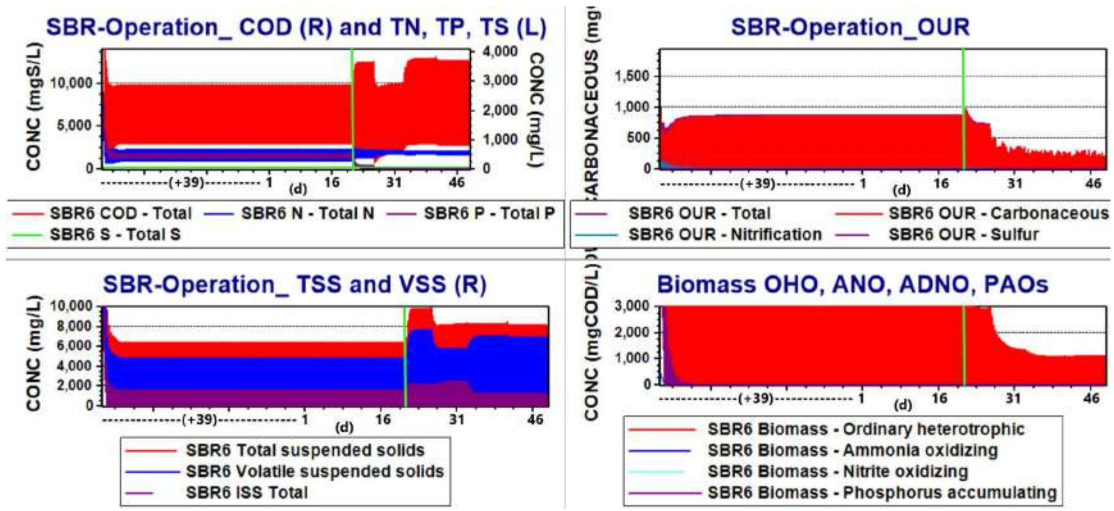

Figure 32. SBR operation chart: for (1) nutrient concentration, (2) OUR, (3) Solids as MLVSS and (4) the most important bio-communities content for the housekeeping wastewater.
Source: Own elaboration running the BioWin software ®.

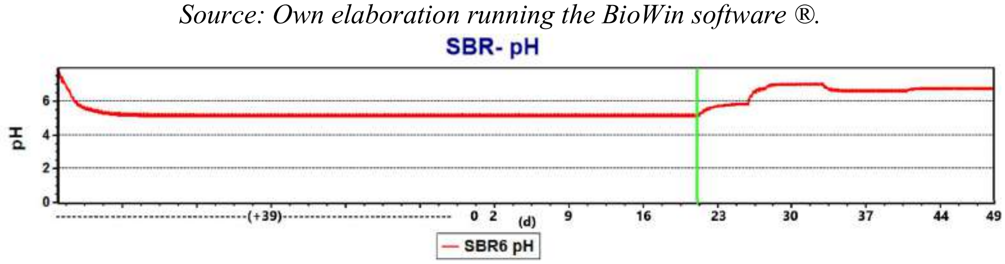

Figure 33. pH control chart during HKWW analysis (Stage II).
Source: Own elaboration running the BioWin software ®.

After every reaction and settling phase, the effluent is pumped out of the system, and contains the effluent performance concentrations. As presented in Figure 34-1 the percentage of COD, and N removal (Figure 34-2) is extremely low, considering the magnitude of the inflow and the drawn effluent results, as a consequence of inhibition conditions mentioned before. For instance, not all BOD is transformed in the system but discharged untransformed by the effluent, which is not common on regular biological systems. Figure 34-4 shows that with the increase in the inflow nutrients load the TSS on the effluent also increase due to the high X_I content in the COD input.

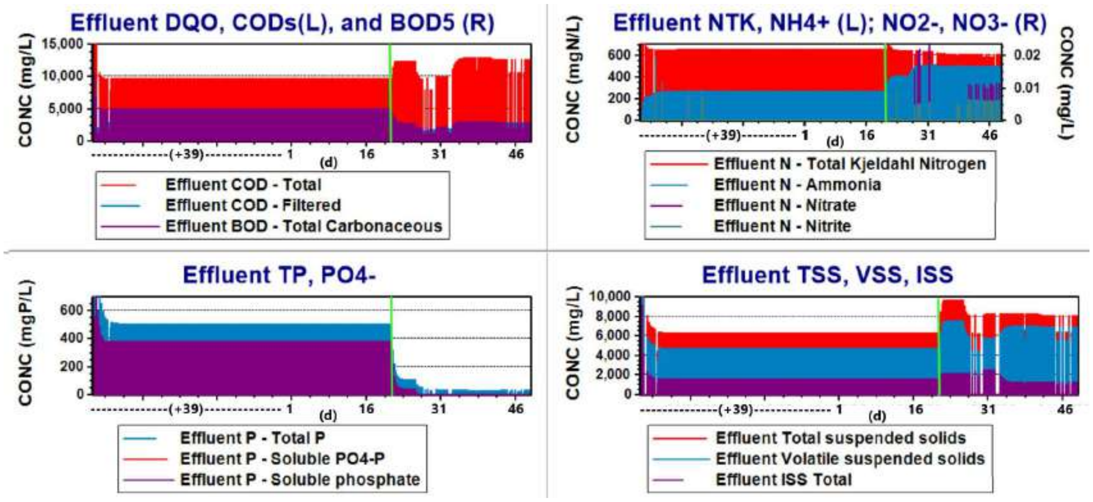

Figure 34. Effluent Performance chart: Effluent concentrations for Carbon (1), Nitrogen (2), phosphorous (3) species, and (4) solids for the housekeeping wastewater. Source: Own elaboration running the BioWin software ®.

As stated before, the KLa coefficient is too high due to the high times of intermittent aeration. This excessive aeration not only limits the denitrification process, but also causes a release, and loss of around 20% of the oxygen (Figure 35) that is transfer by the aerators.

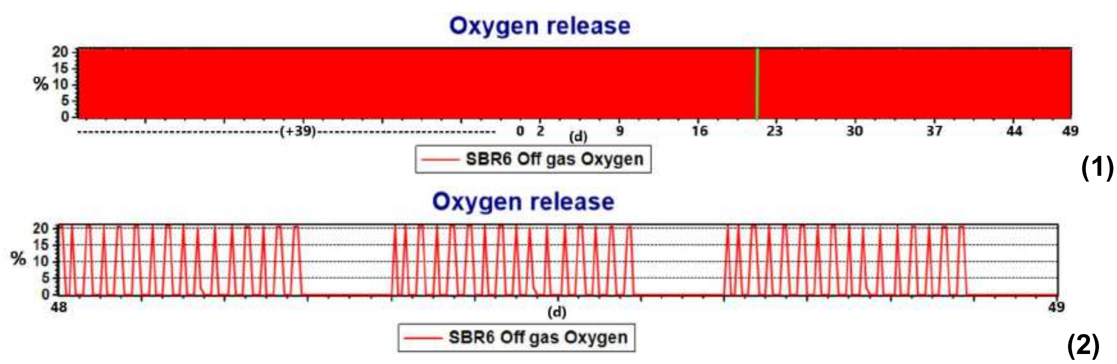

Figure 35. Off gas phase chart % of release of (1) Oxygen, (2) inprocess of the last day of simulation. Source: Own elaboration running the BioWin software ®.

As presented in Figure 36-1 round 60% of the carbon (the majority) is released in the form of carbon dioxide on the stable response period, i.e. The low biodegradable COD is not uptake for new growing cells due to the phosphorus deficit but is taken out the system as CO_2 due to the excessive intermittent aeration since the CO_2 is on agreement with the Oxygen release if comparing the peaks on Figure 36-2 and Figure 36-2.

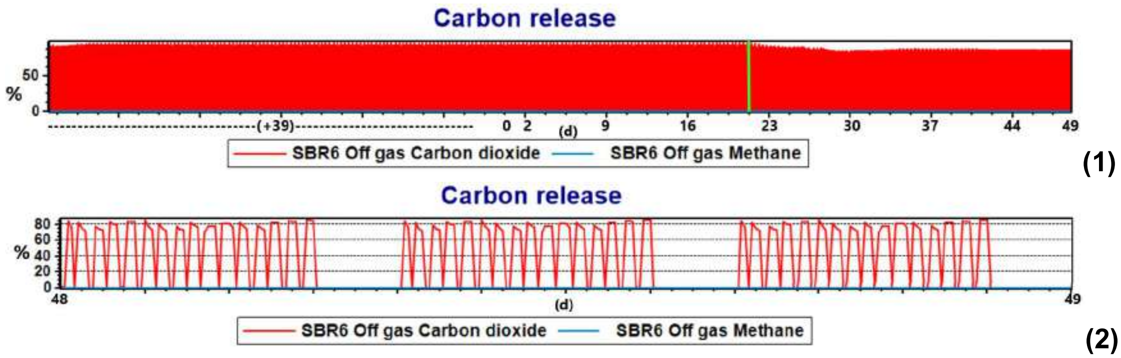

Figure 36. Off gas phase chart % of release of (1) Carbon, (2) in process of the last day of simulation.
Source: Own elaboration running the BioWin software ®.

Finally, Figure 37 at the stable response of stage II shows that only 3% on average of the inflow nitrogen is release out of the system, and this small release of nitrogen also match with the oxygen release (Figure 37-2) similar phenomena as for the carbon release. In the case of HKWW most of the nitrogen is discharged by the effluent.

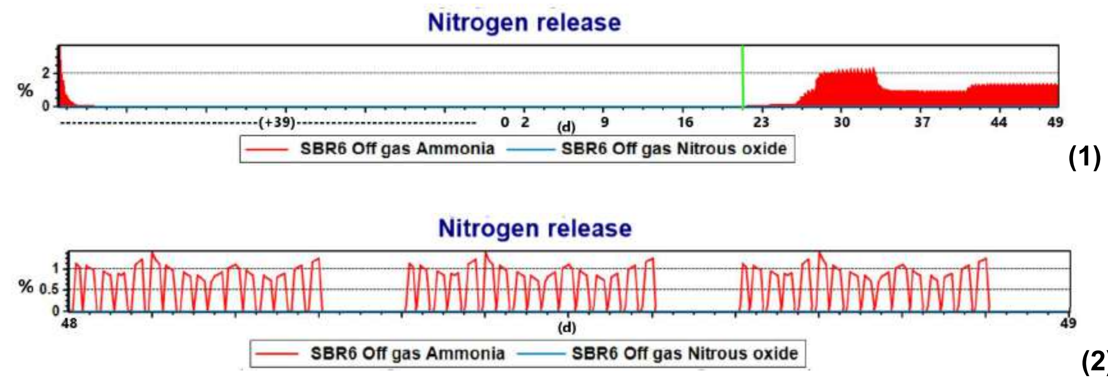

Figure 37. Off gas phase chart % of release of (1) Nitrogen, (2) in process of the last day of simulation.
Source: Own elaboration running the BioWin software ®.

6.3.3. NUMERICAL ASSESSMENT FOR KHWW

As shown Figure 38-1 and -2, the TSS, COD and BOD average (MAE) and standard deviation (RMSE) present relative high error values of 6000, 10000 and 3000mg/L per any new prediction, suggesting a further adjustment of the model. However, only the TSS exceeds the acceptance criteria of 10% (MAPE), which is a standardization to make easy the comparison between models. Although the high MAE and RMSE suggests that the model may not be performing well and could benefit from further calibration, it was also proven than the model prediction was enhanced when fractionating the influent and calibrating the model parameter, as shown for the decreasing values of MAE and RMSE from default values, in comparison with the fractionation of the influent alone, and finally by fractionating the influent and adding the model parameter changes. In general, the ammonia state variable presents the best Good-of-fit, low MAE, RMSE and MAPE.

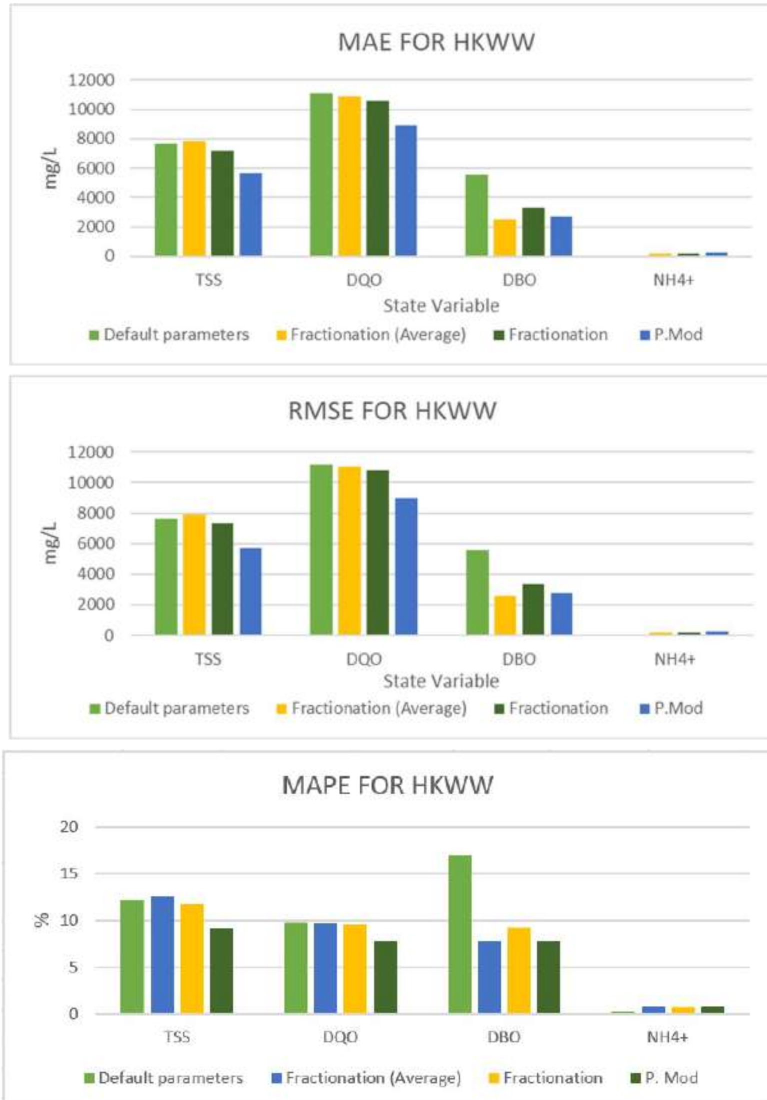

(1)
(2)
(3)

Figure 38. Comparison of good-of-fitness assessment for (1) MAE, (2) RMSE, and (3) MAPE in steady-state with default, fractionation, fractionation average and parameter modifications values. Source: Own elaboration based on the software R-4.0.2.®.

6.3.4. CALIBRATION PROCESS FOR CWW

As follows, the results of the final sensitivity analysis for CWW (stage VIII) were obtained similarly to HKWW calibration.

- **SLUDGE PRODUCTION MODIFICATIONS**

As seeing on Figure 39, the TSS concentration at the effluent from the real system is extremely low, which shows that the system is suffering washout not only because of the hydraulic overload, but also due the microorganism's death due to the high inhibitory environment. In this case, scenario number 4 presents one of the closest results to the observer data. It's also important to note that different to HKWW in this case the fractionation plays a fundamental role in the TSS prediction (scenario 3, 4, or 5 Vs 2). Similar as for HKWW the scenario, with the SRT equals 1d, shows the closest result against the observed data. However, this scenario is made under non-realistic assumptions.

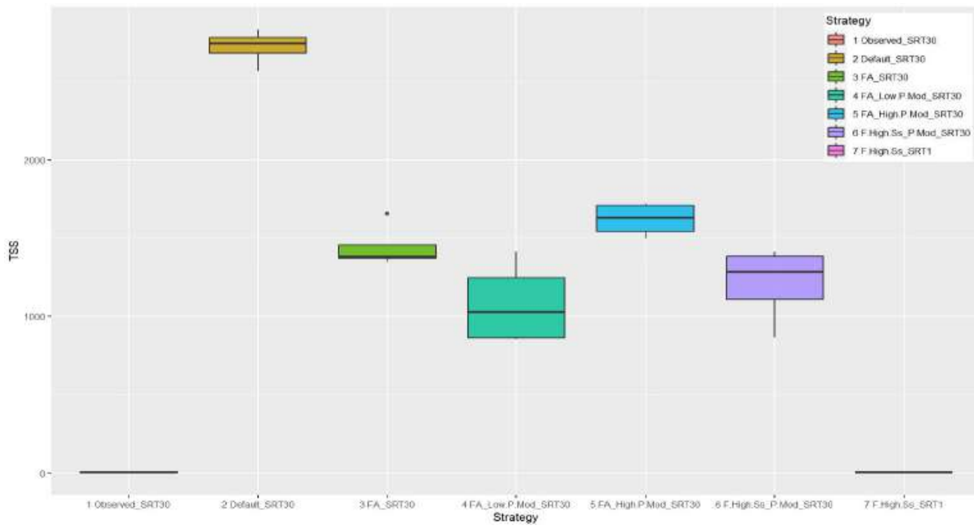

Figure 39. Observed and simulated strategies for TSS calibration based on SRT analysis on Stage VIII (CWW).

Source: Own elaboration using the software R-4.0.2.®, packages "ggplot2", and function "ggplot".

- **CARBBON PERFORMANCE REMARKS**

CWW presents an even lower COD and BOD concentration at the influent than HKWW, and thus the carbon at the effluent is lower (Figure 40). Similarly, as results before for sludge production, scenario 4 presents the better result from the realistic point of view. On the other hand, the closets result belongs to the un-realistic scenario of SRT equals 1d.

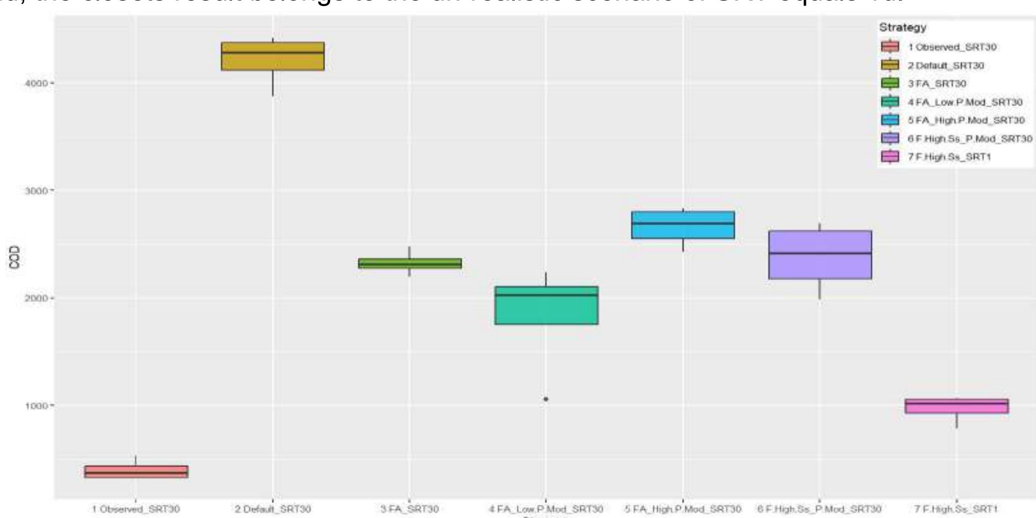

Figure 40. Observed and simulated strategies for TCOD calibration based on SRT analysis on stage VIII (CWW).

Source: Own elaboration based on the software R-4.0.2.®, packages "ggplot2", and function "ggplot".

Similar to HKWW the fractionated (scenario 2) and default (scenario 3) model parameter preset the best BOD performance than scenario 4 with the low model parameter modification (Figure 41), which confirms the relevance of the STOWA fractionation methodology. As mentioned before, TSS calibration has a higher importance criterion than carbon, and thus scenario 4 continuous being the possible selected scenario for describing the simulation of CWW.

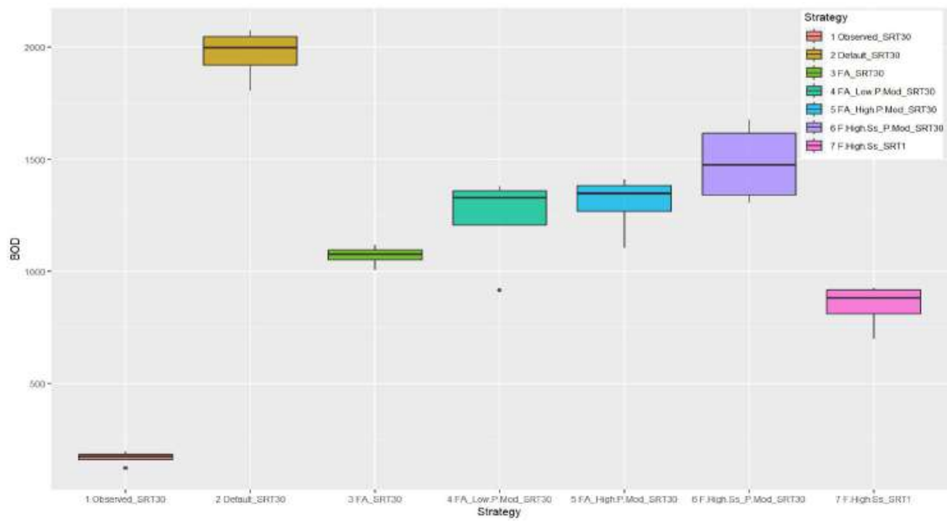

Figure 41. Observed and simulated strategies for BOD calibration based on SRT analysis on stage VIII (CWW).

Source: Own elaboration based on software R-4.0.2.®, packages "ggplot2", and function "ggplot".

- **NITROGEN EFFLUENT REMARKS**

As seen on Figure 42, scenarios 4 with low and 5 high model parameter modifications present respectively an overestimation and underestimation of the ammonia effluent results. The non-realistic scenarios 6 and 7 present the worst ammonia concentration results, supporting the idea that variables to calibrate sludge production are not necessarily the same to nitrogen or other nutrients of analysis.

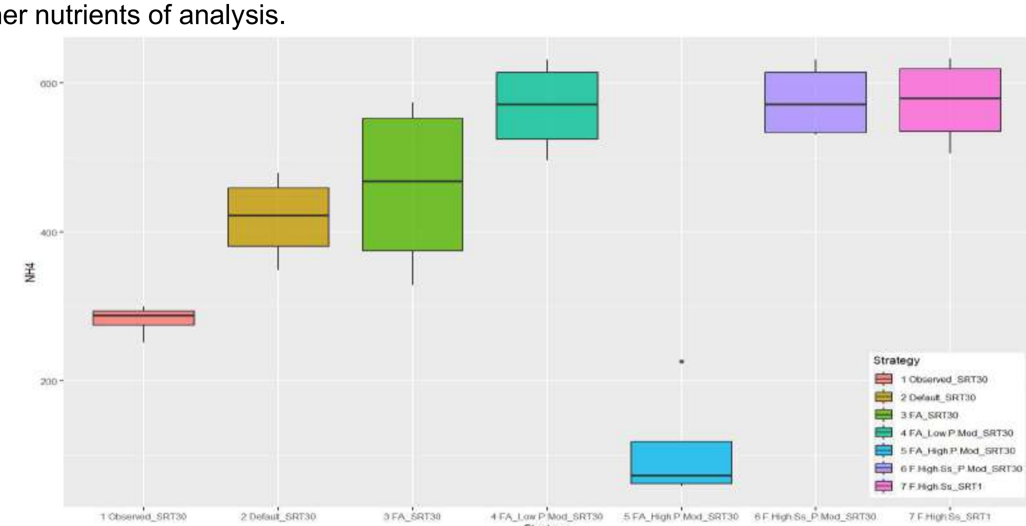

Figure 42. Observed and simulated strategies for TN calibration based on SRT analysis on stage VIII (CWW).

Source: Own elaboration based on software R-4.0.2.®, packages "ggplot2", and function "ggplot".

In general, scenario 4 present the better results for TSS, COD, BOD, but not for effluent ammonia, thus, intending to meet a suitable trade-off the final scenario will be the mean value suggested from Nakhla, Liu & Bassi (2006) and Nowak et al. (1996) that studied CWW of rendering processing facilities, and that will be presented as next.

6.3.5. FINAL CONDESATE WASTEWATER SIMULATION

In this case, the pseudo-steady state begins from day 178, the microorganism's establishment was reached in the first 15 days. Unlike the HKWW, the CWW nitrogen load (red line Figure 43) tends to be as high as the carbon load (purple line Figure 43). For this matrix the carbon compound is of 80% of S_S (where up to 82% was S_F and 18% was S_A) and only 10% X_s according to the STOWA protocol results on numeral 6.1.3. The fractionation of nitrogen is compound of 95% is soluble ammonia the rest is present its organic forms, and 40% is soluble orthophosphates and the rest organic P.

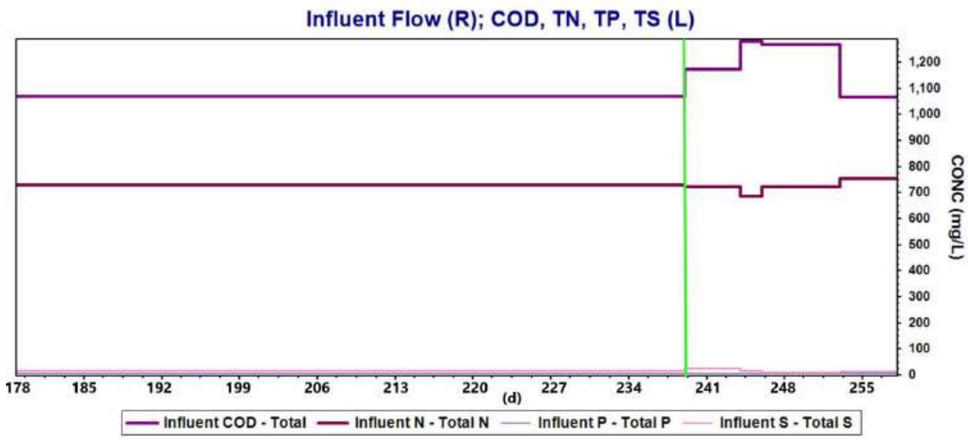

Figure 43. Flow/Nutrient chart: Influent flow (R for right axis) and nutrient concentration (L for left axis) stable stage.
Source: Own elaboration running the BioWin software ®.

The CWW presents a constant carbon load concentration as presented in red on Figure 44-1, and a variable nitrogen load (blue line on Figure 44-1). Similar as for HKWW, the in-process shows that after the reaction phase of any cycle the system can transform a small amount of the TCOD and nutrients, which is demonstrated by the down slope in Figure 44-1. Although the TCOD input for HKWW is higher than for CWW, the COD removal is higher for this matrix than for HKWW, as demonstrated by the amount of OHO microorganism (Figure 44-4) and the oxygen uptake rate (Figure 44-3). This fact is caused because the CWW present a higher biodegradable content (S_S) than for HKWW and the phosphorous content, and the small removal of TCOD is mostly caused by the low input of phosphorus that limits the microorganisms growth in more than 50%, as well as the limitation of calcium and magnesium, which in turns is low for the CWW (10.9 mgCa/L and 0.8mg Mg/L) than for HKWW (26mg Ca/L and 7mg Mg/L). In general, in HKWW and CWW simulations the carbon removal is extremely low, although in this case wash out is happening, which again reconfirms that the system removal is undertaken by physical mechanisms rather than biological.
Additionally, when the biodegradable COD is higher than the inorganic particulate fraction, as

happened for the HKWW, the sludge production is reduced as demonstrated by comparing Figure 44-3 (around 3000mg TSS/L) and Figure 32-3 (around 8000mg TSS/L).
As presented in Figure 44-3, the SBR operation chart shows and average carbonaceous-OUR of 70mg O_2/L*h suggest that only heterotrophs are dominating, but autotrophs are limited completely, fact that is support as well by the Biomass concentration in the bio-communities Figure 44-4, only the red color is plotted, not the blue ones. Therefore, there is no oxygen consumption or ANO microorganisms that perform nitrogen nitrification or removal. In this case, the nitrogen removal is caused mostly by the release of nitrogen as stripped ammonia as presented in Figure 49-1, the off gas of nitrogen demonstrated that more than the 50% of the nitrogen is release as ammonia, rather than being transformed or uptake by microorganisms, making this remotion a physical process due to the harsh environmental condition (pH, alkalinity) rather than biological process. The ammonia stripping occurs when ammonium is speciated as ammonia (NH3) due to the increase in the pH (PH>8), then the ammonia is released by the high aeration pattern. Also, it is not a biological process that governs the nitrogen removal because the high ammonia concentration and high pH inhibit the grow of ANO microorganisms.

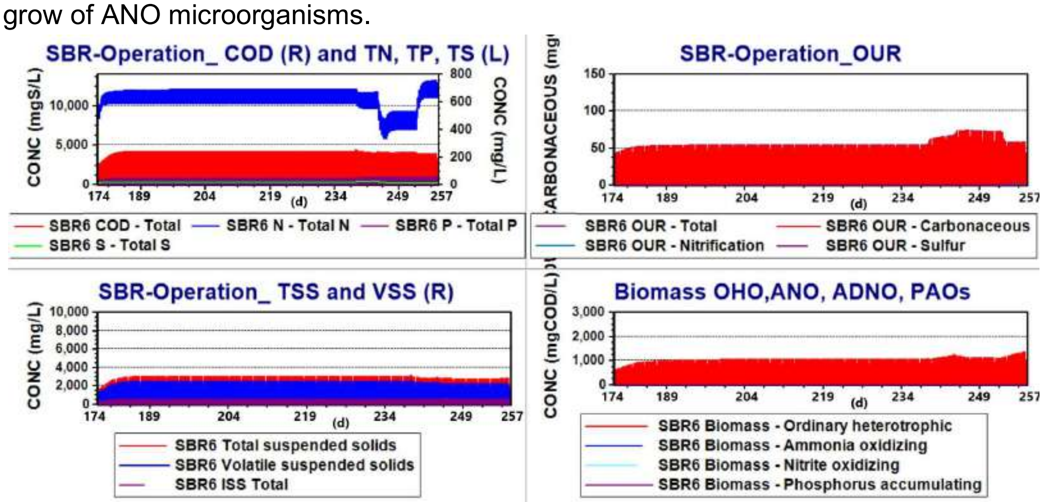

Figure 44. SBR operation chart: for (1) nutrient concentration, (2) OUR, (3) Solids as MLVSS and most important (4) bio-communities content for condensate wastewater.
Source: Own elaboration running the BioWin software ®.

The inhibition of OHO is so extreme that the untransformed BOD concentration is still high at the effluent as presented by the purple line on Figure 45-1 (around 2000mg BOD/L), and similar happened for the nitrogen removal, as seeing on Figure 45-2 the Nitrites and nitrates concentrations are too low because of the ammonia, pH and nutrient concentrations. In this case, the sludge production is not as high as for HKWW, but it is still too far from the measured data due to wash out caused by the nutrient disbalance.

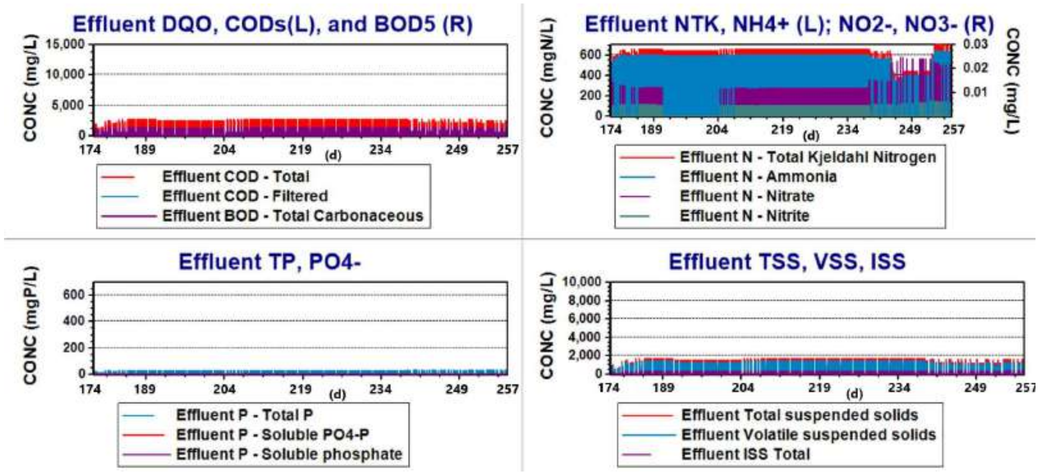

Figure 45. Effluent Performance chart: Effluent concentrations for Carbon (1), Nitrogen (2), phosphorous species (3), and (4) solids for the condensate wastewater.
Source: Own elaboration running the BioWin software ®.

The CWW presents an uncommon pH behavior, since the pH response tends to be basic rather than acid. It is important to highlight that the alkalinity of this matrix is lower than the HKWW, which means a vulnerability due to the pH variations (Figure 46). Additionally, nitrogen aid in the alkalinity contain in the CWW, since the ammonia, produced during the hydrolysis process, and catalyzed by the heat process in the cooker-batch equipment, reacts with the CO_2 to form ammonium bicarbonate contributing to the alkalinity in the reactor (Nakhla et al., 2003).

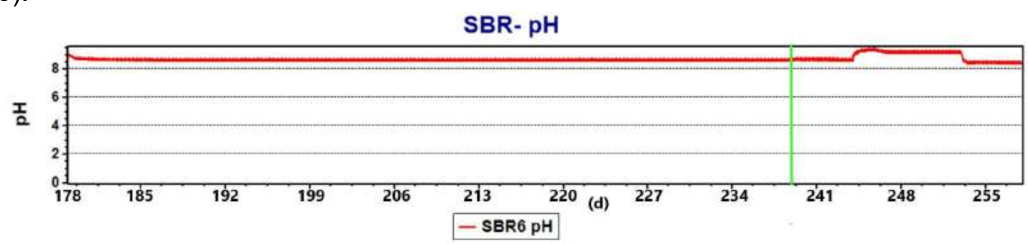

Figure 46. pH control chart during stage VIII.
Source: Own elaboration running the BioWin software ®.

Similar as HKWW, the CWW is operated under a high loaded oxygen pattern and thus the oxygen release arises to 20% of the bubbled oxygen by the aeration system.

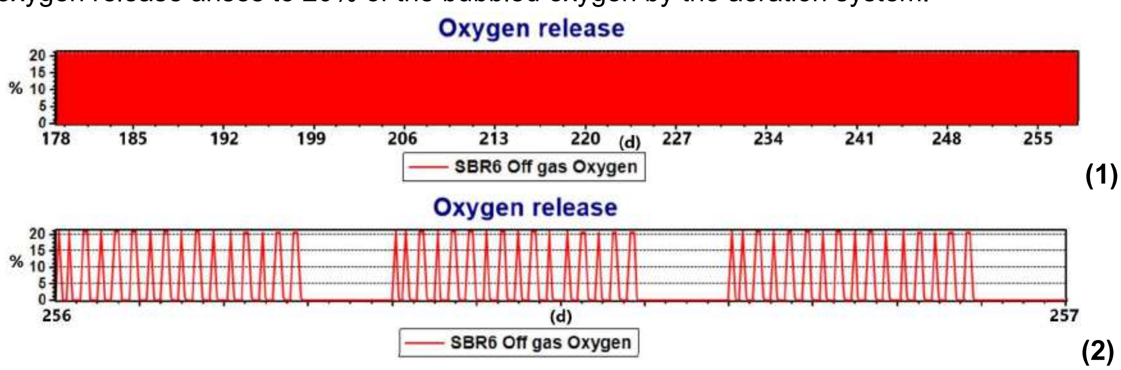

Figure 47. Off gas phase chart % of release of (1) Oxygen, (2) in process of the last day of simulation.
Source: Own elaboration running the BioWin software ®.

The CWW presents a lower release of carbon in the form of carbon dioxide (between 10% and 40%), amount that is less than for the 60% of the HKWW and is also because of the inhibition condition and the aeration pattern (Figure 48). Because S_S fraction is higher for this matrix, the carbon release is lower for this matrix since it is being uptake in high extend by microorganisms than for HKWW.

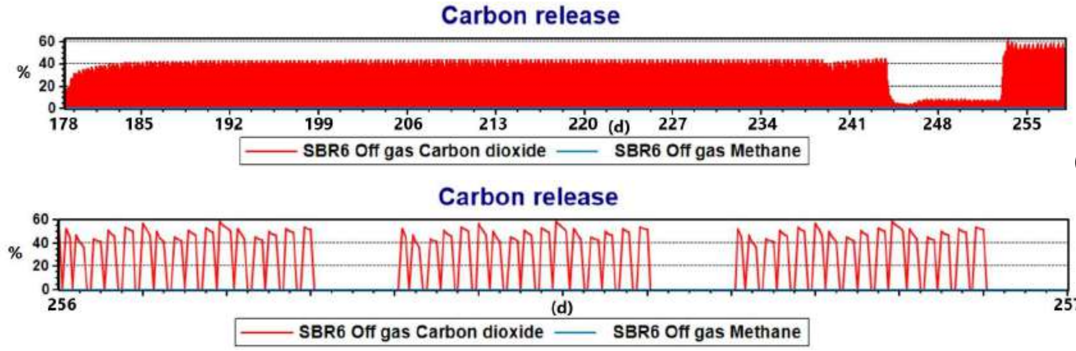

(1)

(2)

Figure 48. Off gas phase chart % of release of (1) Carbon, (2) in process of the last day of simulation.
Source: Own elaboration running the BioWin software ®.

Because this matrix presents a higher nitrogen input and basic pH, the nitrogen release in form of ammonia is also high in comparison with the HKWW (between 40% and 80%). Similar as the carbon release the nitrogen in for of ammonia is caused by the aeration system as presented by comparing the in-process peaks of oxygen (Figure 47-2) and nitrogen release (Figure 49-2).

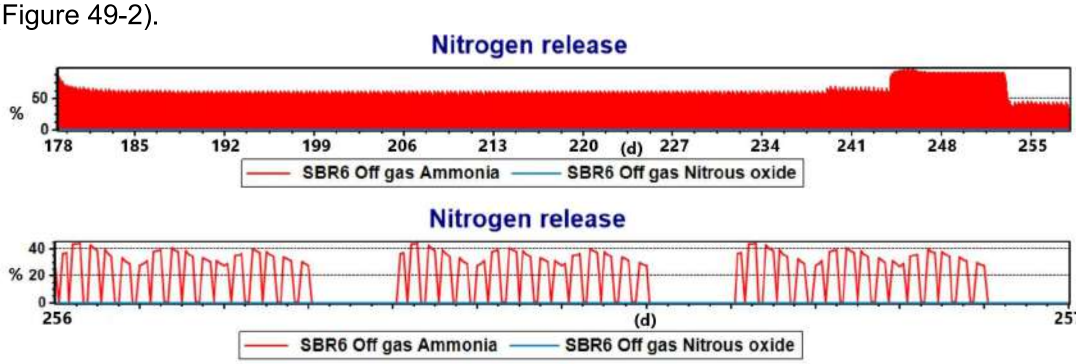

(1)

(2)

Figure 49. Off gas phase chart % of release of (1) Nitrogen, (2) in process of the last day of simulation.
Source: Own elaboration running the BioWin software ®.

Although in literature is suggested to treat the rendering effluent due to its high organic component as VFA, which are easily biodegradable organics (Metzner & Temper, 1990; Brønd & Sund, 1994), the reality is that this kind of effluent also content a high particulate and slowly organic matter content that inhibits the growth of microorganisms (from fats and grease mostly). Thus, it is suggested the use of thermophilic process and use of surfactants to aid the fat and grease removal by increasing solubility, and hereafter, the biodegradability (Nakhla et al., 2003). Additionally, complete denitrification could be achieved with COD/N ratio larger than 5, and high pH should be buffered in range of 6,5 to 7 to prevent shock load, otherwise nitrification could be affected by nitrifiers inhibition (Brønd & Sund, 1994). Auterská & Novák (2006) suggested that external carbon source is not only necessary for enhance of denitrification but also to remedy the nitrifiers inhibition, since ammonia is transformed into biomass.

6.3.6. NUMERICAL ASSESSMENT FOR CWW

As shown in Figure 50-1 and 2 the TSS, COD and BOD average (MAE) and standard deviation (RMSE) of errors change from 2500, 3600 and 1800mg/L to 1200, 1200 and 800 mg/L respectively, when changing from the default parameters to the influent fractionation and model parameter calibration. However, when analyzing the MAPE results its seeing on Figure 50-3 that the TSS present an error of more than 300% for the four evaluation scenarios, not only exciding the acceptance criteria of 10% (MAPE), but also suggesting that the model should be subject to better fitting. In general, the ammonia state variable presents the best Good-of-fit, low MAE, RMSE and MAPE, less than 10%.

(1)

(2)

(3)

Figure 50. Comparison of good-of-fitness assessment for (1) MAE, (2) RMSE, and MAPE in steady-state with default, fractionation, fractionation average and parameter modifications values. Source: Own elaboration using the software R-4.0.2.® packages "zoo" and "hydroGOF" and function "gof".

6.4. SIMULATION AND RESULT INTERPRETATION.

6.4.1. SIMULATION OF DIFFERENTIAL OVERLOAD OF CARBON/NITROGEN

The pseudo-steady state was simulated 60 days (2SRT) before day 0 of measure data, and the microorganism's establishment occurred after day 57 of simulation (Figure 51). As is seen on Figure 51 the system suffers a solids overload at stage V (80% of HKWW and 20% of CWW), which coincides with the nutrient overload presented in Figure 53. The solid and nutrient overload in this specific case does not physically wash microorganisms out of the system but inhibits and reduces its population due to the harsh environmental conditions. This overload is caused mainly by the high grease and oil that enters the system due to the failure in the coagulation process prior to the SBR system as suggested by Rodriguez et al. (2011). Nakhla, Liu & Bassi (2006) stated that the high oil and grease caused 57-70% degradation rate reduction in apparent biomass. Finally, measured data presents even higher values of sludge washout (low TSS) and thus ISS calculation presents some errors.

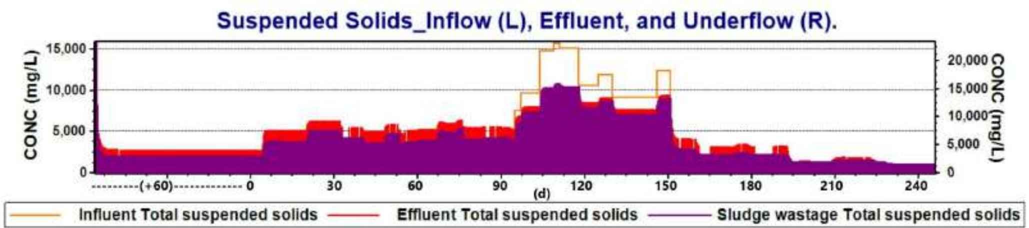

Figure 51. Flow chart: Influent flow at the left axis (L), while the effluent and underflow stay at the right axis (R).
Source: Own elaboration running the BioWin software ®.

This solids and nutrient overload also influence the SRT, since at stage V the SRT is reduced al half of the original (30d) as presented in Figure 52, which basically means that not only the hydraulic overload affect the solid retention time, but also the nutrient overload. Although the SRT is reduced considerably, in climate regions is possible to work nitrification plants with SRT from 5d to 10d, when ensuring enough oxygen supply.

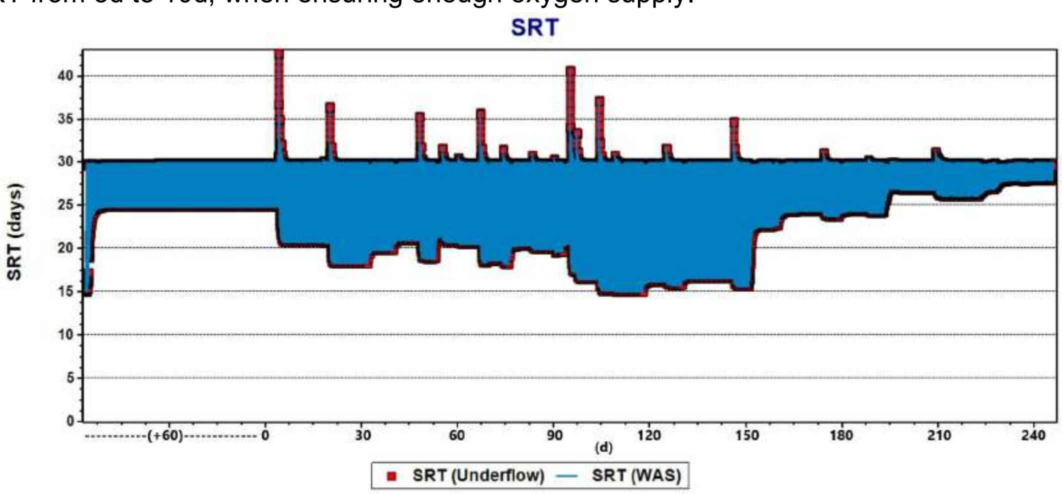

Figure 52. SRT chart: Sludge retention time (sludge age) during stage I to VIII.
Source: Own elaboration running the BioWin software ®.

As presented in Figure 53 the HKWW contents a high carbon load, and low nitrogen load (until day 77 i.e. Stages I, II and III), in contrast, the CWW contents a high nitrogen load, and lower carbon load (from day 233 to 252 i.e. Stage VIII). However, the system presents an unusual carbon overload during stage IV and V that triggers a most difficult environmental condition for the different microorganisms' communities, which is caused by an overload of grease and oil. Although the COD/N or COD/P ratio are lower for the CWW than for HKWW, the CWW is more "biodegradable" than the HKWW fact that is demonstrated based on the amount of S_S, and nutrients availability.

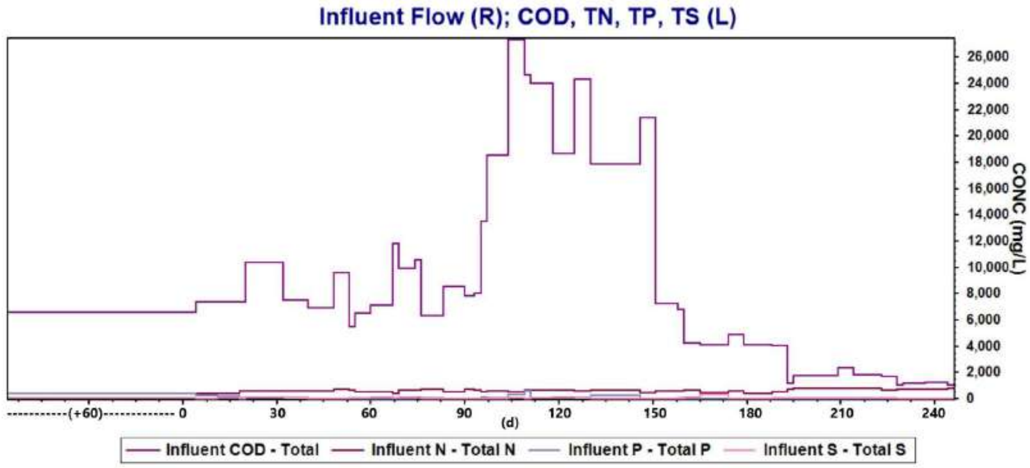

Figure 53. Flow/Nutrient chart: Influent flow and nutrient concentration (L for left axis) stable stage. Source: Own elaboration running the BioWin software ®.

Figure 54-1 and Figure 54-3 confirm the carbon and solids overload that occurred at stage IV and V due to the rapid increment in the red line (both cases), and thus, the system is not removing enough carbon at the effluent as will be present on Figure 55-1. This carbon overload affects microorganisms and its effect is represented by the reduction in the oxygen uptake rate and the microorganisms biomass, as seeing in Figure 54-2 and Figure 54-4, where the carbonaceous OUR and OHO biomass decreased at stage IV and V as a result of the carbon and solids overload, i.e., previously it was announced that the CWW present a higher biodegradable and soluble COD fraction that enhance the existence of OHO microorganisms and it removal, but for the whole simulation campaign it is seeing than after the carbon overload the OUR (Figure 54-2) and OHO microorganisms (Figure 54-4) remains the same as for HKWW (around 100mg O/L*h and 2000mg OHO/L).

Nether the HKWW nor CWW ANO microorganisms are growing and developing in the SBR system as presented by the absence of Nitrification OUR (Figure 55-2) and Ammonia oxidizing biomass (Figure 54-4) due to the nutrient deficit as phosphorous (for the entire project), calcium and magnesium (specially for CWW) and pH inhibition (specially for the HKWW).

In many scientific reports authors stated that COD/TKN> 6 or more would maximize nitrogen removal (Filali-Meknassi et al., 2004), which is specially need it, in the denitrification process, but this guideline it is right when the majority of COD is in the form of S_S fraction, especially S_A, which is for example one of the main components in the CWW contain in the volatile fatty acids components (Metzner & Temper, 1990), also, when the aeration pattern is not a limiting factor for denitrification, and pH dont limited the OHO or ANO growth, because they are also two factors that plays an important role on the growth of microorganisms to ensure the nitrification process.

When the carbon and solids overload occur, the solid in the SBR system increases dramatically (Figure 54-3). This fact could be attributed to the high amount of particulate inert COD fraction that is content in the HKWW, 90% and 80% of HKWW respectively on stage IV and V. As a result, the system is not removing neither the solid at the effluent as presented in Figure 55-4.

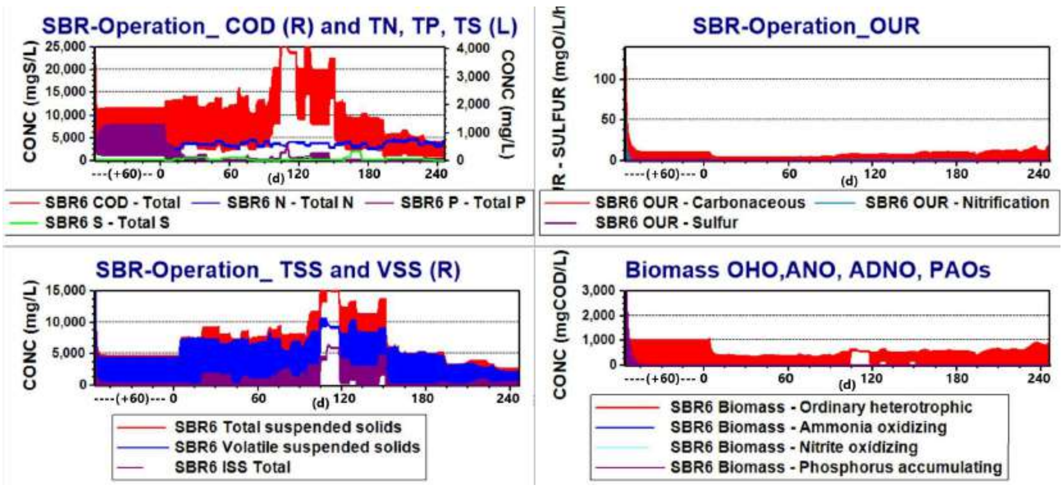

Figure 54. SBR operation chart: for (1) nutrient concentration, (2) OUR, (3) Solids as MLVSS and most important (4) bio-communities content for condensate wastewater.
Source: Own elaboration running the BioWin software ®.

Fully nitrification/denitrification is not occurring in this SBR system, as represented by the low concentrations on NO_2^- and NO_3^- on Figure 54-2, and the low difference between NH_4^+ at the influent and effluent. The nitrogen is not fully nitrified by autotrophs microorganisms in the entire different load project due to problems with the excess of aeration, low alkalinity, pH inhibition, and nutrient deficit (phosphorus) concentrations. Autotrophs microorganisms need non-organic carbon sources as CO_2 and HCO_3^- (autotrophs), but the excess of aeration is stripping the CO_2 first, and then the low HCO_3^- tries to compensate the CO_2 deficit by transforming itself due to the pH conditions. Additionally, the meat industry wastewater presents low base HCO_3^- concentrations (HKWW and CWW) that is represented by the low alkalinity, so there is not enough non-organic carbon source for nitrifiers to thrive.

Another reason why nitrifiers do not survive is due to the pH inhibition, in both wastewater matrices the pH was out the optimal range for autotroph growth (6.8 to 7.5 of pH, Figure 56). The pH inhibition reduces more than 50% the growth rate of heterotrophs and autotrophs microorganisms and is also related with the low alkalinity. When there is low alkalinity in the wastewater, the acid (H^+) produced for ammonia oxidizers inhibit the nitrate oxidizers growth. Thus, if nitrification were correctly working the system pH should not be so basic as it is for CWW, since the nitrification process produces large amounts of hydrogen that creates an acid environment (Chen et al., 2020).

Although it seems to be a good pH range for stage VI, VII and VIII, there is another issue for the correct treatment related with the nutrient deficit, which is another inhibition source, since Nitrifiers also required phosphorus to reproduce new cells (Chen et al., 2020). Finally, for the current treatment system, the only requirement for nitrifiers that was over met, was the oxygen supply due to the intensive aeration.

The denitrification is not performing correctly since the system do not nitrifying and produce NO_3^- to denitrify, the high amount of oxygen do not allow the developing of anoxic zones in the system, and do not force heterotrophic bacteria (alkalinity production as OH^-) to take nitrate as electro receptor, instead of oxygen to denitrify, neither the heterotrophic microorganisms do not count with enough biodegradable carbon to produce nitrogen gas due to the low S_S content. When there is a long sedimentation time, the problem is that the system becomes very anoxic and denitrifying, which causes bulking of microorganisms and poor settling conditions hereafter.

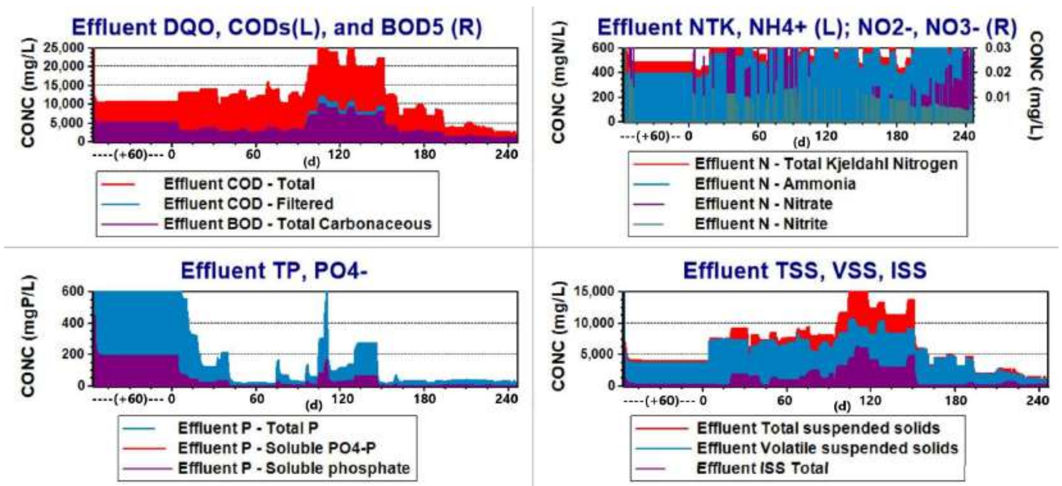

Figure 55. Effluent Performance chart: Effluent concentrations for Carbon (1), Nitrogen (2), phosphorous (3) species, and (4) solids for the housekeeping wastewater.
Source: Own elaboration running the BioWin software ®.

As mentioned before, nitrogen aid in the alkalinity contain in the CWW, since the ammonia, produced during the hydrolysis process, and catalyzed by the heat process in the cooker-batch equipment, reacts with the CO_2 (the non-organic carbon source that is also required for nitrifiers) to form ammonium bicarbonate contributing to the alkalinity in the reactor (Nakhla et al., 2003), and thus the pH change from acidic to alkaline from HKWW to CWW respectively (Figure 56). As Brønd & Sund (1994) suggests, sufficient upstream buffering should be ensured to prevent shock loads.

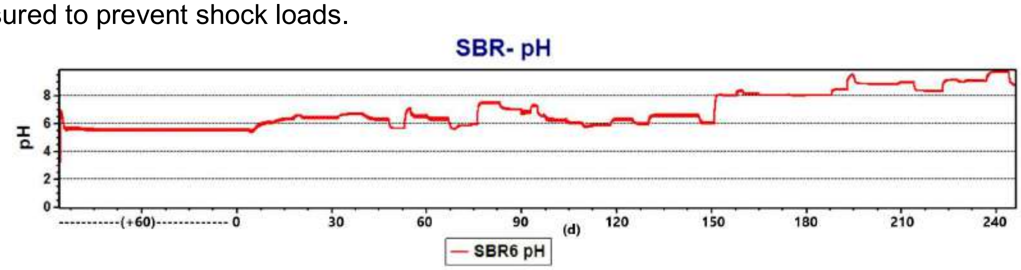

Figure 56. pH control chart during stages I to VIII.
Source: Own elaboration running the BioWin software ®.

The equilibrium between ammonia and ammonium is heavily impacted by the pH, thus the

CWW lose most of the nitrogen in the form of ammonia due the basic pH that favored the ammonia gas existence and its releasing by the strong aeration pattern than for the HKWW, as presented in Figure 57-3, i.e., this process happed due a physical phenomenon rather than a biological process as it supposed to be.

When HKWW or CWW are discharged in natural water bodies under anaerobic conditions, increase the release probability of high nitrogen oxides emission to the atmosphere. However, the excess of aeration of the current SBR system neither allow the anaerobic conditions that favors the formation of this kind of GHG, as seen in Figure 57-3, nor the anoxic condition to complete denitrification, which is the objective of the nitrogen removal process. These findings suggest that with proper control and monitoring GHG emissions could be avoided without stopping using biological treatments (Tian et al., 2020).

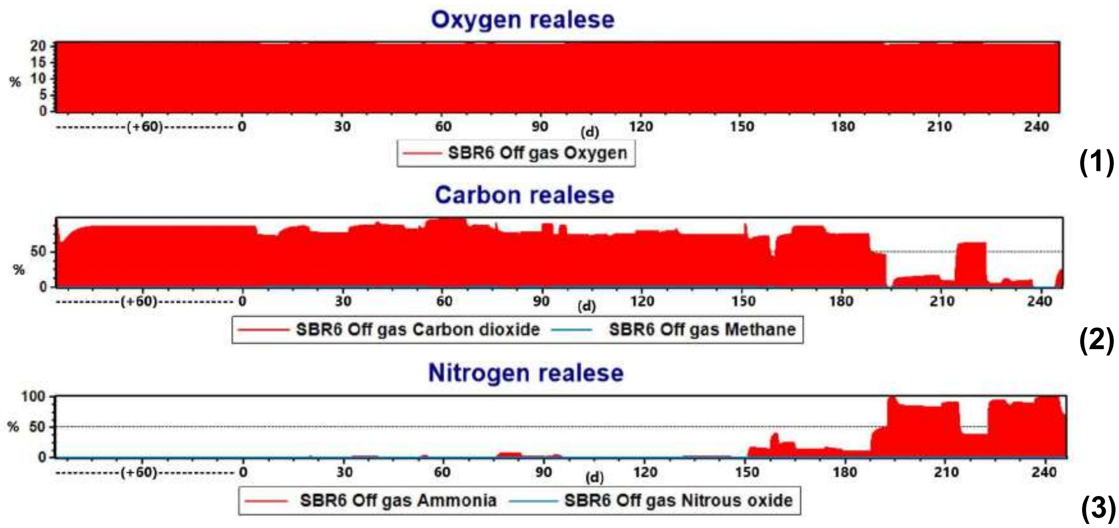

Figure 57. Integrated off gas phase chart % of release of (1) Oxygen, (2) carbon, and (3) nitrogen species for stages I to VIII.
Source: Own elaboration running the BioWin software ®.

Finally, the SBR system is a good option to avoid the appearance of filamentous bacteria, since this kind of system provide a strong substrate gradient that favors the floc forming bacteria, minimizing the bulking, due to the selection theory (Wilderer et al., 2001; Liao et al., 2004).

6.4.2. GRAPHICAL EFFLUENT PERFORMANCE

Although the measured and simulated results differ strongly in magnitude, the response trend is kept for the entire project. As expected, the solids simulation was the most difficult to represent, and the better result was for the ammonia (Figure 58). Those result are in accordance with the fact that solids are the most sensitive variable due to the multiple sources of transformation and the fact that biomass are compound not only by microorganisms, also by organic matter, nutrients, extracellular polymeric substances, among others, while the nitrogen is not working well in the system and thus the representation from the physical point of view is more accurate than the biological state variables as COD or BOD.

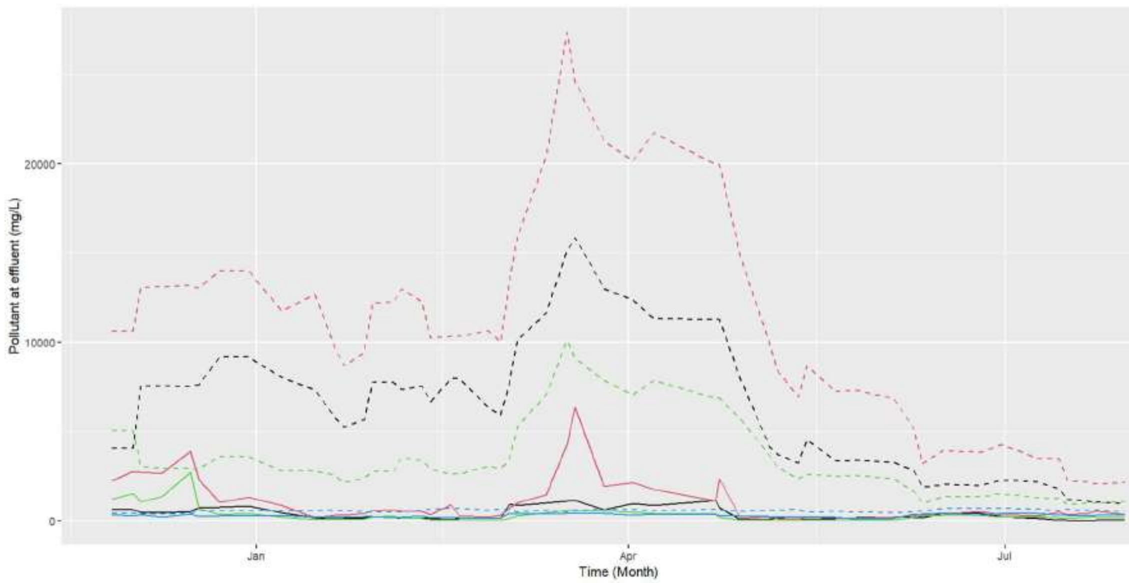

Figure 58. Effluent measured data (continuous line) and corresponding simulated results (dashed line) of TSS (Black), COD (Red), BOD5 (Green), and NH4+ (Blue) concentrations for the whole differential load analysis.
Source: Own elaboration.

6.4.3. GOOD-OF-FIT OF PRE-RUN MODEL PERFORMANCE

To evaluate numerically the performance of the default and fractions adjustments, the good-of-fit for differential overload simulations must be assessed.

- **MODEL PERFORMANCE ASSESSMENT**

As shown in Figure 59-1, for the general experiment the DQO state variable present the highest average and standard deviation error (MAE and RMSE, respectively), and conversely the lowest for the ammonia prediction. It is highlighted that the MAE and RMSE of the HKWW were around 10000mg/L and in the general differential load simulation those values remain unchanged, suggesting that the fractionation and model parameters were an outstanding strategy. As in the individual HKWW and CWW simulation the ammonia state variable was the best predicted. Because the MAPE of the TSS is close to 51%, the prediction is inaccurate, the COD of 22% and BOD of 34% can be considered reasonable predicted, and the $NH4^{+}$ of 1.23% is highly accurate for forecasting.

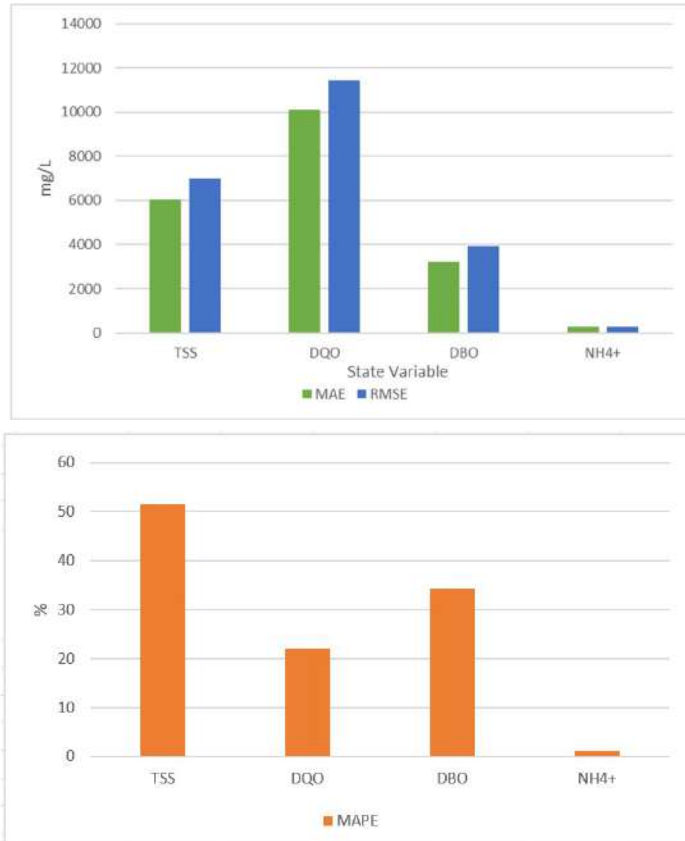

(1)

(2)

Figure 59. Comparison of good-of-fitness assessment for (1) MAE and RMSE, and (2) MAPE with fractionation average and model parameter modification.
Source: Own elaboration using the software R-4.0.2.®.

- **VALIDATION**

In general, 8 points, one for overload stage, were evaluated. The change in model efficiency between calibration and validation was acceptable for four variables, but the lower change on the distribution is presented to the BOD variable (0.6333 J^2 on Figure 60), as suggested by the MAPE of 34%. However, as presented in the previous sections for calibration, to enhance the similarity between observed and simulated need further improvement.

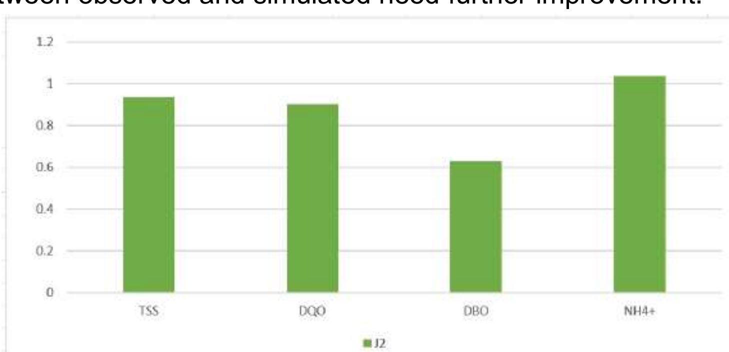

Figure 60. Validation assessment with fractionation average and model parameter modification.
Source: Own elaboration using the software R-4.0.2.®.

According to Meijer, & Brdjanovic (2012) after feeding the model with plant design and preliminary flow data, it is very unlikely that the first simulation with default parameter values will lead to reliable results. Therefore, calibration must be embraced for this simulation study. Melcer (2004) recommended that instead of beginning with parameter adjustment (calibration), modelers should look at other possible reasons of matching bias as: influent inhibition (e.g. high chlorine that inhibits EBPR, or poor information (e.g. sludge wastage). In this case, the inhibition is mostly presented by the grease and oil overload, low alkalinity, and deficit of phosphorus at the influent.

7. CONCLUSIONS

OBJECTIVE 1

- The SBR transport and conversion models were successfully set by checking the hydraulic configuration for the former and the bioreactor model ($ASDM_i$) for the latter. Data processing was performed by missing data completion based on literature review, and the fractionation of both HKWW and CWW were performed by the STOWA fractionation protocol. While kinetic and stoichiometric model parameters were modified in the calibration stage.

OBJECTIVE 2

- The proposed calibration methodology was based on sludge production, and carbon and nitrogen performance values by changing the influent fractionation and model parameter. At next, the most sensible parameters will be presented: The calibration of the sludge production was achieved by the SRT, followed by the maximum growth of OHO microorganisms, and the UpFlow factor related with the settling parameters. On the other hand, for the carbon description the most sensible parameters were a combination of the fractionation of state variables, and the lowest model parameter values from the sensitivity analysis. Finally, for the nitrogen description in both HKWW and CWW, were selected common model parameter values from literature of slaughterhouse and rendering effluents.

OBJECTIVE 3

- The TSS MAPE evaluation was 51% (6991mg/L RSME) suggesting that the prediction of solids is inaccurate, the COD of 22% and BOD of 34% (11443mg/L and 3923mg/L RSME, respectively) can be both considered reasonable predictable, and the nutrient (NH_4^+) of 1.23% (295.23mg/L RSME) is highly accurate for forecasting. In terms of validation, eight measured data points, one per differential load stage, were reserved for the validation assessment. The BOD variable was the worst in change on model efficiency between calibration and validation with a Janus coefficient of 0.63 J^2, while the rest variables present values higher than 0.9 and lower than 1. However, the calibration stage suggested an adjustment in the model parameters for using the model in the operation plant.

GENERAL OBJECTIVE

- The actual SBR system does not remove the carbon as other common biological systems treating meat industrial wastewater (HKWW and CWW), neither nitrify and denitrify completely due to the high X_I, and ammonium content, lack of nutrients, pH inhibition. In general, the failure in the preliminary and primary treatment (FOG removal) affects completely the secondary treatment, overloading and creating dying of more than half of OHO microorganisms' populations, and thus, high loads of BOD and ammonia are discharged into the receiving water body. When the BOD removal is ineffective, the heterotrophic bacteria are numerous and out-compete autotrophic bacteria. On the other hand, for the correct biological treatment performance, the system requires the reduction in the aeration pattern or the addition of non-organic carbon (stripped CO_2, or similar) to promote the growth of nitrifiers, and the addition of alkali species to buffer the acidity and prevent nitrifiers inhibition. Finally, the system also requires an addition of a phosphorous source to supply the OHO and ANO demand.
- The fractionation and average fractionation inflow scenarios shows relatively same results for all the control performance variables (effluent TSS, TCOD, BOD_5, NH_4^+) and

for both effluents (HKWW and CWW), suggesting that calibration could be realized by the average fractionation instead of looking for a fractionation of every control simulation point.

- HKWW presents an excess of grease and oil, which is characterized by a high fraction of X_I with poor settleability (SVI=450mm/h), that affects the TSS removal, as well as the COD, and BOD removal due to its low biodegradability. This wastewater matrix is characterized as 51% X_I and only 33% biodegradable carbon fraction (where up to 57% was S_F and 43% was S_A). While the nitrogen content is 92% soluble ammonia, the rest is present in its organic forms. Finally, 23% of phosphorus is soluble orthophosphates and the rest organic P. Only carbon is partially being transformed in the SBR system, since phosphorus deficit, and pH inhibition caused the OHO growth reduction. On the other hand, nitrogen and other nutrients present almost no removal because of pH and ammonia inhibition. According to the CO_2 release (more than 60%) the system is removing carbon physically rather than biologically, due to the acute inhibition conditions. In the case of nitrogen, is not being transformed but rather biological nor physically.
- The overall system performance of CWW is critical, considering that the average TSS response is equals to 5.59mg TSS/L which indicates that this wastewater matrix is facing solids wash out. The CWW fractionation is compound of 80% of S_S (where up to 82% was S_F and 18% was S_A) and only 10% X_s. The fractionation of nitrogen is compound of 95% soluble ammonia; the rest is present in its organic forms. Finally, 40% of phosphorus is present as soluble orthophosphates and the rest organic P. Although the TCOD input for HKWW is higher than for CWW, the COD removal is higher for this matrix than for HKWW, as demonstrated by the amount of OHO microorganisms and the oxygen uptake rate, since CWW present a higher biodegradable content (S_S), and the phosphorous content, since it is being uptake in high extend by microorganisms than for HKWW. Similar as for HKWW only carbonaceous OUR is happening on the system, which demonstrated that the nitrification process is also inhibited by the pH (pH>8), nutrient deficit, and the ammonia concentration. Similar as for HKWW the CWW behavior tends to be more a physical process due to the harsh environmental condition (pH, alkalinity), rather than biological process, the only difference is, in this case the major nutrient removal is nitrogen, which is probably release by the high aeration. Because this matrix presents a higher nitrogen input and basic pH, the nitrogen release in form of ammonia is also high in comparison with the HKWW (between 40% and 80%). This pH increases because NH_4^+ reacts with the CO_2 to form ammonium bicarbonate contributing to the alkalinity in the reactor, and hereafter the pH increment. Finally, The TSS in the system is lower than the HKWW, which is caused because of nutrient disbalance.
- Although the COD/N or COD/P ratio are lower for the CWW than for HKWW, the CWW is more “biodegradable” than the HKWW, based on the amount of S_S, and nutrients availability. From the calibration it is concluded that the higher the S_s the lower the TSS at the effluent for both matrices.
- Differential overload: Not only the hydraulic overload affects the solid retention time. The solid and carbon overload (Stage IV and V, mostly HKWW content), because of the grease and oil surplus, in this specific case do not physically wash microorganisms out of the system but inhibits and reduces at half (stage V) its population due to the harsh environmental condition. Fact that is proven by the carbonaceous OUR and

OHO biomass decreased at stage IV and V when the overload occurred. Neither the HKWW nor CWW ANO microorganisms are growing and developing in the SBR system as presented by the absence of Nitrification OUR (Figure 54-2) and Ammonia oxidizing biomass (Figure 54-4) due to the nutrient deficit as phosphorous (for the entire project), calcium and magnesium (specially for CWW) and pH inhibition (specially for the HKWW). Nitrification does not thieve since pH inhibition, low CO2, and neither denitrification due to the high aeration, and pH inhibition. Nitrogen removed from the system is a consequence of the high aeration system rather than the biological conversion as expected.

8. RECOMMENDATIONS

- Pollution caused by the rendering wastewater can be reduced by means of treatment removal or material recovery. If the objective is the treatment removal, pre-treatments compound of gravity and physical separation and lipids dissolution must be carried out to avoid microorganisms' inhibition, microorganism cell transport and sedimentation issues, and unpleasant odor in the secondary treatment of rendering wastewater.
- Gravity separation like grease trap, grease interceptor (autonomous systems), or settlers with skimmer technologies are selected according to the rendering size and production loads. Those technologies are used to reduce the free FOG content, and particulate COD by physical force (Klaucans & Sams, 2018). However, disperse and emulsifying oil remains in the system.
- Surfactants like biosurfactants (plant-base), increase not only the oil dissolution of disperse and emulsifying materials, but also the degree of degradability of particulate and soluble COD to improve degradability of oily wastewater (Nakhla et al., 2003).
- At this point, it's suggested to change the technology of the primary treatment with coagulant/flocculation to biosurfactants materials to avoid the production of hazardous foam waste (i.e. with ion metal remains) that increases the disposition cost and affects the posterior biological treatment.
- After releasing disperse and emulsifying oil, primary treatment like DAF technologies is suggested, instead of settlers, to avoid the emulsifying oil overload that inhibits and is the main failure responsible of biological treatment process (Nakhla, Liu & Bassi, 2006). This excess of wasted lipids promoted by the pretreatment and primary treatment could be conveyed to the municipal anaerobic systems (digestors) as a co-digestion solution to increase its the gas production (Klaucans & Sams, 2018).
- Finally, the dissolved oil should be reduced by means of secondary treatment like UASB or SBR reactor. In the first case, enzymatic hydrolysis processes by means of lipase addition is suggested, since it splits ester bonds of triacylglycerols with the consumption of water molecules (Jeganathan et al., 2006), i.e. transforms complex regnant of FOG to VFA, materials easy to synthesize in the anaerobic biological treatment, and addition of alkali species to buffer the acidity and prevent nitrifiers inhibition. In the case of SBR, the system requires the right set of aeration patterns to promote heterotrophic growth without CO_2 releasing necessary for nitrifying organisms, the addition of extra-organic carbon source according to the pre and primary treatment removal efficiency, the addition of alkali species prevent nitrifiers inhibition, and the addition of a phosphorous source to supply the OHO and ANO demand (Nowak et al., 1996; Filali-Meknassi et al., 2004).
- When HKWW or CWW are discharged in natural water bodies under anaerobic conditions, increase the probability of high nitrogen oxides emission to the atmosphere. With proper control and monitoring GHG emissions could be avoided without stopping using biological treatments (Tian et al., 2020).
- On the other hand, the rendering wastewater could be subjected to material recovery. Different to slaughterhouse or housekeeping wastewater the rendering or CWW produces valuable wastewater that is less harmful on pathogenic microorganisms' content, due to the reduction and sterilization in the cooker-batch process, allowing its use as a fertilizer, rather be submitted to biological treatment process (Meeker & Hamilton, 2006). Additionally, Housekeeping wastewater could be pre and primary

treated by biosurfactants and DAF technologies, and the secondary treatment could add external carbon sources to increase the gas production, if it’s the case.

- The field measured information does not have the specificity necessary to be used in a sophisticated model such as ADM1, therefore, for future works, the parameters necessary (fractionations) to feed the simulation model must be taken into account in the analyses to be carried out on raw and treated wastewater.

9. REFERENCES

- Abbasi, N., Ahmadi, M., & Naseri, M. (2021). Quality and cost analysis of a wastewater treatment plant using GPS-X and CapdetWorks simulation programs. Journal of Environmental Management, 284, 111993.
- Alex, J., Hübner, C., & Förster, L. (2020). Planning, testing and commissioning of automation solutions for waste water treatment plants using simulation. IFAC-PapersOnLine, 53(2), 16665-16670.
- American Public Health Association (APHA), American Water Works Association (AWWA), Pollution Control Federation (WPCF). (2005). Standard methods for examination of wáter and wastewater 16th ed. Washington.
- Andreottola, G., Bortone, G., & Tilche, A. (1997). Experimental validation of a simulation and design model for nitrogen removal in sequencing batch reactors. Water Science and Technology, 35(1), 113-120.
- Ángulo, L. F., Gómez Rojas, J. F., Arango Villegas, V., & López, J. (2020). Documento Sectorial Servicios Públicos Domiciliarios para la debida diligencia en derechos humanos-Aseo, Acueducto y Alcantarillado.
- Artan, N., Wilderer, P. A., Orhon, D., Tasli, R., & Morgenroth, E. (2002). Model evaluation and optimization of nutrient removal potential for sequencing batch reactors. Water SA, 28(4), 1-10.
- Auterská, P., & Novák, L. (2006). Successful solution for high nitrogen content wastewater treatment from rendering plants. Water science and technology, 54(10), 23-30.
- Bentancur, S., López-Vázquez, C. M., García, H. A., Duarte, M., Travers, D., & Brdjanovic, D.(2021) Modelling of a pulp mill wastewater treatment plant for improving its performance on phosphorus removal. Process Safety and Environmental Protection, 146, 208-219.
- Besharati Fard, M., Mirbagheri, S. A., & Pendashteh, A. (2020). Removal of TCOD and phosphate from slaughterhouse wastewater using Fenton as a post-treatment of an UASB reactor. Journal of Environmental Health Science and Engineering, 1-10.
- Brdjanovic, D., Meijer, S. C., Lopez-Vazquez, C. M., Hooijmans, C. M., & van Loosdrecht, M. C. (Eds.). (2015). Applications of activated sludge models. Iwa Publishing.
- Brennan, B., Gunes, B., Jacobs, M. R., Lawler, J., & Regan, F. (2021). Potential viable products identified from characterisation of agricultural slaughterhouse rendering wastewater. Water, 13(3), 352.
- Brenner, A. (2000). Modelling of N and P transformations in an SBR treating municipal wastewater. Water science and technology, 42(1-2), 55-63.
- Brønd, S., & Sund, C. (1994). Biological removal of nitrogen in toxic industrial effluents, high in ammonia. Water Science and Technology, 29(9), 231-240.
- Bustillo, C. L., & Mehrvar, M. (2017). Slaughterhouse wastewater: treatment, management and resource recovery. Physico-chemical wastewater treatment and resource recovery, 153-174.
- Casellas, M., Dagot, C., Pons, M. N., & Baudu, M. (2008). Influent fractionation for the use of ASM1 to optimize urban wastewater treatment: Application to the removal of C and N in a SBR. Revue des sciences de l'eau/Journal of Water Science, 21(4), 451-462.

- Chang, H. N., Moon, R. K., Park, B. G., Lim, S. J., Choi, D. W., Lee, W. G., ... & Ahn, Y. H. (2000). Simulation of sequential batch reactor (SBR) operation for simultaneous removal of nitrogen and phosphorus. Bioprocess Engineering, 23(5), 513-521.
- Chen, G. H., van Loosdrecht, M. C., Ekama, G. A., & Brdjanovic, D. (Eds.). (2020). Biological wastewater treatment: principles, modeling and design. IWA publishing.
- Coen, F., Petersen, B., Vanrolleghem, P. A., Vanderhaegen, B., & Henze, M. (1998). Model-based characterisation of hydraulic, kinetic and influent properties of an industrial WWTP. Water Science and Technology, 37(12), 317–326. doi:10.2166/wst.1998.0557
- Corominas Tabares, L. (2006). Control and optimization of an SBR for nitrogen removal: from model calibration to plant operation.
- Cuadros, F., López-Rodríguez, F., Ruiz-Celma, A., Rubiales, F., & González-González, A. (2011). Recycling, reuse and energetic valuation of meat industry wastes in Extremadura (Spain). Resources, conservation and recycling, 55(4), 393-399.
- Domingo, F. C., Pellicer-Nàcher, C., Petersen, M. S., Jensen, M. M., Plósz, B. G., & Smets, B. F. (2017). Heterotrophs are key contributors to nitrous oxide production in activated sludge under low C-to-N ratios during nitrification—Batch experiments and modeling. Biotechnology and bioengineering, 114(1), 132-140.
- Echavarría, N., Atehortúa, N. y Tobón, O. (2016). Manual Gestión del Recurso Hídrico. Plantas de beneficio animal. Corantioquia y Centro Nacional de Producción Más Limpia. Recuperado de: http://www.corantioquia.gov.co/SiteAssets/PDF/Gesti%C3%B3n%20ambiental/Producci%C3%B3n%20y%20Consumo%20Sostenible/Manuales_GIRH/Plantas_Beneficio.pdf
- Envirosim (2021). BioWin user Manual 5.3. (Reviewed: 2023.03.09). Source: http://www.envirosim.com/downloads/BW5Manual.pdf
- Federación Colombiana de Ganaderos (FEDEGAN) & Fondo Nacional del Ganado (FNG) (2020). “Balance y Perspectivas del sector ganadero colombiano (2019-2020)”. Oficina de Planeación y Estudios Económicos. Recuperado
- Filali-Meknassi, Y., Auriol, M., Tyagi, R. D., & Surampalli, R. Y. (2004). Treatment of slaughterhouse wastewater in a sequencing batch reactor: simulation vs experimental studies. Environmental technology, 25(1), 23-38.
- Filali-Meknassi, Y., Auriol, M., Tyagi, R. D., Comeau, Y., & Surampalli, R. Y. (2005). Design strategy for a simultaneous nitrification/denitrification of a slaughterhouse wastewater in a sequencing batch reactor: ASM2d modeling and verification. Environmental technology, 26(10), 1081-1100.
- Gernaey, K. V., Van Loosdrecht, M. C., Henze, M., Lind, M., & Jørgensen, S. B. (2004). Activated sludge wastewater treatment plant modelling and simulation: state of the art. Environmental modelling & software, 19(9), 763-783.
- Gujer, W., & Henze, M. (1991). Activated sludge modelling and simulation. Water Science and Technology, 23(4-6), 1011-1023.
- Hansen, C. L., & West, G. T. (1992). Anaerobic digestion of rendering waste in an upflow anaerobic sludge blanket digester. Bioresource technology, 41(2), 181-185.
- Hauduc H., Gillot S., Rieger L., Ohtsuki T., Shaw A., Takács I. and Winkler S. (2009). Activated Sludge Modelling in Practice - An International Survey. Water Science and Technology, 60(8), 1943–1951.
- Hauduc, H., Neumann, M. B., Muschalla, D., Gamerith, V., Gillot, S., & Vanrolleghem,

P. A. (2015). Efficiency criteria for environmental model quality assessment: A review and its application to wastewater treatment. Environmental Modelling & Software, 68, 196-204.

- Hauduc, H., Rieger, L., Oehmen, A., Van Loosdrecht, M. C. M., Comeau, Y., Héduit, A., ... & Gillot, S. (2013). Critical review of activated sludge modeling: state of process knowledge, modeling concepts, and limitations.
- Henze, M., Grady Jr, C. L., Gujer, W., Marais, G. V. R., & Matsuo, T. (1987). A general model for single-sludge wastewater treatment systems. Water research, 21(5), 505-515.
- Ifak Magdeburg (2020). SIMBA# Kläranlagen | Petrinetz für SBR-Steuerung [Archivo de Vídeo]. Youtube. https://www.youtube.com/watch?v=3iF6KAgKMiw&t=1s
- Karpinska, A. M., & Bridgeman, J. (2016). CFD-aided modelling of activated sludge systems – A critical review. Water Research, 88, 861–879. doi:10.1016/j.watres.2015.11.008
- Kim, Y. H., Yoo, C., & Lee, I. B. (2008). Optimization of biological nutrient removal in a SBR using simulation-based iterative dynamic programming. Chemical Engineering Journal, 139(1), 11-19.
- Knobeloch, L., Salna, B., Hogan, A., Postle, J., & Anderson, H. (2000). Blue babies and nitrate-contaminated well water. Environmental health perspectives, 108(7), 675-678.
- Ky, R. C., Comeau, Y., Perrier, M., & Takacs, I. (2001). Modelling biological phosphorus removal from a cheese factory effluent by an SBR. Water science and technology, 43(3), 257-264.
- Larrea, L., Albizuri, J., Irizar, I., & Hernandez, J. M. (2007). Design and operation of SBR processes for small plants based on simulations. Water science and technology, 55(7), 163-171.
- Lobo, C. C., Bertola, N. C., & Contreras, E. M. (2016). Approximate expressions of a SBR for wastewater treatment: Comparison with numeric solutions and application to predict the biomass concentration in real cases. Process Safety and Environmental Protection, 100, 65-73.
- Lopez-Vazquez, C. M., Hernández García, H. A., Buitrón Méndez, G., & Cervantes Carrillo, F. J. (2017). Tratamiento biológico de aguas residuales: principios, modelación y diseño. IWA publishing.
- Mace, S., & Mata-Alvarez, J. (2002). Utilization of SBR technology for wastewater treatment: an overview. Industrial & engineering chemistry research, 41(23), 5539-5553.
- Makinia, J., & Zaborowska, E. (2020). Mathematical modelling and computer simulation of activated sludge systems. IWA publishing.
- Mao, G., Hu, H., Liu, X., Crittenden, J., & Huang, N. (2021). A Bibliometric Analysis of Industrial Wastewater Treatments from 1998 to 2019. Environmental Pollution, 115785. doi:10.1016/j.envpol.2020.115785
- Mariotti, F., Tomé, D., & Mirand, P. P. (2008). Converting nitrogen into protein—beyond 6.25 and Jones' factors. Critical reviews in food science and nutrition, 48(2), 177-184.
- Marsili Libelli, S., Ratini, P., Spagni, A., & Bortone, G. (2001). Implementation, study and calibration of a modified ASM2d for the simulation of SBR processes. Water Science and Technology, 43(3), 69-76.

- Meeker, D. L., & Hamilton, C. R. (2006). An overview of the rendering industry. Essential rendering, 1-16.
- Meijer, S. C. F. (2004). Theoretical and practical aspects of modelling activated sludge processes. Delft, The Netherlands: Delft University of Technology.
- Meijer, S. C. F., & Brdjanovic, D. (2012). A practical guide to activated sludge modeling. UNESCO-IHE Institute for Water Education.
- Melcer, H. (2004). Methods for wastewater characterization in activated sludge modelling. IWA publishing.
- Metcalf & Eddy, Abu-Orf, M., Bowden, G., Burton, F. L., Pfrang, W., Stensel, H. D., ... & AECOM (Firm). (2014). Wastewater engineering: treatment and resource recovery. McGraw Hill Education.
- Metzner, G., & Temper, U. (1990). Operation and optimization of a full-scale fixed-bed reactor for anaerobic digestion of animal rendering waste water. Water science and technology, 22(1-2), 373-384.
- Mincomercio, Colombia Productiva (revisado el 30.11.2020). Eje:Carne Bovina, Sector: Agroindustria. tomado de: https://www.colombiaproductiva.com/ptp-sectores/agroindustria/carne-bovina
- Morgenroth, E., Arvin, E., & Vanrolleghem, P. (2002). The use of mathematical models in teaching wastewater treatment engineering. Water Science and Technology, 45(6), 229-233.
- Muniozguren, A. P. (2020). Advanced Oxidation Processes for the Treatment of Real Slaughterhouse Wastewater After a Biological Treatment.
- Nakhla, G., Al-Sabawi, M., Bassi, A., & Liu, V. (2003). Anaerobic treatability of high oil and grease rendering wastewater. Journal of Hazardous Materials, 102(2-3), 243-255.
- Nakhla, G., Liu, V., & Bassi, A. (2006). Kinetic modeling of aerobic biodegradation of high oil and grease rendering wastewater. Bioresource technology, 97(1), 131-139.
- Ng, M., Dalhatou, S., Wilson, J., Kamdem, B. P., Temitope, M. B., Paumo, H. K., ... & Kane, A. (2022). Characterization of slaughterhouse wastewater and development of treatment techniques: a review. Processes, 10(7), 1300.
- DATAtab. Online statistics calculator (reviwed 22/01/2023). Link: https://datatab.net/
- Nowak, O., Svardal, K., & Kroiss, H. (1996). The impact of phosphorus deficiency on nitrification-case study of a biological pretreatment plant for rendering plant effluent. Water Science and Technology, 34(1-2), 229-236.
- O'Flynn, T. (1999). Operating experiences of a treatment plant designed for biological nutrient removal by pilot trials and mathematical modelling. Resources, conservation and recycling, 27(1-2), 117-124.
- Oles, J., & Wilderer, P. A. (1991). Computer aided design of sequencing batch reactors based on the IAWPRC activated sludge model. Water Science and Technology, 23(4-6), 1087-1095.
- Olsson, G., & Newell, B. (1999). Wastewater treatment systems. IWA publishing.
- Orhon, D., Babuna, F. G., & Karahan, O. (2009). Industrial wastewater treatment by activated sludge. IWA publishing.
- Pitk, P., Kaparaju, P., & Vilu, R. (2012). Methane potential of sterilized solid slaughterhouse wastes. Bioresource technology, 116, 42-46.
- Pons, M. N., Spanjers, H., & Jeppsson, U. (1999). Towards a benchmark for evaluating control strategies in wastewater treatment plants by simulation. Computers & Chemical Engineering, 23, S403-S406.

- Qasim, S. R., & Zhu, G. (2018). Wastewater treatment and reuse theory and design examples: Volume 2: Post-treatment, reuse, and disposal. In Wastewater Treatment and Reuse Theory and Design Examples: Volume 2: Post-Treatment, Reuse, and Disposal. https://doi.org/10.1201/b22366.
- Rahman, U. U., Sahar, A., & Khan, M. A. (2014). Recovery and utilization of effluents from meat processing industries. Food Research International, 65, 322-328.
- Rajab, A. R., Salim, M. R., Sohaili, J., Anuar, A. N., & Lakkaboyana, S. K. (2017). Performance of integrated anaerobic/aerobic sequencing batch reactor treating poultry slaughterhouse wastewater. Chemical Engineering Journal, 313, 967-974.
- Reijken, C., Giorgi, S., Hurkmans, C., Pérez, J., & van Loosdrecht, M. C. (2018). Incorporating the influent cellulose fraction in activated sludge modelling. Water research, 144, 104-111.
- Rendón Echeverri, C. P. (2020). Impacto ambiental generado por las plantas de beneficio de ganado bovino en Colombia.
- Rieger, L., Gillot, S., Langergraber, G., Ohtsuki, T., Shaw, A., Takacs, I., & Winkler, S. (2012). Guidelines for using activated sludge models. IWA publishing.
- Rodríguez, D. C., Pino, N., & Peñuela, G. (2011). Monitoring the removal of nitrogen by applying a nitrification–denitrification process in a Sequencing Batch Reactor (SBR). Bioresource Technology, 102(3), 2316-2321.
- Roeleveld, P. J., & Van Loosdrecht, M. C. M. (2002). Experience with guidelines for wastewater characterisation in The Netherlands. Water Science and Technology, 45(6), 77-87.
- Rönner-Holm, S. G. E., Mennerich, A., & Holm, N. C. (2006). Specific SBR population behavior as revealed by comparative dynamic simulation analysis of three full-scale municipal SBR wastewater treatment plants. Water science and technology, 54(1), 71-80.
- Sin, G., De Pauw, D. J., Weijers, S., & Vanrolleghem, P. A. (2008). An efficient approach to automate the manual trial and error calibration of activated sludge models. Biotechnology and bioengineering, 100(3), 516-528.
- Singureanu, C., & Woinaroschy, A. (2019). Obtaining a guide operator of wastewater treatment by SBR process using simulation and sensitivity analysis. Environmental Engineering & Management Journal (EEMJ), 18(2).
- Snowling, Spencer [Hydromantis]. (14 de Febrero de 2020). Modelling Sequencing Batch Reactors (SBRs) with GPS-X [Archivo de Video]. Youtube. https://www.youtube.com/watch?v=C5XH26P1q4w
- Tian, H., Xu, R., Canadell, J. G., Thompson, R. L., Winiwarter, W., Suntharalingam, P., ... & Yao, Y. (2020). A comprehensive quantification of global nitrous oxide sources and sinks. Nature, 586(7828), 248-256.
- Tilche, A., Bortone, G., Malaspina, F., Piccinni, S., & Stante, L. (2001). Biological nutrient removal in a full-scale SBR treating piggery wastewater: results and modelling. Water Science and Technology, 43(3), 363-371.
- Triana, K. M. (2019). Impactos ambientales generados en plantas de beneficio bovino (Trabajo de grado). Universidad Nacional Abierta ya Distancia, Colombia.
- Van Loosdrecht, M.C.M., Lopez-Vazquez, C.M., Meijer, S.C.F., Hooijmans, C.M., Brdjanovic, D., 2015. Twenty-five years of ASM1: past, present and future of wastewater treatment modelling. J. Hydroinf. 17.

- Venegas, C. B. (2015). Eliminación biológica de nutrientes en aguas residuales con alto contenido de nitrógeno amoniacal utilizando un reactor biológico secuencial (tesis doctoral). Universidad de Cantabria, Cantabria, España. Recuperado de http://hdl.handle.net/10902/8451
- Waki, M., Yasuda, T., Fukumoto, Y., Béline, F., & Magrí, A. (2018). Treatment of swine wastewater in continuous activated sludge systems under different dissolved oxygen conditions: Reactor operation and evaluation using modelling. Bioresource technology, 250, 574-582.
- Woodard, C. I. (2006). 10-wastes from industries (case studies). Industrial waste treatment handbook, 2nd edn. Butterworth-Heinemann, Burlington, 409-496.
- Woodard, F. (2001). Industrial waste treatment handbook. Elsevier.
- Zamudio, L. E. V. (2019). El plan nacional de desarrollo 2018-2022:" Pacto por Colombia, pacto por la equidad". Apuntes del CENES, 38(68), 12-14.
- Cammarota, M. C., & Freire, D. M. (2006). A review on hydrolytic enzymes in the treatment of wastewater with high oil and grease content. Bioresource technology, 97(17), 2195-2210.
- Jeganathan, J., Bassi, A., & Nakhla, G. (2006). Pre-treatment of high oil and grease pet food industrial wastewaters using immobilized lipase hydrolyzation. Journal of Hazardous Materials, 137(1), 121-128.
- Pintor, A. M., Vilar, V. J., Botelho, C. M., & Boaventura, R. A. (2016). Oil and grease removal from wastewaters: sorption treatment as an alternative to state-of-the-art technologies. A critical review. *Chemical Engineering Journal*, *297*, 229-255.
- Klaucans, E., & Sams, K. (2018). Problems with fat, oil, and grease (FOG) in food industry wastewaters and recovered FOG recycling methods using anaerobic co-digestion: A short review. Key Engineering Materials, 762, 61-68.
- Sultana, N., Roddick, F. A., & Pramanik, B. K. (2024). Fat, oil and grease wastewater and dishwashers: Uncovering the link to FOG deposition. Science of the Total Environment, 907, 168032.
- Kosseva, M. R. (2020). Sources, characteristics, treatment, and analyses of animal-based food wastes. In *Food Industry Wastes* (pp. 67-85). Academic Press.
- Muster-Slawitsch, B., Dow, N., Desai, D., Pinches, D., Brunner, C., & Duke, M. (2021). Membrane distillation for concentration of protein-rich waste water from meat processing. *Journal of Water Process Engineering*, *44*, 102285.
- Bedoić, R., Špehar, A., Puljko, J., Čuček, L., Ćosić, B., Pukšec, T., & Duić, N. (2020). Opportunities and challenges: Experimental and kinetic analysis of anaerobic co-digestion of food waste and rendering industry streams for biogas production. *Renewable and Sustainable Energy Reviews*, *130*, 109951.

10. APPENDIX

10.1. INFLUENT FRACTIONS

Table 17, Table 18, Table 19 and Table 20 use the nomenclature of the unified protocol, and the fractionation input order, in the way that BioWin software prompts the fractionation data. For instance, SS/FBS (1) stands for the readily degradable soluble substrate, the S_S is the standard nomenclature, the F_{BS} the BioWin one, and number (1) indicates that is the first prompt in the fractionation tap in the BioWin software. It important to recognized that the S_A (2) and X_{SP} (3) fraction belong to the S_S fraction.

Table 17. Inflow COD fractionation in soluble and particulate components.

		COD										
		Solubable COD				Particulate COD						
	DATE	SS/FBS (1) (gCOD/m3)	SA/FAC (2) (gCOD/m3)	XSP/FXsp (3) (gCOD/m3)	SI/FUS (4) (gCOD/m3)	XI/FUP (5) (gCOD/m3)	XS (gCOD/m3)	XH (gCOD/m3)	XPAO (gCOD/m3)	XPHA (gCOD/m3)	XGLY (gCOD/m3)	XAUT (gCOD/m3)
PSEUDO-STEADY STATE	11/27/2008	0.800	0.176	0.950	0.040	0.070	0.091	0	0	0	0	0
STABLE RESPONSE	12/18/2008	0.390	0.360	0.950	0.027	0.538	0.044	0	0	0	0	0
	12/23/2008	0.392	0.359	0.950	0.005	0.384	0.219	0	0	0	0	0
	12/30/2008	0.263	0.535	0.950	0.007	0.547	0.183	0	0	0	0	0
	1/7/2009	0.268	0.524	0.950	0.048	0.613	0.071	0	0	0	0	0
MEAN		0.328	0.445	0.950	0.022	0.521	0.129	0	0	0	0	0

Source: Own elaboration.

Table 18. Inflow TKN characterization in soluble and particulate components.

	TKN							
	Ammonia	Organic Solubable			Organic Particulate		Inorganic	
	SNH4/Fna (7) (gN/m3)	SF*iNSF (gN/m3)	SA*iNSA (gN/m3)	SI*iNSI/Fnus (9) (gN/m3)	XI*iNXI (gN/m3)	XS*iNXS/Fnox (8) (gN/m3)	SNO2 (gN/m3)	SNO3 (gN/m3)
PSEUDO-STEADY STATE	0.872	0.083	0.012	0.004	0.011	0.016	0.016	0.115
STABLE RESPONSE	0.931	0.007	0.006	0.001	0.051	0.004	0.016	0.730
	0.927	0.012	0.003	0.000	0.034	0.019	1.114	1.937
	0.934	0.016	0.015	0.001	0.018	0.029	0.822	0.002
	0.827	0.017	0.019	0.007	0.116	0.013	1.473	1.137
MEAN	0.905	0.013	0.011	0.002	0.054	0.016	0.856	0.952

Source: Own elaboration.

Table 19. Inflow TP characterization into soluble and particulate components.

	TP							
	Mineral	Poly-Phoshate	Organic Solubable			Organic Particualte		
	SPO4/Fpo4 (11) (gP/m3)	XPP (gP/m3)	SF*iPSF (gP/m3)	SA*iPSA (gP/m3)	SI*iPSI (gP/m3)	XPAO*iPBM (gP/m3)	XI*iPXI (gP/m3)	XS*iPXS (gP/m3)
PSEUDO-STEADY STATE	0.529	0.000	0.256	0.048	0.022	0.000	0.046	0.099
STABLE RESPONSE	0.529	0.000	0.046	0.038	0.007	0.000	0.335	0.027
	0.529	0.000	0.126	0.047	0.003	0.000	0.128	0.220
	0.000	0.000	0.000	0.000	0.000	0.000	0.000	0.000
	0.529	0.000	0.087	0.064	0.044	0.000	0.277	0.096
MEAN	0.397	0.000	0.064	0.037	0.014	0.000	0.185	0.086

Source: Own elaboration.

Table 20. Additional inflow soluble components.

Others	
SO2 (gO2/m3)	SALK (mmol HCO/l)
0	11.7

Source: Own elaboration.

10.2. SENSITIVITY ANALYSIS FOR HKWW

This section aims for the calibration of the HKWW following the calibration procedure from Figure 7 and the completed fractionated influent (5.2.5) rather than default influent.

10.2.1. SLUDGE PRODUCTION FOR HKWW

Sludge production is related with the TSS, VSS and ISS for: Mixed Liquor (MLVSS), the effluent, and the wastage underflow. Sludge production can be adjusted by modifying inert fractions (F_{XI}, iN_{Xi}, iP_{XI}**,** etc), biomass growth and decay ratios of heterotrophic microorganisms ($\mu_{H,Max}$, $\mu_{AUT,Max}$, B_H, b_{AUT}), settling parameters, and the SRT (related with the wastage sludge). In the present study, the TSS, VSS and ISS will be analyzed for both SBR Mixed Liquor and effluent point in four simulation results against four measured (observed) points from “steady state” timespan, presented in
Table 7.

10.2.1.1. INFLUENT FRACTIONS

To calibrate and analyze the ISS simulated response, $\mathbf{X_I}$ and $\mathbf{iNX_I}$**,** $\mathbf{iPX_I}$**,** will be modified following the STOWA fractionation protocol, since the inert particulate materials is the main contributor to the waste sludge production (Meijer & Brdjanovic, 2012). The simulation should result in an accurate prediction of the mixed liquor ISS concentration (Melcer, 2004). At next, it will present the Inert solids results in both mixed liquor and the effluent, to calibrate the inert fractions.

10.2.1.1.1. INERT PARTICULATED COD FRACTION (X_I)

F_{XI}/X_I fraction is modified from the STOWA fractionation by changing the **X_S** fraction. This later fraction, at the same time, is changed by the food/microorganism ratio (Y_{BOD}) and the k constant from the BOD model, while other parameters remain constant. Two scenaries will be supposed to analyze the effect of low and high inert COD fraction from the sludge production, modifying the Y_{BOD} ratio and k constant. The high X_I scenario (55% of X_I) that corresponds to the maximal inert COD content allowed by the STOWA protocol, for this specific wastewater state variables, without altering other variables, k will be equal to 0.8 while Y_{BOD} ratio will be kept at 0.55. On the other hand, In the low inert COD scenario (5% of X_I) which is the minimum allowed amount) the k constant is equals to 0.13 (typical k range for domestic effluent of 0.15-0.6d^{-1}) and the Y_{BOD} ratio will be 0.2 (Y_{BOD} typical range for domestic effluent of 0.1-0.2).

According to Melcer (2004), when the inert particulate carbon fraction is increased, the system will produce more sludge, and vice versa. This hypothesis was proven comparing the X_I fraction of 5% (called down) and 55% (called up) on Figure 61, the increment of F_{XI} (blue line) produces little less ISS sludge in the mixed liquor (Figure 61-1), and in the effluent (Figure 61-2) and favoring the inert sludge removal. Also, when the F_{XI} (green line) was decreased the ISS was increased for both mixed liquor and effluent. Figure 61-1 and Figure 61-2 present in general that the simulation is far from the measured points (big yellow dots), although the increment or reduction in the inner particulates COD fraction, this fraction present low sensitivity for this wastewater matrix.

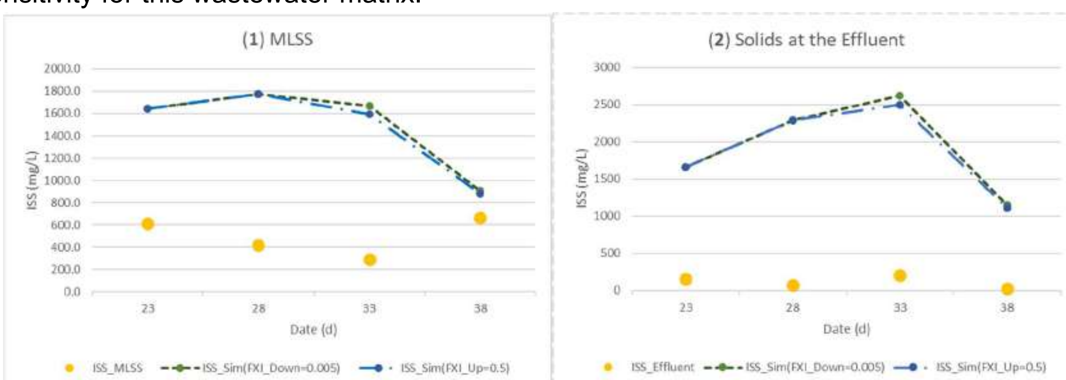

Figure 61. Inert sludge production analysis for (1) Mixed liquor solids in the reactor and (2) solids at the effluent, modifying the inert particulate fraction by the k constant of the BOD model in the STOWA protocol.
Source: Own elaboration.

10.2.1.1.2. INERT PARTICULATED NITROGEN AND PHOSPHORUS FRACTIONS (iNX & iPX_I)

Nitrogen and phosphorus inert fractions (iN_{XI} and iP_{XI}) exhibit a direct relationship between TKN and TP respectively on the sludge (Melcer, 2004; Roeleveld & Van Loosdrecht, 2002), therefore this parameter should be also tuned to meet stringent standards. iN_{XI} and iP_{XI} fractions are changed directly in the STOWA fractionation (e.g. iNS_F, iNS_A, iNS_I, iNBM, iNX_I, iNX_S, and similar for the phosphorous fractionation) until matching the nitrogen (TKN-N) and phosphorous (TP) influent content. As a reference, it is suggested default values present by

Roeleveld & Van Loosdrecht (2002) for nitrogen and phosphorus fractions base on COD components for domestic wastewater.

Figure 62 presents the low (1, original fractionation as present in Table 15 and
Table 16) and augmented (2) fractionation for nitrogen and phosphorus in its soluble and particulates fractions obtained from the STOWA protocol for the four calibrations points. In the low inert fractioning (Figure 62-1) the percentage of inert fraction was less than 30%, but in the augmented case (Figure 62-2), the inert fractions rise up to 70%.

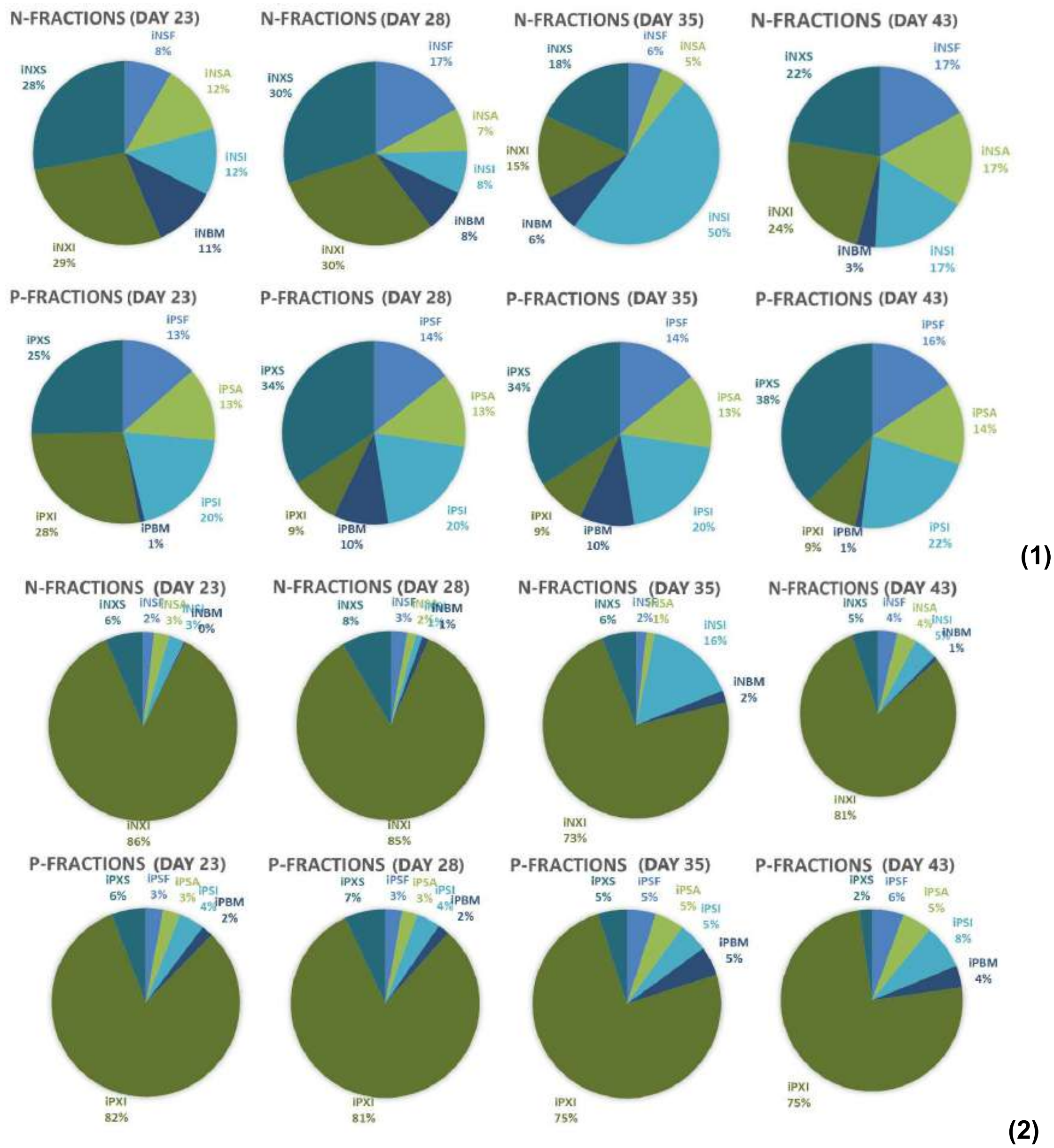

Figure 62. (1) low and (2) augmented inert fractionations of the four simulation points from stage II, for nitrogen in the top and phosphorous in the bottom.
Source: Own elaboration.

Although the visible difference between low and augmented inert fraction for nitrogen and phosphorous (from Figure 62-1 and Figure 62-2) for the low scenario (original fractionation, brown dotted lines, Figure 63-1) and high scenario (augmented, yellow dashed line, Figure

63-1), there is not a notable effect while changing both inert fractions in the inert sludge production for SBR Mixed liquor and effluent. Both cases are still far from matching the measured inert solids (big yellow dots), namely the system is overestimating the amount of inert sludge production whatever the case. This suggests that the increment in the inert influent carbon fraction does not present a notable sensitivity for this wastewater matrix under the current conditions. However, the better visual approximation between observed and simulated ISS solids is for the mixed liquor rather than the effluent concentration.

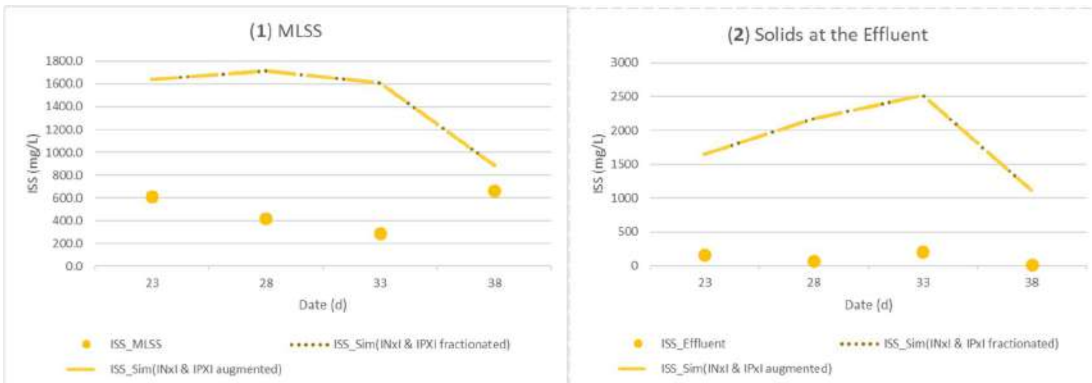

Figure 63. Inert sludge production analysis for (1) SBR Mixed liquor and (2) solids at the effluent, modifying the nitrogen and phosphorus inert fractions from Figure 7.
Source: Own elaboration.

10.2.1.2. MODEL PARAMETERS

The volatile sludge production is influenced by kinetic parameter as the maximum heterotrophic growth rate ($\mu_{H,Max}$) and its respective decay (b_H) (Rieger et al., 2012) and also stoichiometric parameter as (Y_H), especially for high strength load of industrial applications, by contrast, domestic application not always need this fitting process for kinetic parameters (Melcer, 2004).

10.2.1.2.1. BIOMASS GROWTH RATES (μ_H)

Two scenarios will be tested base on the suggestion of Andreottola et al. (1997): The high maximum growth rate as $\mu_{H,Max}$=13d^{-1} called "mu_Up", versus a the low maximum growth rate $\mu_{H,Max}$=1 d^{-1}, called "mu_Down". This high $\mu_{H,Max}$ value was taken following the suggestion by Henze et al. (1987), Gujer & Henze (1991) and Oles & Wilderer (1991) who stated that heterotrophic bacteria depends markedly on the actual feeding pattern, in this case fast fill, and experimenting 10 times higher $\mu_{H,Max}$ values. However, in the praxis, it is recommended to perform respirometric test to evaluate the kinetic ratios for industrial wastewaters (Meijer & Brdjanovic, 2012).

The decrease of the maximum growth rate of heterotrophs (mu_Down=1 d^{-1}), reduces the VSS concentration in both the mixed liquor (Figure 64-1) and effluent (Figure 64-2) and vice versa, i.e. the higher the number of viable microorganisms the higher the VSS concentration. In general, the effluent VSS presents higher sensitivity than the mixed liquor suspended solids. Finally, the VSS in the mixed tank (dotted and dashed) are graphically, more similar to the measured data (blue big dots) than from the effluent, which is common in activated sludge system since the reaction phase (mixed liquor) keep the higher number of microorganisms, but for the effluent is expected to present relatively low (i.e. removed) volatile solids.

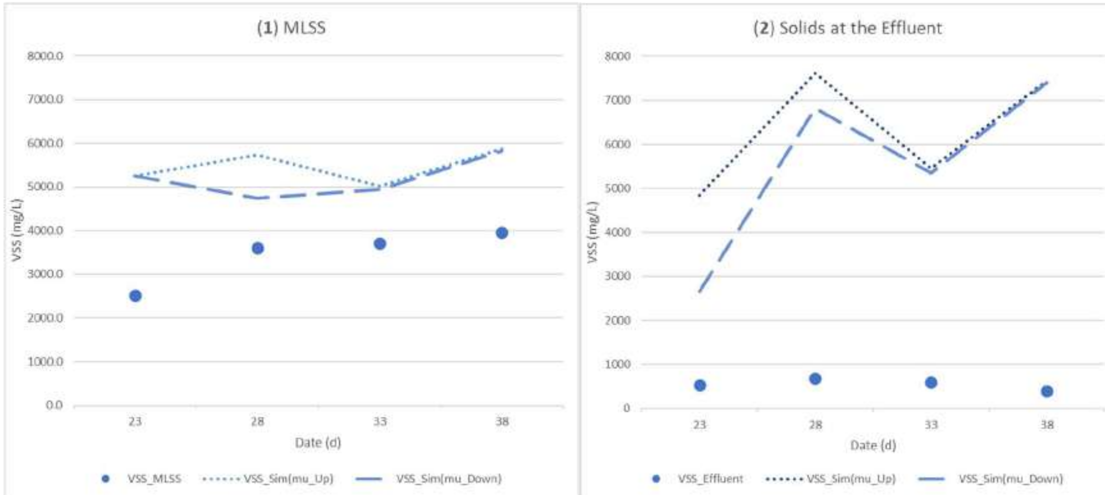

Figure 64. Volatile sludge production analysis for (1) SBR Mixed liquor solids in the reactor and (2) solids at the effluent, modifying the maximum growth rates of heterotrophs microorganisms. Source: Own elaboration.

10.2.1.2.2. BIOMASS DECAY RATES (b_H)

The decay rate from the same heterotrophic microorganism groups and that stands for decay, lysis, maintenance, endogenous respiration and predation (Gujer & Henze, 1991), will be simulated with under a high decay rate B_H=1.5d^{-1}called “b_Up” and low decay rate B_H=0.15d^{-1} called “b_down” scenarios, values are taking by suggestion of Oles & Wilderer (1991) and Andreottola et al. (1997) for SBR systems on industrial application, while for domestic wastewater is b_H=0.24d^{-1} a common value.

It was found that augmenting the decay rates (dotted green line) reduces the VSS in both mixed (Figure 65-1) and effluent (Figure 65-2), as expected. Additionally, the decay of heterotrophic transforming microorganisms is less sensitive than the maximum growth rates. Finally, augmenting the decay rates presents better visual fine tuning especially in the mixed liquor as for the growth rates analysis.

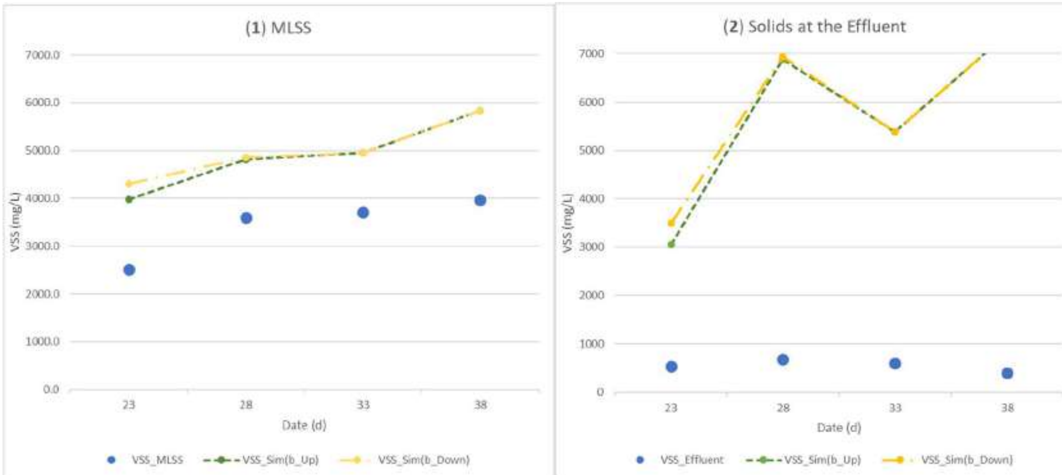

Figure 65. Volatile sludge production analysis for (1) SBR Mixed liquor solids in the reactor and (2) at the effluent, modifying the decay rate of heterotrophs microorganisms.
Source: Own elaboration.

10.2.1.3. YIELD PARAMETERS (Y_H)

The yield of OHO for industrial applications could be affected by fast fill SBR pattern (Melcer, 2004). Taking this into consideration, two scenarios will be tested based on the suggestion of Andreottola et al. (1997) for meat industry wastewater: The high maximum growth rate $\mathbf{Y_H}$=0.9mgCOD/mgCOD called "mu_Up" and the low maximum growth rate as $\mathbf{Y_H}$=0.3mg COD/mgCOD called "mu_Down".

The decrease of the stoichiometric parameter Y_H will produce less VSS in both MLSS and Effluent, reproducing a better fine tuning for the MLSS than for the effluent (Figure 66). The Y_H_Down=0.3 scenario, presents the better visual fine-tuning approximation to the MLSS volatile solids. However, this parameter does not present a clear sensitivity pattern in both responses, as found by Oles & Wilderer (1991) for SBR systems analysis.

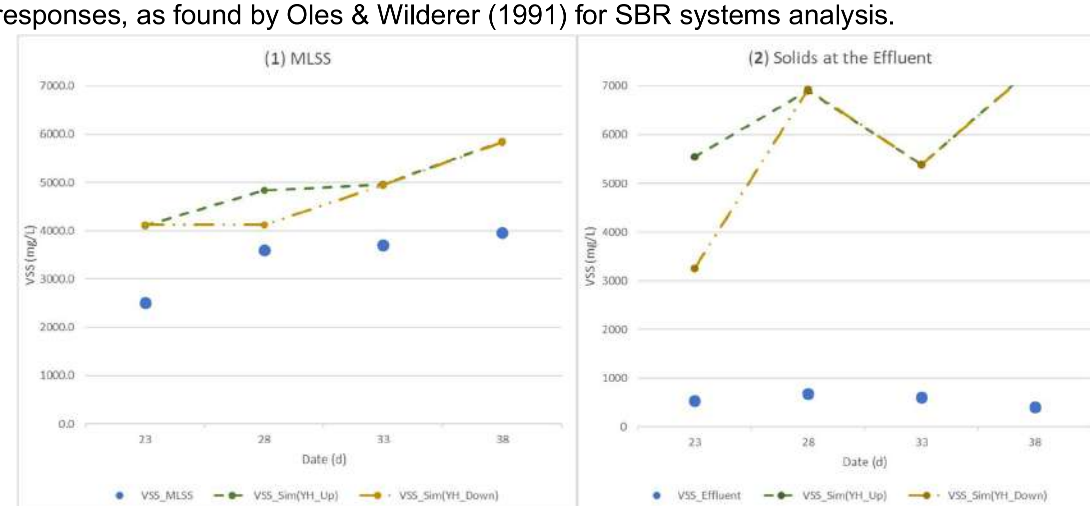

Figure 66. Volatile sludge production analysis for (1) SBR Mixed liquor solids in the reactor and (2) at the effluent, modifying the yield coefficient of heterotrophs.
Source: Own elaboration.

10.2.1.4. SETTLING PARAMETERS

BioWin software allows to estimate the sludge settling extent in a SBR system by means of the “Upflow Factor”, for instance, a high UF produce a worse sedimentation response, in continuous AS this is called “percent of solids removal” and is adjusted in the secondary clarifier (Envirosim, 2021). This parameter produces high changes in the TSS, MLVSS and COD effluent response. The sensitivity analysis in this parameter will be performed by an Upflow factor of 0.5 (Called “UF_up=0.5”, 50% of poor sedimentation process) and other of 0.005 (called “UF_down=0.005”, 0.5% a well sedimentation process).
Figure 67 presents the effect from an Upflow Factor (UF) of 0.005 (0.5% a well sedimentation process) and other of 0.5 (50% a poor sedimentation process). Low UF for the MLSS response but no for the effluent as expected. This parameter presents a relative high sensitivity to the TSS response. However, is not enough an UF of 0.5% to be closer to the observed values.

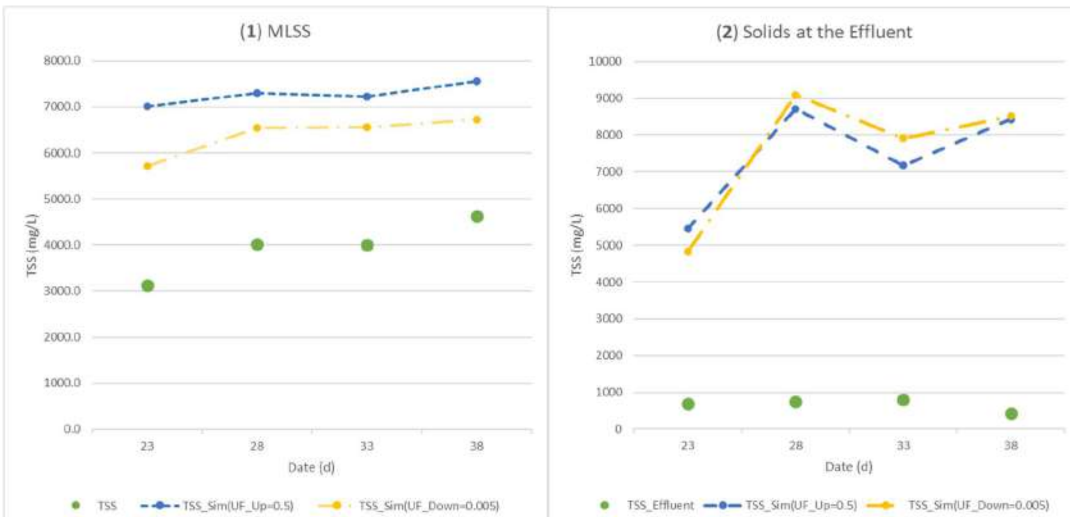

Figure 67. Total suspended solid production analysis for (1) SBR Mixed liquor solids in the reactor and (2) at the effluent, modifying the Upflow Factor.
Source: Own elaboration.

10.2.1.5. SRT

Filali-Meknassi et al. (2004) suggested that the SRT correction for solid matching is valid when no wastage sludge flow is known, otherwise this value is fixed according to the measured data, which is a more accurate practice. The sludge retention time produces the highest changes in the sludge production (Meijer & Brdjanovic, 2012), and therefore, much attention should be paid during the calibration of SRT value, which is suggested by means of closing the total phosphorus balance. Melcer (2004) suggests the adjustment of the wastage flow implies the modification of the SRT.

In the current project, a value of SRT to 30d was adopted from the measure data, however, SRT, especially in SBR systems, present difficulties in the estimation due to the high interferences on quantifying the mass of sludge in the system, compactability, sludge concentration changes during the settle/decant phase, and loss of sludge when high wastage rate is carried out (Envirosim, 2021). Therefore, an additional analysis for a high SRT=60d (called “SRT=Up”) and low SRT=1d (called “SRT=Down”) will be analyzed.

The possible reason why sludge production does not match the actual measured data could include an incorrect measurement of wastage sludge in: Flow, mass flow or chemical addition in the plant that generates more inorganics to the MLSS, as the addition of the coagulant prior to the SBR system of analysis. The reduction of the SRT to 1d (dashed line, called Down), decreases the TSS in both the Mixed liquor (Figure 68-1) and effluent (Figure 68-2). The higher sensitivity was presented for the effluent TSS, where both scenaries are far from each other. Finally, the SRT=1d presents the better approximation of the mixed liquor and effluent TSS values. However, this is not a common condition, since SRT lower than 5d is not suggested for BNR (Meijer & Brdjanovic, 2012).

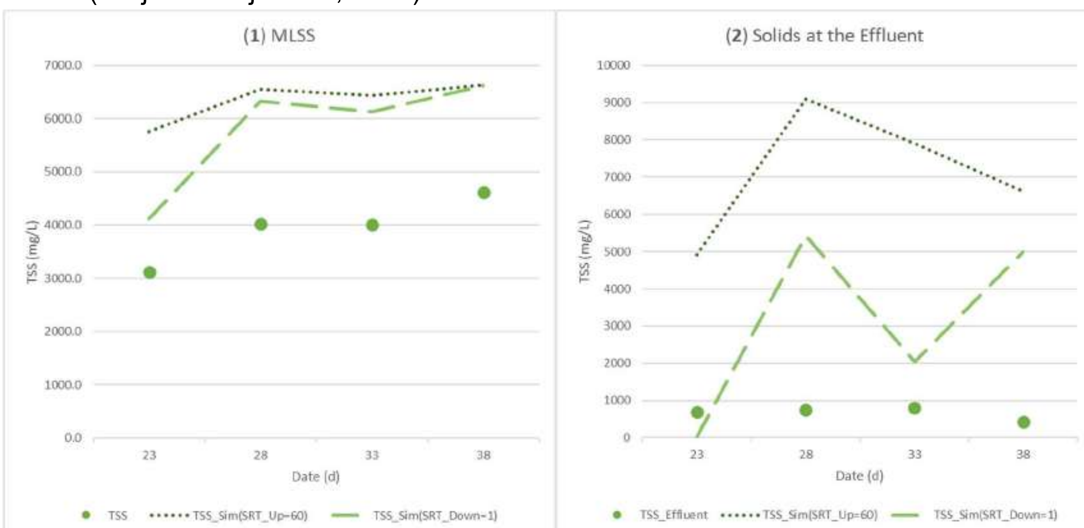

Figure 68. Total suspended solid production analysis for (1) SBR Mixed liquor solids in the reactor and (2) suspended solids at the effluent, modifying the SRT.
Source: Own elaboration.

10.2.1.6. FINAL REMARKS OF SENSITIVITY ANALYSIS FOR SLUDGE PRODUCTION

For this specific wastewater the most sensible variables were the SRT, follow by other less sensible variables like growth of ordinary heterotrophic organisms-OHO (μ_H), upflow factor (UF, which is a settling parameter), and the last group with the inorganic particulate COD fraction (X_I), OHO decay (b_H), and Y_H.
The lower the value of SRT, the lesser the TSS in the MLSS and Effluent solids. Decrease of μ_H will reproduce a decrease of VSS on MLSS and Effluent solids, presenting high sensitivity for the Effluent response, but better fine-tuning for the MLSS. The lower the UF, the lower the TSS response. High X_I produces less inert sludge production, especially for the MLSS. When b_H is augmented, it produces less VSS in both MLSS and Effluent, with better fine-tuning for the MLSS. The decrease of Y_H parameter reduces the VSS response for both MLSS and Effluent. However, is not a clear pattern. Finally, iNX_I & iPX_I do not present a visual effect on inert MLSS and Effluent. Most of the parameters that do not present high sensitivity can be because of the inhibition effect of the system.

10.2.2. CARBON PERFORMANCE FITTING FOR HKWW

COD_S at the effluent is fitting by adjusting of S_I and S_S fractions since S_I is not converted (Meijer & Brdjanovic, 2012). In many industrial application S_I is also composed by volatile components that could be limiting for heterotrophic organisms (Gernaey et al., 2004). Under the current project, using the STOWA fractionation protocol, some state variables are not possible to change, for instance, the S_I fraction since this fraction is computed based on the COD_S and BOD_5 at the effluent, already observed data. However, the biodegradable and particulates fractions are changeable and will be examined next.

10.2.2.1. BIODEGRADABLE SOLUBABLE FRACTION (S_S)

The BOD_5 effluent response will be analyze though the soluble biodegradable fraction (S_S), which is composed by S_F and S_A. Variations in the S_S fraction is only possible by changing the S_A fraction, when the COD from VFAs concentration (COD_{AC}) is unknow as in this project. In this sense, two scenarios will be proven for the DBO analysis, a low S_A scenario with a VFA/TCOD ratio of 330mg COD_{ac}/10813mg COD_T as an approximation from the rendering wastewater of Ng et al. (2022) for Slaughterhouse wastewater, instead of 1519.7mg COD_{AC} that was used for the default analysis. And a high S_A scenario with a theoretical VFA/TCOD ratio of 2800mg COD_{ac}/10813mg COD_T, which is the maximal COD_{Ac} allowed for the STOWA protocol under the current project conditions. At next it will present that in general the S_A fraction and with this the S_S fraction is increased from on average 14% to 26% (Figure 69-1 and Figure 69-2).

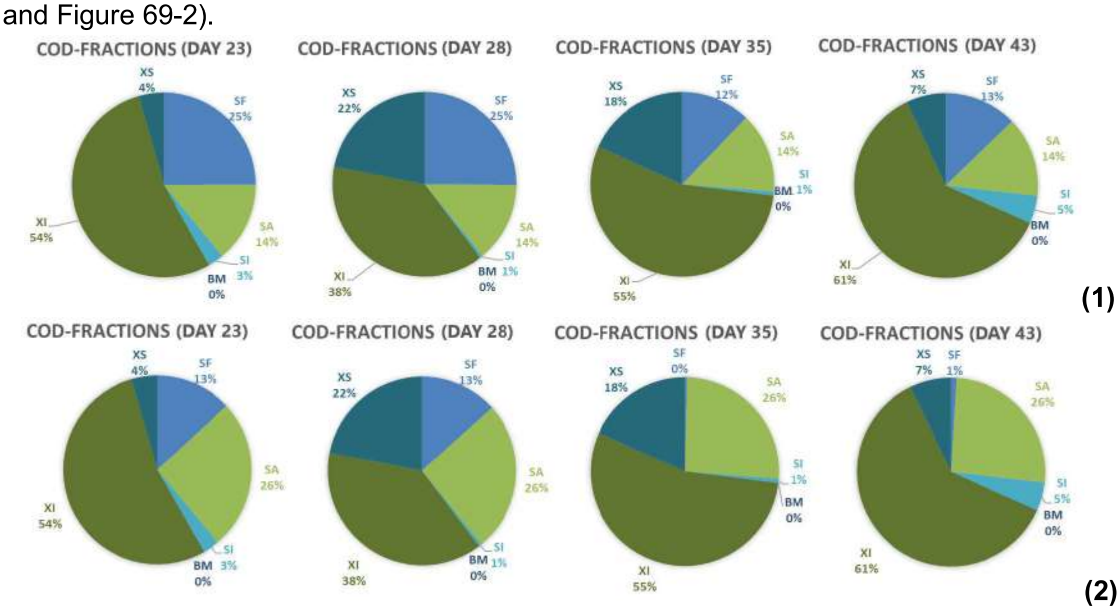

Figure 69. (1) low and (2) augmented SA fractionation to the COD fractionation for the four simulation points from stage II.
Source: Own elaboration.

When the S_A fraction is increased (orange dashed line) the BOD response increases slightly as well but is still a relatively small variation showing that under the current project conditions this parameter presents low sensitivity (Figure 70). Different from the sludge production simulated response, in this case, the difference between the first and the next three simulation points present a high deviation, which is explained by the difference in fractionation in those inputs' points.

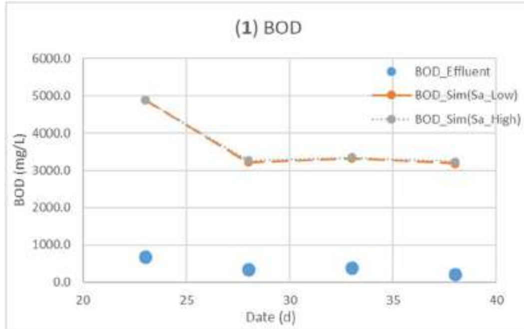

Figure 70. Carbon performance analysis for BOD concentration at the effluent, modifying the SA in the influent input.
Source: Own elaboration.

10.2.2.2. THE COMBINED EFFECT OF S_A and X_I

The total COD, and CODs will be analyzed by means of the sensitivity analysis of S_A and X_I alterations, since both parameters count for part of soluble and particulates COD fractions. Two scenarios will be evaluated as high and low S_A and X_I fraction scenarios. The low scenarios stand for a VFA/TCOD ratio of 330mg COD_{ac}/10813mg COD_T, as in the previous analysis, and low X_I fraction (5% on average) by changing the BOD model from the STOWA fractionation the k constant to 0.13, and Y_{BOD} to 0.2. On the other hand, the high scenario considers the S_A fraction increment for a VFA/TCOD ratio of 2800mg COD_{ac}/10813mg COD_T, as in the previous analysis, and the X_I fraction will increase (55% on average) varying the k constant to 0.8, and Y_{BOD} to 0.55.

As seen in Figure 71-2, this time the X_I fraction augmented in comparison to the X_I fraction of Figure 69-2, as a result of the theoretical and allowed X_I alteration by the STOWA fractionation.

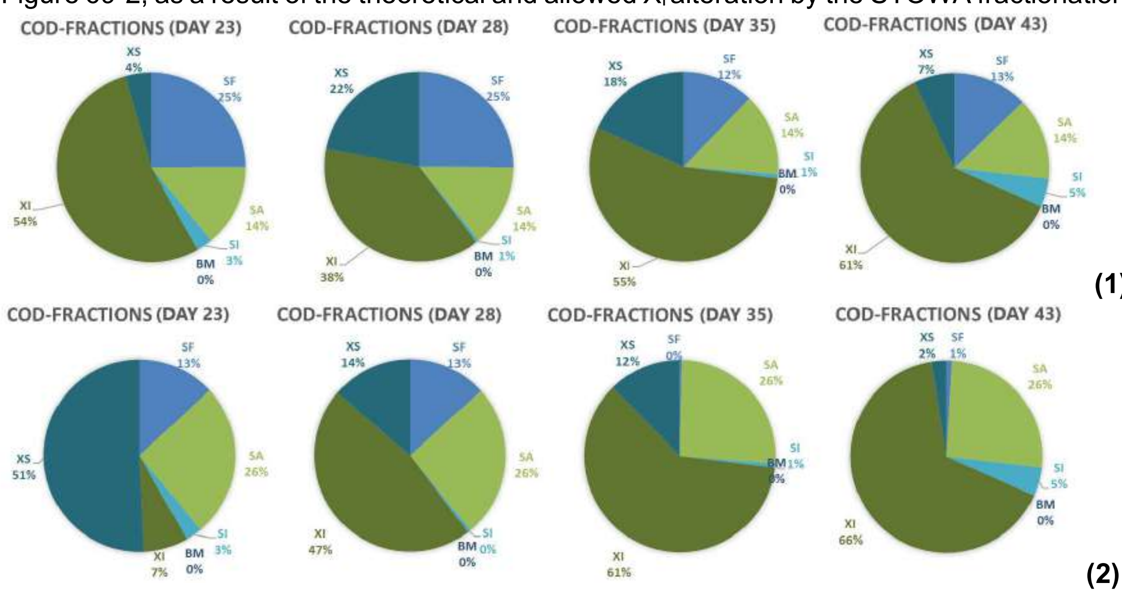

Figure 71. (1) low and (2) augmented SA and XI fractionation to the COD fractionation for the four simulation points from stage II.
Source: Own elaboration.

Figure 72-1 shows that high S_A and X_I fraction produces slightly low TCOD and CODs at the effluent, as seeing in Figure 70 the S_A effect is relatively low, but the X_I effect suggest that augmenting this parameter not only reduces the sludge production but also reduces the TCOD

and CODs response under the current project conditions. The sensitivity of this modification is high in comparison with the previous analysis.
The influent inert soluble COD (S_I) ranges from 32 to 412 mgCOD/L suggesting that the CODs at the effluent is possible to achieve, which range from 602 to 803mgcOD/L. However, the simulation is still far from the observed data points (big blue dots). This effect could be as a result of the pH, ammonia inhibition and lack of phosphorous contain.

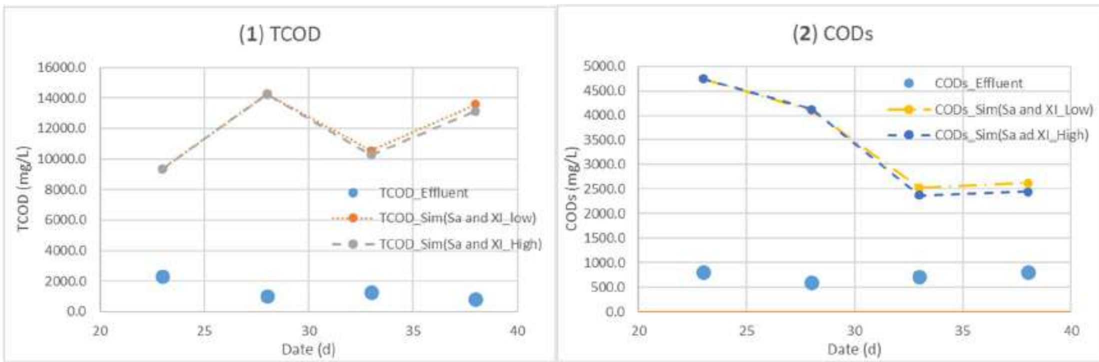

Figure 72. Carbon performance analysis for (1) TCOD concentration and (2) CODs at the effluent, modifying the SA and XI in the influent input.
Source: Own elaboration.

10.2.2.3. FINAL REMARKS OF SENSITIVITY ANALYSIS FOR CARBON PERFORMANCE

Neither S_S fraction nor S_A and X_I fraction reproduce high sensitivity in the COD or BOD response as expected and suggested by the literature. Thus, many protocols as GMP protocol do not calibrate the carbon state variables.

10.2.3. NITROGEN EFFLUENT CONCENTRATIONS FOR HKWW

The nitrogen sensitivity analysis will be performed based on the proposition on Figure 7, first changing model parameters as $\mu_{Ammonia}$, $b_{Ammonia}$, K_{O2}, k_{NH4} for autotrophic nitrifying bacteria and after influent fractions as S_a and iNSa and iNPa and, since nitrification process is calibrated against ammonium, while denitrification is calibrated against nitrite and nitrate concentrations.

10.2.3.1. MODEL PARAMETERS (NITRIFICATION)

μ_{AUT} should be modified to achieve the NTK and NH_4^+ effluent concentrations and hence to fine-tuning the nitrification process (Melcer, 2004). If the result does not match correctly then $b_{AUT,}$ and inhibition factors as K_{O2}, k_{NH4}, should also be proven (Rieger et al., 2012), zinc ammonium could cause acute nitrification inhibition by the toxic components of industrial wastewater (Gernaey et al., 2004). Also, environmental conditions are suggested to be checked as D.O. set point and alkalinity (Meijer & Brdjanovic, 2012; Rieger et al., 2012).

10.2.3.1.1. BIOMASS GROWTH RATES ($\mu_{Ammonium}$=⅕ μ_{OHO})

Two scenarios will be tested base on the suggestion of Andreottola et al. (1997) and Nowak et al. (1996) for meat industry wastewater studies: The high maximum growth rate $\mu_{Ammonia,Max}=5d^{-1}$ called “mu_Up” and the low maximum growth rate as $\mu_{Ammonia,Max}=0.3d^{-1}$ called "mu_Down". However, It is recommended to perform respirometric test to evaluate the kinetic rates for industrial wastewaters (Meijer & Brdjanovic, 2012).

The increment in the maximum growth rate of ammonium oxidizers ($\mu_{Ammonium}$) produce less NTK at the effluent (Figure 73-1), but the trend is not clear for the ammonium concentration (Figure 73-2), i.e. the $\mu_{Ammonium}$ produces a highly sensitive response for the NTK than the NH_4^+. Although this parameter presents higher sensitivity for NTK response than NH_4^+, the better approximation (fitting) between observed and simulated data is for the NH_4^+ response. The BioWin software presents two alarms: "Phosphorous limited condition" and "PH inhibition for autotrophs" that confirms the reason why the nitrogen removal is too low.

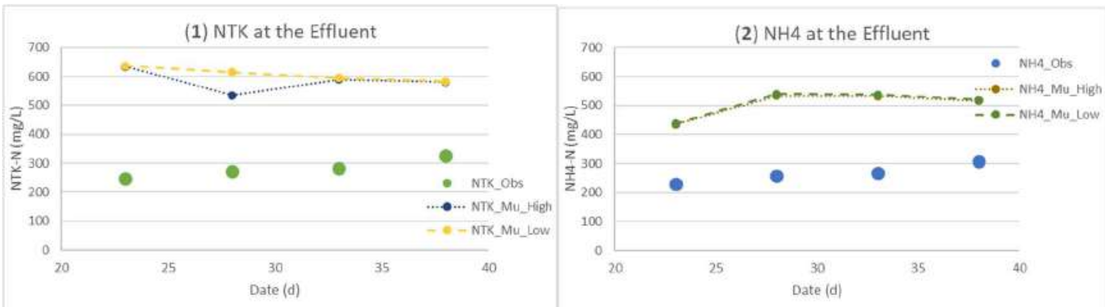

Figure 73. Nitrogen performance analysis for (1) NTK and (2) NH4+ at the effluent, varying the biomass growth rate of maximal ammonium oxidizers bacteria.
Source: Own elaboration.

10.2.3.1.2. BIOMASS DECAY RATES ($b_{Ammonium}$=0.04d^{-1})

Also two different decay rates scenarios will be evaluated for high decay rate $B_{H,ammonia}$=0.5d^{-1} called "b_Up", and for low decay rate $B_{H,ammonia}$=0.05d^{-1} called "bn_Down".
Different from the heterotrophic microorganisms, the decay rate of ammonium oxidizers does not present a notable sensitivity (Figure 74Figure 73), and the NH_4^+ effluent results are similar as those in Figure 73-2.

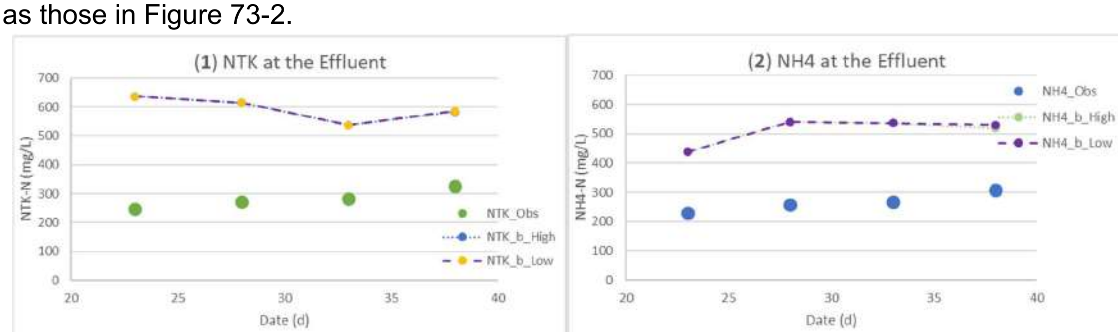

Figure 74. Nitrogen performance analysis for (1) NTK and (2) NH4+ at the effluent, varying the decay rate of ammonium oxidizers bacteria.
Source: Own elaboration.

10.2.3.1.3. SATURATION/INHIBITION FACTORS O_2 (K_{O2})

For fitting the NH_4^+ at the effluent inhibition factors for autotrophic microorganism as ammonium oxidizers are suggested to be corrected (Rieger et al., 2012). When some of those parameters are increased the system inhibition decreases, for example, when K_{O2} is increased, the anoxic process inhibition is reduced. i.e. increasing the K_{O2} the treatment

system does not see that oxygen is present in the reaction tank and allowing the nitrifying continues (Meijer & Brdjanovic, 2012). K_{O2} for ammonia oxidizing bacteria typical value is 0.2 mg O_2/L, while for ammonium half saturation concentration is 1mg NH_4^+/L.
The wrong prediction of ammonium at the effluent is usually caused by wrong D.O. (**K_{O2}**) in the reaction chamber (Rieger et al., 2012; Meijer & Brdjanovic, 2012). High aeration rates inhibit the nitrifiers performance, this is not only proven by the meaning of the K_{O2} factor, but also Larrea et al. (2007) has stated that the number of intermittent aerations (e.g. four sub cycles of aeration) increases the K_{La} coefficient causing an excess of aeration that reduces the overall nitrogen removal performance. Therefore, due to the low denitrification performed by the actual SBR system the effect of dissolved oxygen concentration will also be analyzed. Thus, two different oxygen-nitrification inhibition scenarios will be evaluated: for low inhibition K_{O2}=1mg O_2/L called “K_Up”, and for high nitrification inhibition K_{O2}=0.1mg O_2/L called “K_Down”.

The increment to 1.2 mg O_2/L produces less NTK at the effluent (Figure 75-1) as expected, but the trend in not clear for the ammonium concentration (Figure 75-2), i.e., this parameter neither presents high sensitivity in the ammonium-nitrogen response.

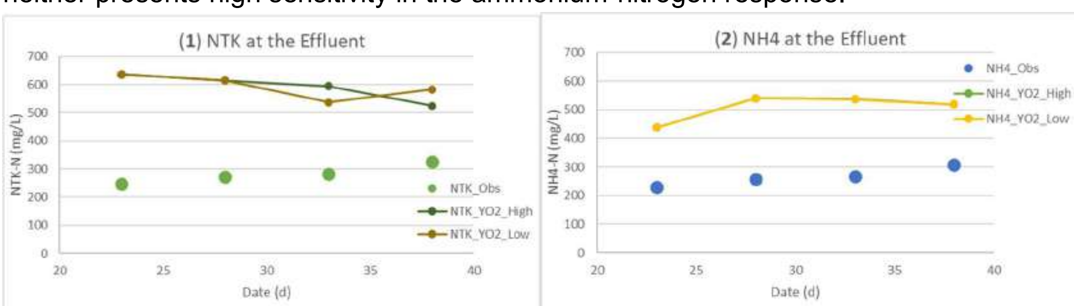

Figure 75. Nitrogen performance analysis for (1) NTK and (2) NH4+ at the effluent, varying the decay rate of ammonium oxidizers bacteria.
Source: Own elaboration.

10.2.3.1.4. SATURATION/INHIBITION FACTORS NH_4^+ (K_{NH4})

Also, the wrong prediction of ammonium (**K_{NH4}** , related with alkalinity) is caused by the toxic effect from the same ammonium concentration (Rieger et al., 2012; Meijer & Brdjanovic, 2012). Two different ammonium-nitrification inhibition scenarios will be evaluated: for low inhibition K_{NH4}=3mg NH_4^+/L, called “K_Up” and high inhibition K_{NH4}=0.3mg NH_4^+/L, called “K_Down”.

This parameter presents the lower sensitivity since nitrogen response remains unchangeable at the effluent for both NTK (Figure 76-1) and NH_4^+ (Figure 76-2).

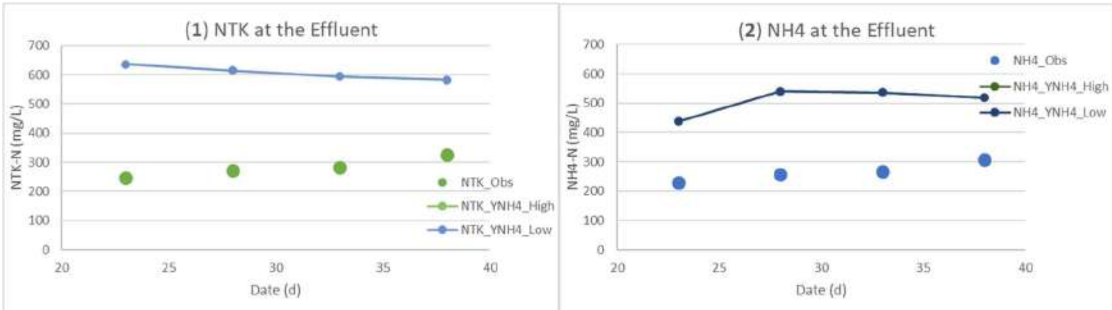

Figure 76. Nitrogen performance analysis for (1) NTK and (2) NH4+ at the effluent, varying the decay rate of ammonium oxidizers bacteria.
Source: Own elaboration.

10.2.3.2. INFLUENT FRACTIONS (DENITRIFICATION)

Usually, the denitrification is calibrated against the nitrite and nitrate effluent concentrations with the next parameter: Decay of heterotrophs (b_H), reduction factor (η_{NO3}), and inhibition factor (K_{O2}, K_{NO3}, K_{OH}) (Melcer, 2004; Meijer & Brdjanovic, 2012). Additionally, alkalinity must be considered (Rieger et al., 2012). However, for the current inhibition project condition the sensitivity analysis will be based on the readily biodegradable fraction (S_S) and the VFAs in form of acetate for nitrogen and phosphorus fractions.

10.2.3.2.1. READILY BIODEGRADABLE COD FRACTION (S_F-S_A)

Soluble biodegradable COD fractions play an important role for denitrification fine-tuning and should be changed in the calibration process (Melcer, 2004; Rieger et al., 2012). Not only direct S_s should be analyzed, since another source of S_S comes from the hydrolysable $\mathbf{X_S}$ COD, in this sense, $\mathbf{X_S}$ is also important in the denitrification fine-tuning (Orhon et al., 2009). Two analysis scenarios will be also evaluated for the sensitivity analysis of S_S fraction called S_A_low (with the original fractionation with VFA ratio (from literature approximated) of 330mg COD_{ac}/10813mg COD_T) and F_{BS}_High (VFA ratio (approximated) of 2800mg COD_{ac}/10813mg COD_T instead of 1519.7mg COD_{ac}/10813mg COD_T as was used for the past experiments as the original fractionation). The fractionation for this analysis is the same as in Figure 69-1 for low and Figure 69-2 for high S_A fraction.

The increment in S_S fraction do not produce high sensitivity for the NO_3^- and NO_2^- nitrogen species (Figure 77). In general, for the simulation study, the TKN and NH_4^+ are overestimated for the software and NO_3^- and NO_2^- are underestimated.

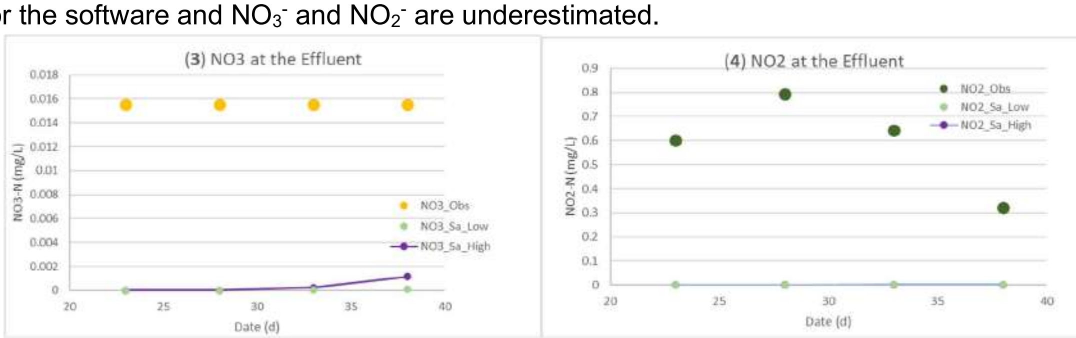

Figure 77. Nitrogen performance analysis for (1) NO3 and (2) NO2 at the effluent, varying the SA fraction.
Source: Own elaboration.

10.2.3.2.2. INERT NITROGEN FRACTIONS (iN_{Sa} and iP_{Sa})

As S_S fraction, the associated nitrogen and phosphorous readily carbon source can affect the nitrogen response. Also, in high strength industrial effluents, large effluent amounts of inert soluble nitrogen (iN_{SI}) are common (Roeleveld & Van Loosdrecht, 2002), which is possible to determine by respirometric test. However, in the present study this parameter was not recorded. Two analysis scenarios will be evaluated low and high organic fractionation of N and P called Low_iNSa and iPSa (original fractionation, Figure 62-1), and high_iNSa and iPSa respectively Figure 78).

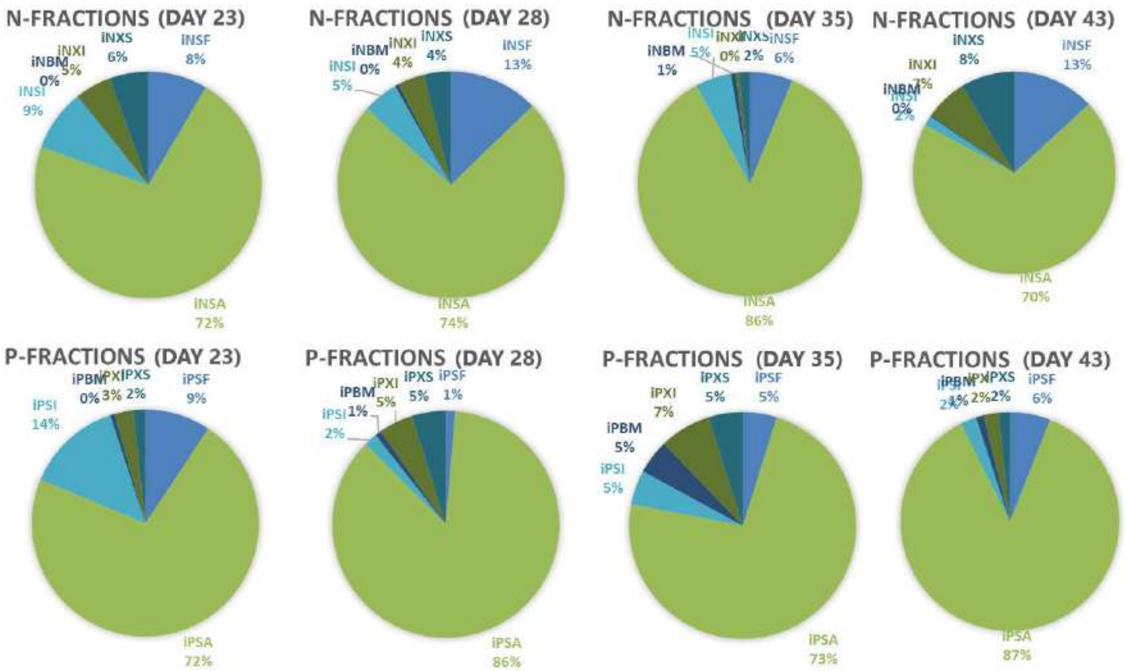

Figure 78. Augmented fractionation of the four simulation points from stage II, for nitrogen (top) and phosphorus (bottom).
Source: Own elaboration.

The sensitivity analysis shows in general that the modification of VFAs in form of acetate for nitrogen and phosphorous fraction do not reproduce a notable change in the effluent nitrogen species results under this specific wastewater matrix (Figure 79), since there is not different between low and high INS_A and IPS_A fraction from the influent.

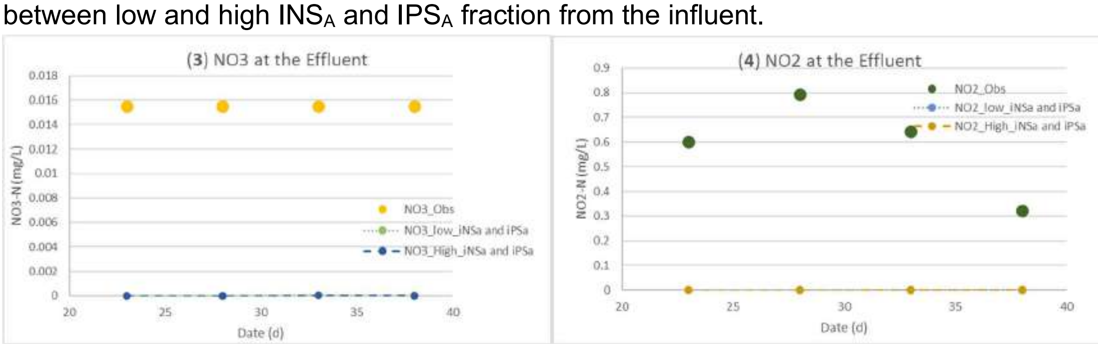

Figure 79. Nitrogen performance analysis for (1) NO3 and (2) NO2 at the effluent, varying the INSA and IPSA fractions.
Source: Own elaboration.

10.2.3.3. FINAL REMARKS OF SENSITIVITY ANALYSIS FOR NITROGEN PERFORMANCE

In general, nitrogen calibration presented the lower sensitivity since the biological process is being affected by the nutrient deficit, pH attack and aeration pattern. The maximum growth rate of ammonium oxidizers and the oxygen half saturation inhibition factor (K_{O2}) present a relatively sensitive response, but not the remaining parameters. The increase on $\mu_{Ammonium}$ will reduce the NTK at the effluent, but the effect is not clear for the NH_4^+ ion. Similarly, the increase of K_{O2} will reduce the NTK at the effluent, but low to the NH_4^+ ion. Finally, neither $b_{ammonium}$ nor K_{NH4}, S_A, INSa and IPSa does not present a significant sensitivity.